Abstract

A total of 602 rock samples for paleomagnetism were collected from the McMurdo Sound region, southern Victoria Land, Antarctica. These collected samples, ranging from the Cambro-Ordovician to the Cenozoic age, were examined using several tests of rock magnetism to check the evidence of stability of natural remanent magnetization (NRM) and were then studied paleomagnetically as follows:

The samples of the Cenozoic volcanic rocks have stable NRM. The position of Antarctica has been almost the same from the late Pliocene age up to the present. The position of the virtual geomagnetic pole (VGP) (11 normals and 3 reverses) from the Pliocene age to the present is within a polar cap area of about 30 colatitude. The sequence of lava eruption was determined by synthetic evidence from paleomagnetic, geological and geochronological data.

The almost samples of Ferrar dolerite of Jurassic age have stable NRM. All these samples were magnetized to the normal polarity, and the calculated VGP positions were 45.3°S, 152.0°W for the Wright Valley, 47.0°S, 133.2°W for the Allan Hills and 68.6°S, 139.5°W for Mt. Fleming. These VGP positions are in reasonable agreement with other Jurassic VGPs from Antarctica.

The most samples of Beacon Supergroup have stable NRM of parallel direction to that of Ferrar dolerite. These samples were remagnetized in the Jurassic age and the primary magnetization disappeared. However part of the samples has stable depositional remanent magnetization of the Permo-Triassic age. The direction of NRM is parallel to that of Ferrar dolerite. East Antarctica had no shift from the Permo-Triassic to the Jurassic and Australia must have been linked to Antarctica at least up to the Jurassic age.

The basement complex of Cambro-Ordovician age of Wright Valley has a stable component of NRM. The directions of NRM distributed on a meridian gathered gradually to low in latitude by thermal demagnetization up to 500°C, however distributed in high latitude dispersed by that demagnetization. These characteristics are related to the Curie points of the samples. These rocks were heated to 500°C in the Jurassic age by a hidden Ferrar dolerite body. Consequently primary magnetization was remagnetized for the samples which have a Curie point lower than 500°C in the Jurassic age by a hidden Ferrar dolerite body, but survived for the samples included in magnetite grains. The obtained VGP positions of the Cambro-Ordovician age

consistent with previous date of the same age in East Antarctica. The differences in the declination of the Cambro-Ordovician age from East Antarctica are consistent with an angular rifting of 15–20° having occurred subsequently with in East Antarctica, probably along the line of the Amery Ice Shelf and Lambert Glacier.

From these viewpoints, following synthetic results were obtained: The reconstruction model of Gondwanaland by SMITH and HALLAM (1970) is available; the southern continents and India were continuous large land mass until Jurassic age, and the break-up had begun after intrusion of dolerite in Gondwanaland at that time; newly apparent polar-wander path for Antarctica was determined.

1. Introduction

This paper is summarized about paleomagnetic investigation of McMurdo Sound region in southern Victoria Land, East Antarctica, from Cambro-Ordovician age to present, based on rock magnetic evidence, and then the results were expanded to whole East Antarctica. A part of this study has been published already by FUNAKI (1979, 1983a, b, c).

By general agreement, the geological and geophysical evidences of Antarctica have been subdivided into East and West Antarctica. The boundary passes through the Ross and Weddell Seas. Although East Antarctica is clearly a large continental block mass, consisting largely of a Precambrian Shield, and was one of the main fragments of Gondwanaland, it appears that West Antarctica could be found to consist of a number

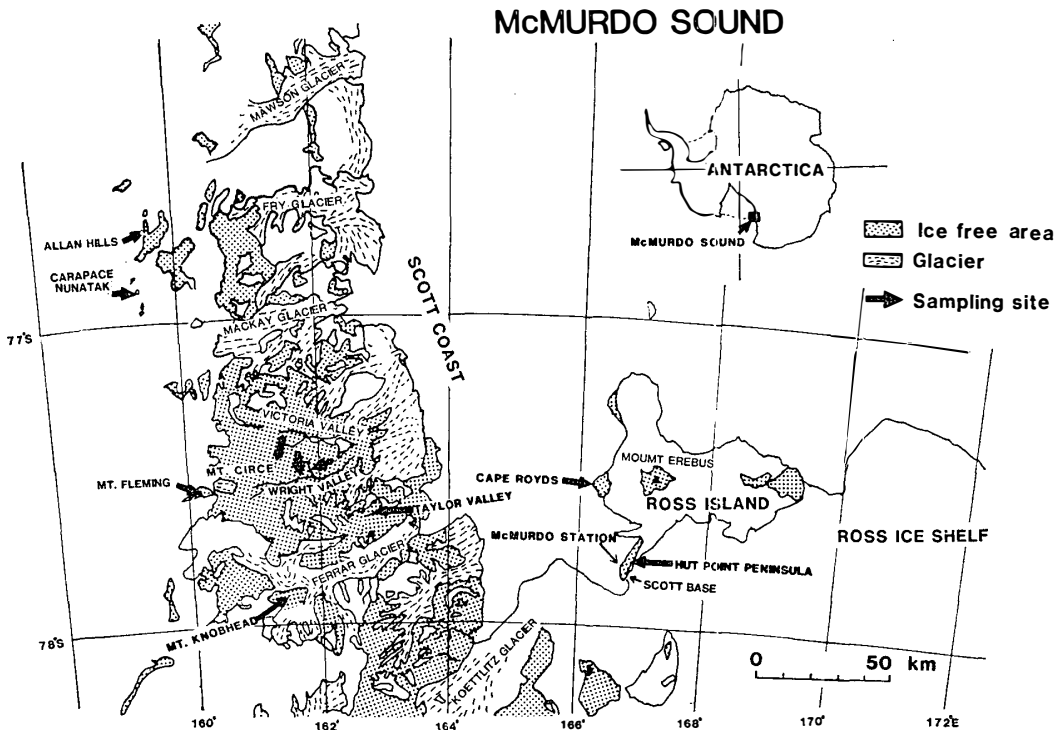

Fig. 1. A topographic map of McMurdo Sound region and the sampling sites.

of isolated regions, if its ice cap were melted (*e.g.* HAMILTON, 1967). The continental drifts of these blocks are mutually different (*e.g.* SCHARNBERGER and SCHARON, 1982). Therefore this study will be limited to the paleomagnetism of East Antarctica.

The McMurdo Sound area, mapped in Fig. 1, in the Ross Sea, has a wide icefree area along the coast line of southern Victoria Land, Antarctica. In particular the Dry Valley region consists of three major excavated valleys, from the north to the south, namely Victoria Valley, Wright Valley and Taylor Valley. The McMurdo Sound region consists of Precambrian metasediments, a Cambro-Ordovician basement complex, Devonian-Jurassic sediments, a Jurassic dolerite sills and Cenozoic volcanics, and consequently this region has an advantage over the other parts of East Antarctica paleomagnetically.

As mentioned later, clearly defined VGP positions for East Antarctica were obtained for only two points for the Jurassic and Cambro-Ordovician ages. However the reliability of these points is low compared to those of other continental fragments of Gondwanaland. Therefore the main purpose of this study is to clarify the polar-wander path from the Paleozoic to the Cenozoic age. Previous paleomagnetic investigations of East Antarctica were carried out as follows:

Paleomagnetic investigations of Cenozoic volcanics in the Hut Point Peninsula, Ross Island, were carried out by COX (1966), MCMAHON and SPALL (1974a, b), KYLE and TREVES (1974), ARMSTRONG (1978) and FUNAKI (1979). COX (1966) reported that surface samples of trachyte from Observation Hill, at the tip of Hut Point Peninsula, were found to be reversely magnetized, whereas the majority of lava flows and cones in the McMurdo Sound showed normal magnetization. MCMAHON and SPALL carried out paleomagnetic studies of Core No. 1 (196.54 m long) and Core No. 2 (171.38 m long) obtained during the Dry Valley Drilling Project (DVDP), as shown in Fig. 2, and reached the general conclusion that natural remanent magnetizations (NRMs) of all samples of No. 1 and No. 2 cores, except those of a layer of 1 m in thickness, show Matuyama reverse polarity, and predate the Jaramillo event (0.89 to 0.95 m.y.), the average inclination of NRM being $-83°$ (upward magnetization in the southern hemisphere). They examined the NRM stability of pilot samples of No. 2 core, and found that the samples possessed a very stable magnetization direction. KYLE and TREVES (1974) measured the NRM to decide the volcanic sequence of 5 rock masses collected from the Hut Point Peninsula, *i.e.* Twin Crater, Second Crater, Half Moon Crater, Observation Hill and lava flows 250 m north of Scott Base (see Fig. 2). However, these samples were not magnetically clean. ARMSTRONG (1978) reported that late Cenozoic basalts are magnetized in the normal direction (at Half Moon Crater in the Hut Point Peninsula), but reversely magnetized in the Taylor Valley, except for one site. FUNAKI (1979) studied the area of drift of the south geomagnetic pole using ten rock masses collected from the Hut Point Peninsula. His results show that the position of the virtual geomagnetic pole (VGP) (8 normals and 2 reverses) is within a polar cap area of about 30° latitude. However, the NRM stability is not fully discussed in this study.

Previous paleomagnetic investigations of Ferrar dolerite have been carried out at six sites along the Transantarctic Mountains. The virtual geomagnetic pole (VGP) positions obtained from these rocks were 54°S, 136°W for the Theron Mountains

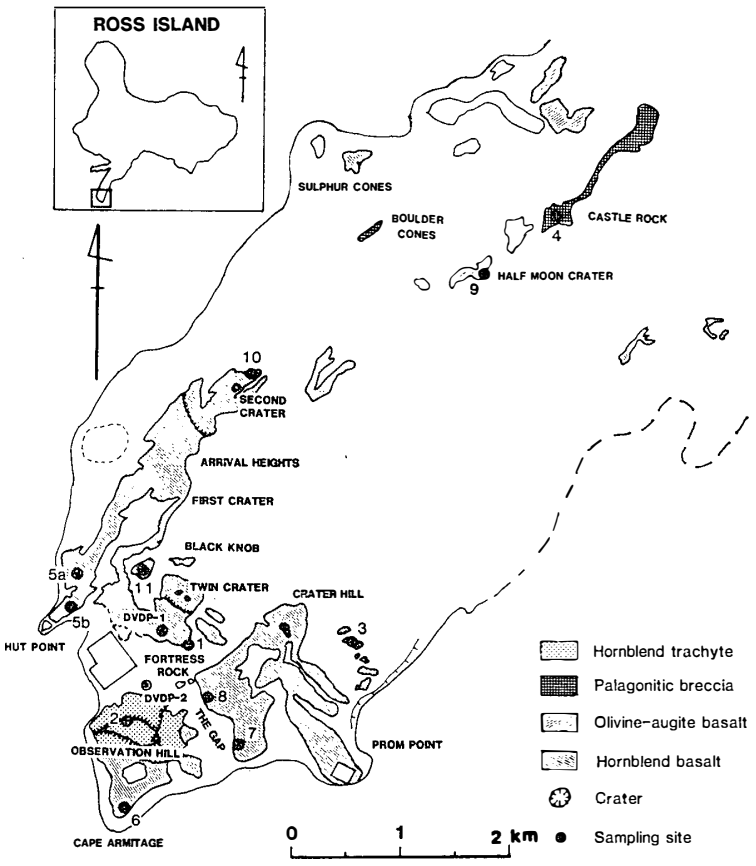

Fig. 2. Sampling sites and geological map (COLE et al., 1971) of Hut Point Peninsula. The names of sampling sites are as follows: 1. Fortress Rock, 2. Observation Hill, 3. Crater Hill, 4. Castle Rock, 5a. North of Hut Point, 5b. Near Hut Point, 6. Cape Armitage, 7. Site between Cape Armitage and Scott Base, 8. East side of the Gap, 9. Half Moon Crater, 10. Second Crater, 11. Black Knob.

(BLUNDELL and STEPHENSON, 1959), 45°S, 140°W for the Wright Valley and the Victoria Valley (BULL *et al.*, 1962), 59°S, 139°W for the Beadmore Glacier (BRINDEN and OLIVER, 1963), 57°S, 168°W and 60°S, 137°W for the Dufec intrusion (BECK, 1972; BURMESTER and SHERIFF, 1980) and 41.8°S, 134°W for Queen (Dronning) Maud Land (LØVLIE, 1979). That is, these VGPs cluster around the present South Pacific.

It is important to ascertain the paleomagnetic pole positions for the period when dolerites were intruding into the Transantarctic Mountains, in order to solve the problem of the break-up of Gondwanaland (MCDOUGALL, 1963). Since the strata surrounding the dolerite are magnetically affected by the igneous activity of the intrusion, it is also important to determine the direction of NRM in the dolerite to evaluate other paleomagnetic data in East Antarctica.

Paleomagnetic investigations of the Beacon Supergroup were carried out for the samples collected from Ferrar Glacier (78°S, 163°E) by TURNBULL (1959), and for the Wright and Victoria Valleys (77.5°S, 161.6°E) by BULL *et al.* (1962). They reached the general conclusion that NRM at these sites is parallel to that of indubitably younger dolerite sills (Ferrar dolerite) in spite of a separation of 150 m from the lower boundary of the sill. That is, a large intrusive mass of Ferrar dolerite nearby caused sufficient

heating to raise the Beacon Supergroup to the Curie point and must have been remagnetized in alignment with the ambient geomagnetic field in the Jurassic age.

According to the geological evidence, the formations from the middle Paleozoic to the Mesozoic age in East Antarctica consist of only the Beacon Supergroup in the Transantarctic Mountains and Prince Charles Mountains of the Lambert Glacier (*i.g.* RAVICH and FEDOROV, 1982). Therefore it is very important to carry out an investigation of the Beacon Supergroup paleomagnetically in order to solve the history of Gondwanaland, as the East Antarctic plate is probably situated in the center of that region.

Paleomagnetic investigations of the basement complex of the McMurdo Sound region were carried out at Wright Valley and Victoria Valley (BULL and IRVING, 1960; BULL *et al.*, 1962) and at Taylor Valley (MANZONI and NANNI, 1977). The main results obtained from these investigations are as follows: The directions of the stable component of natural remanent magnetization (NRM) in the Wright and Victoria Valleys area are parallel in all the units of the basement complex (Cambro-Ordovician age) and dolerite sills (Jurassic age). This uniformity in direction could have resulted from the geomagnetic field in this region being constant in direction for a long period of time in the Paleozoic and Mesozoic ages, or from the reheating of the whole area during the last phase of intrusion (that of Ferrar dolerite) in Mesozoic time. Calculated paleomagnetic pole positions from these data are located in the present South Pacific. In the case of Taylor Valley, the mean NRM direction of four lamprophyric dykes (Cambro-Ordovician age) yielded a declination of 222.6° and an inclination of 0.6°, but the other dykes and the amphibolitic basement were not fully reliable magnetically. The corresponding paleomagnetic pole position lay at 9.3°S and 26.7°E, consistent with the previous results for lower Ordovician rock from a distant area of East Antarctica. This suggests that the basement complex in the Wright and Victoria Valleys region was heated to above the Curie point by Ferrar dolerite in the Jurassic period.

2. Geology of McMurdo Sound Region

2.1. Geological review of East Antarctica and McMurdo Sound region

East Antarctica, the older part of the continent, is a Precambrian Shield, in much of which charnockites are characteristic. The high Transantarctic Mountains, along

Table 1. Geochronological data of basement complex and Ferrar dolerite for McMurdo Sound, Antarctica.

Age	Group	Formation	K-Ar (m.y.)	Rb-Sr (m.y.)	U-Pb (m.y.)
Mesozoic-Cenozoic		McMurdo volcanics Ferrar dolerite Beacon Supergroup	147-163 (9)		
	Kukri peneplain				
Lower Paleozoic	Victoria Intrusives	Vanda lamprophyre	—	—	
		Vanda porphyry		470±7 (5) 480±44 (6)	
		Vida granite	210 (2), 185 (2) 220 (2), 211 (2) 451.4±6.2 (8) 461.2±8.8 (8) 459.9±8.0 (8)	480±44 (6) 486±14 (7)	
Upper Cambrian-Lower Ordovician	Wright Intrusives	Theseus granodiorite	—	—	—
		Loke microdiorite	463.2±8.2 (8) 469.0±8.2 (8) 458.9±8.1 (8) 464.9±8.2 (8) 482.1±8.52 (8)		
		Dais granite		500±43 (6)	
		Olympus granite-gneiss	520 (1)	480−495 (3) 500±43 (6)	610 (4)
Cambrian-Precambrian	Skelton Group	Asgard formation	469.1±8.1 (8)		

(1) GOLDICH *et al.* (1958), (2) MCDOUGALL (1963), (3) DEUTSCH and WEBB (1964), (4) DEUTSCH and GRÖGLER (1966), (5) JONES and FAURE (1967), (6) FAURE and JONES (1973), (7) STUCKLESS (1975), (8) MCDOUGALL and GHENT (1970), (9) MCDOUGALL (1963).

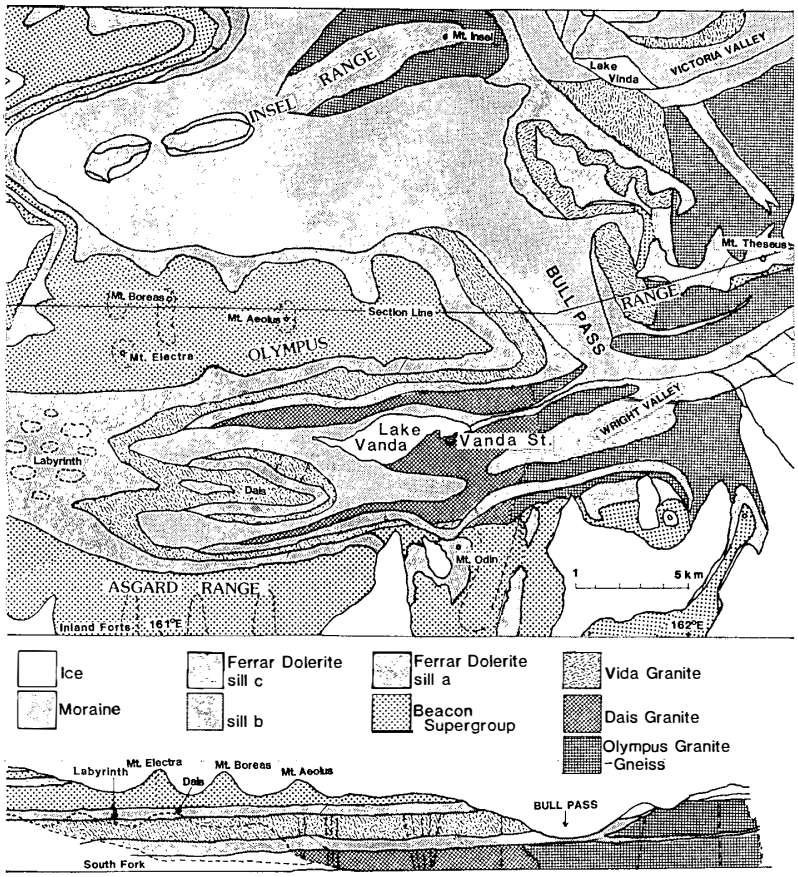

Fig. 3. Geology of Wright Valley region in Dry Valley (McKelvey and Webb, 1961).

the Ross and Weddell Seas, largely follow a geosyncline of upper Precambrian marine sedimentary rocks that were deformed, metamorphosed and intruded by granitic rocks during Cambro-Ordovician time. The rocks of the orogen were peneplained, then covered by late Paleozoic–early Mesozoic terrestrial sediments of the widespread southern Gondwana System, which were intruded by Jurassic dolerite sheets. The main tectonic disturbances in East Antarctica appear to be block faulting of a late Tertiary–Quaternary age, with which, volcanism is widely associated (Hamilton, 1967). Many stratigraphic comparisons can be made with the other southern continents, especially Australia and southern Africa.

The geology of the Dry Valley region may be held to be essentially representative of that of the McMurdo Sound region (*i.e.* McKelvey and Webb, 1961). The summarized geological sequence exposed in Dry Valley is shown in Table 1 and illustrated in Fig. 3.

The basement complex consists of Precambrian–lower Cambrian metasediment intruded by plutonic rocks. These can be divided into the Asgard Formation (the earliest), the Wright Intrusive and the Victoria Intrusive (the latest). The surface of the basement complex, peneplain, is overlaid unconformably with mid-Paleozoic to mid-Mesozoic sediment called Beacon Supergroup (sandstone). The basement complex and Beacon Supergroup were intruded by dolerite sills called Ferrar dolerite in the Jurassic age. Finally late Cenozoic volcanic activities occurred along the coast line.

Since the strata of Beacon Supergroup is horizontal, there must have been no tilting and folding tectonics apparently did not occur after mid-Mesozoic time in McMurdo Sound, although there was volcanic activity in Jurassic and Cenozoic time.

2.2. Geology of McMurdo volcanics

Volcanic cones and lava flows may be observed at the tip of the Hut Point Peninsula. These volcanics consist of basanite and basanitoid with a smaller amount of hawaiite and phonolite. Most of the volcanic cones are concentrated on a prominent lineation whose strike is NNE along the western side of the peninsula. The late Quaternary surface geology of this area has been described by WELLMAN (1964), COLE *et al.* (1971) and KYLE and TREVES (1973). Figure 2 shows the geology of the Hut Point Peninsula as summarized by COLE *et al.* (1971). Studies of the subsurface geology in this area were carried out by DVDP, and the results were reported by TREVES and KYLE (1973). KYLE and TREVES (1974) summarized the relationships between surface and subsurface geology based on paleomagnetic and chronological data. According to these results, the inferred eruptive sequence for the Hut Point Peninsula is as follows: First a very early pile of palagonitic breccias (Castle Rock Sequence); olivine-augite basalt (Crater Hill Sequence); hornblende trachyte (Observation Hill Sequence); hornblende basalt (Half Moon Crater Sequence); and finally a later olivine-augite basalt (Twin Crater Sequence). According to the results of analyses of DVDP Nos. 1, 2 and 3 cores, these cores are assigned to five stages in the sequence of volcanic activity, namely, from the latest to the earliest Twin Crater, Half Moon Crater, Observation Hill, Crater Hill and the palagonitic breccia of Castle Rock (TREVES and KYLE, 1973; KYLE and TREVES, 1974). The palagonitic breccia of Castle Rock is thought to be of submarine or subglacial origin (KYLE and TREVES, 1974).

The volcanic rock at Cape Royds consists of at least three major kenyte flows which are partially mantled by volcanic agglomerate, breccia and lithic tuff (TREVES, 1962).

Relatively small volcanic eruptions took place during the Pleistocene period in Taylor Valley, and the rock types are similar to late cinder cones at Cape Armitage (ANGINO *et al.*, 1962). HARRINGTON (1958) reported that the volcanic rocks in Taylor Valley are fragments of the McMurdo volcanic rocks.

Table 2. Cenozoic chronological data at Hut Point Peninsula, Cape Royds and Taylor Valley.

Sampling site		K-Ar age (m.y.)	References
Hut Point Peninsula	Black Knob	0.43±0.07	ARMSTRONG (1978)
	Southwest of Black Knob	0.57±0.03	ARMSTRONG (1978)
	Half Moon Crater	1.0±0.15	ARMSTRONG (1978)
	Castle Rock dyke	1.1±0.4	KYLE and TREVES (1974)
	Observation Hill	1.18±0.03	FORBES *et al.* (1974)
Cape Royds		0.68±0.14	TREVES (1967)
Taylor Valley (below Marr Glacier)		2.93±0.10	ARMSTRONG (1978)
Taylor Valley (below Marr Glacier)		2.89±0.10	ARMSTRONG (1978)
Taylor Valley (below Marr Glacier)		2.87±0.15	ARMSTRONG (1978)

Geochronological data for the McMurdo volcanics at Hut Point Peninsula, Cape Royds and Taylor Valley are summarized in Table 2. The K-Ar ages of lavas from Black Knob, southwest of Black Knob, Half Moon Crater, Observation Hill and the dyke of Castle Rock have been determined as 0.43 ± 0.07, 0.57 ± 0.03, 1.0 ± 0.15, 1.18 ± 0.03 and 1.1 ± 0.4 m.y. respectively (ARMSTRONG, 1978; KYLE and TREVES, 1974; FORBES *et al.*, 1974). TREVES (1967) reported that the K-Ar age of anorthoclase from the Cape Royds area is 0.68 ± 0.14 m.y. In Taylor Valley, the age of basaltic rock from our sampling sites was reported to be 2.93 ± 0.10 and 2.87 ± 0.15 m.y. by ARMSTRONG (1978).

2.3. Geology of Ferrar dolerite

In Wright Valley, Ferrar dolerite sills intrude into the metamorphic and plutonic basement complex of Precambrian to lower Paleozoic rocks and the flat lying stratum of the Beacon Supergroup sandstone from the Devonian to the Permian age (WEBB, 1963). In Allan Hills sandstone and diamictite are intruded by the dyke, and are locally overlain by basalt. BALLANCE and WATTERS (1971) estimated the age of the basaltic volcanism at Allan Hills to be the middle, perhaps the lower, Jurassic period. According to them, a thick sequence of Jurassic Kirkpatrick basalt, with a thick hyaloclastite breccia with pillow lava, overlies lithic sandstones and conglomerates of the Beacon Supergroup at the Carapace Nunatak. On Mt. Fleming, Ferrar dolerite sills and dykes intrude into Triassic siltstone of the Beacon Supergroup (GUNN and WARREN, 1962).

MCDOUGALL (1963) measured the age of Ferrar dolerite from the Victoria Valley, the Skelton Glacier and the Beardmore Glacier area by the K-Ar method for pyroxenes and plagioclaces; the obtained ages range from 147 to 163 m.y., namely the middle Jurassic age. Geomagnetic polarity is the normal interval for these ages according to the international geomagnetic chart by MCELHINNY and BUREK (1971).

2.4. Geology of Beacon Supergroup

In the McMurdo Sound more than 2100 m of sedimentary sequence, predominantly pale yellow quartz sandstone, is found, overlying unconformably the igneous and metamorphic rocks of the basement complex. These sandstone sequences, together with carbonaceous siltstone, feldspathic sandstone, and minor limestones commonly associated with them, were provisionally brought together under the same Beacon System, with the Beacon sandstone (Supergroup) of the McMurdo Sound area, as the type rock (HARRINGTON, 1958). The inferred sedimentation ages of these Beacon sandstone sequences are from Devonian to Jurassic using the evidence of fossils and tracefossils (MCKELVEY and WEBB, 1961; WEBB, 1963). In almost every section where an appreciable thickness of Beacon Supergroup is exposed, one or more horizontal sills of dolerite are present. These sills are from a few meters to more than 300 m thick and most of the sills are of uniform thickness (GUNN and WARREN, 1962). Some recrystallization of the clastic quartz is found close to the contacts (especially near the lower surface of sills) but this is confined to a band only a few centimeters thick in most places.

The geology of the Beacon Supergroup in the Dry Valley region was described by WEBB (1963), from the oldest to the youngest, the sandstone includes dark subgraywacke

breccia and conglomerate (Boreas subgraywacke member), pink to gray arkose (Odin Arkose), almost pure quartz sandstone (Beacon Heights Orthoquartzite), a thin formation of red and green siltstone (Aztec Siltstone) and formations of quartz sandstone, carbonaceous sandstone, siltstone, and shale (Weller Sandstone). This geological evidence expands into the Beacon Heights and Knobhead regions.

Exposed formations at Mt. Circe, located in the upper Olympus Range between Wright Valley and Victoria Valley, consist of Odin Arkose including Boreas subgraywacke member and Beacon Heights Orthoquartzite from the early pre-Devonian to middle-Devonian period. Their lower boundary is dolerite sill "c" 180 m thick, as described by McKELVEY and WEBB (1961). Formations of Beacon Heights Orthoquartzite and Aztec Siltstone of the Devonian period are exposed at Knobhead, located in the upper Ferrar and Taylor Glaciers. Intrusions of two dolerite sills, one on the top of the mountain and one about 470 m below the top, can be observed on that mountain (WEBB, 1963). A thick sequence of flat-laying Beacon Supergroup with lower or middle Triassic age plant fossils and carbonaceous beds is found at Mt. Fleming, on the upper Wright Glacier (GUNN and WARREN, 1962). Ferrar dolerite sills with dykes 50–200 cm in thickness intrude in this place according to our field observations.

Allan Hills is situated about 200 km northwest of McMurdo Station in Ross Island. A synthesized geology of this area was given by BALLANCE and WATTERS (1971) as follows: Sedimentary rocks referred to the Beacon Supergroup, having a coal bed and fossil plants, which dominated *Glossopteris* from Permian to Triassic age, are exposed at Allan Hills. Diamictite from volcanic mudflows is deposited on this sequence and basaltic dykes intrude into these formations. They estimate that basaltic activity occurred sometime in the middle, perhaps the lower, Jurassic age.

2.5. Geology of basement complex in Wright Valley

Geological investigations within the ice-free area in the Dry Valley region have been carried out in Victoria Valley (WEBB and McKELVEY, 1959; ALLAN and GIBSON, 1961), in Wright Valley (McKELVEY and WEBB, 1961) and in Taylor Valley (McKELVEY and WEBB, 1959). According to these results, the whole region consistently shows essentially the same geological structure. The geological sequence exposed in Wright Valley, summarized by McKELVEY and WEBB (1961), is shown in Fig. 3, and is interpreted as follows:

The basement complex consists of more than 4500 m of folded Precambrian–lower Cambrian marbles, hornfelses and schists (Asgard Formation), invaded by acid plutonic rocks. The oldest intrusives are a granitic gneiss (Olympus granite) and a porphyritic granite (Dais granite). The second intrusive phase consists of microdiorite (Loke microdiorite) and granodiorite (Theseus granodiorite) dykes intruding into the Asgard Formation, and Olympus and Dais granite. The third intrusive phase includes a granite (Vida granite) containing dense swarms of younger Vanda lamprophyre and porphyry dykes invading all the earlier rocks. Besides these formations, dykes of a peculiar red or pink color, and 1 to 2 m in thickness, is intrude into the basement complex at Bull Pass. This dyke is referred to as "red dyke" in this paper. Since the Vanda lamprophyre and porphyry dykes are cut by this dyke, according to field evidence by K. YANAI, "red dyke" represents the latest stage of intrusion.

The surface of the basement complex is overlain unconformably by more than 1200 m of mid-Paleozoic to mid-Mesozoic sediment called Beacon Supergroup (sandstone). In the Olympus Range, between Wright and Victoria Valleys, this basement complex and Beacon Supergroup were intruded by three sills of Jurassic Ferrar dolerite. McKELVEY and WEBB (1961) have described these sills, referred to as "a", "b" and "c", from lower to higher altitude. Sill "a", 240 m thickness, intrudes into the basement complex; sill "b", 180 m thickness, intrudes into the boundary (peneplain) of the basement complex and Beacon Supergroup; sill "c", 120 m thickness, intrudes into Beacon Supergroup. From the bottom of the valley, the mutual vertical distances of "a", "b" and "c" are about 600, 490 and 650 m respectively. At the eastern end of Wright Valley, relatively small volcanic cones called the McMurdo volcanics intruded into the basement complex in the Cenozoic period.

Geochronological data for the basement complex of McMurdo Sound were obtained by GOLDICH *et al.* (1958), McDOUGALL (1963), DEUTSCH and WEBB (1964), DEUTSCH and GRÖGLER (1966), JONES and FAURE (1967), McDOUGALL and GHENT (1970), FAURE and JONES (1973) and STUCKLESS (1975), and are summarized in Table 1. The K-Ar ages of Vida granite show two distinct ranges, 185–220 and 451–461 m.y. The younger samples were collected 15 to 75 m below the area of contact of the lower dolerite sheet with granite in Victoria Valley (McDOUGALL, 1963). In general the ages given by the K-Ar method are younger than those by Rb-Sr method. To explain this discrepancy, it is probable that the development of the basement complex in the Dry Valley region is related to the heating which accompanied the intrusion of Ferrar dolerites, with consequent loss of Argon by diffusion. The more reliable ages for the basement complex are those obtained by means of the rubidium-strontium technique; and the inferred ages of the Wright and Victoria Intrusives are 480–500 and 470–486 m.y. respectively.

3. Samples and Sampling Sites

In the 1977 austral summer season paleomagnetic block rock samples were collected from Hut Point Peninsula, Wright Valley, Taylor Valley, Allan Hills and Mt. Fleming. In the same season of 1978, 2.5 cm diameter cylindrical samples were collected from Taylor Valley, Mt. Circe, Knobhead, Mt. Fleming, Allan Hills and Carapace Nunatak by means of an engine core drill. These sampling sites are mapped out in Fig. 1. As the inclination of the geomagnetic field in McMurdo Sound is $-83.5°$, the direction of these samples was checked using a sun compass; a magnetic compass was used in bad weather. The orientation of volcanic samples was determined using only the sun compass. Paleomagnetic samples, 2.5 cm in both diameter and length, were cut from these rock mass samples in the laboratory.

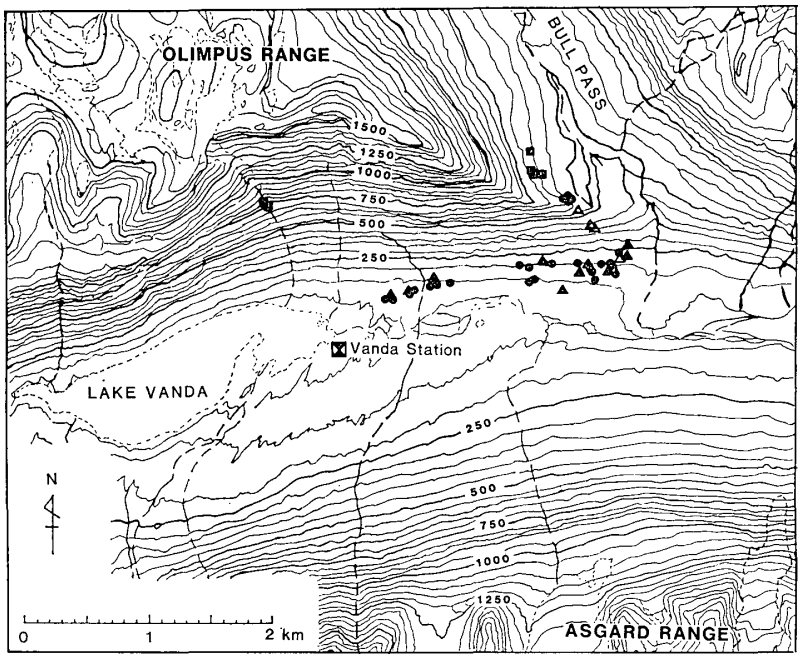

Fig. 4. A topographical map of Wright Valley and sampling sites for basement complex and Ferrar dolerite. Square: Ferrar dolerite, Circle: Granitic rock, Open triangle: "Red dyke", Solid triangle: Lamprophyre and porphyry dykes.

A total of 212 paleomagnetic rock samples from the Cenozoic McMurdo volcanics were collected from Hut Point Peninsula and Cape Royds in Ross Island and from Taylor Valley. The sampling sites in Hut Point Peninsula are illustrated in Fig. 2; they are (1) Fortress Rocks, (2) Observation Hill, (3) Crater Hill, (4) Castle Rock, (5a) north of Hut Point, (5b) near Hut Point, (6) Cape Armitage, (7) site between Cape Armitage and Scott Base, (8) east side of the Gap, (9) Half Moon Crater, (10) Second Crater and (11) Black Knob. At Cape Royds, the samples were collected at two sites; one (12), Cape Royds A, is 300 m northeast of Shackleton Hut, and the other (13), Cape Royds B, is 1000 m north of the Hut. In Taylor Valley, the samples (14) were collected from basaltic cones under the Marr Glacier in the middle of the Valley.

Paleomagnetic sampling of Ferrar dolerite was carried out in Wright Valley, Allan Hills, Carapace Nunatak and Mt. Fleming in the McMurdo Sound region. The sampling sites are shown in Figs. 4, 5 and 6. In Wright Valley, 22 samples were obtained from Bull Pass and 4 from the south slope of the Olympus Range behind Vanda Station. On the samples from Bull Pass, 3 were supplied by Prof. Y. YOSHIDA, Na-

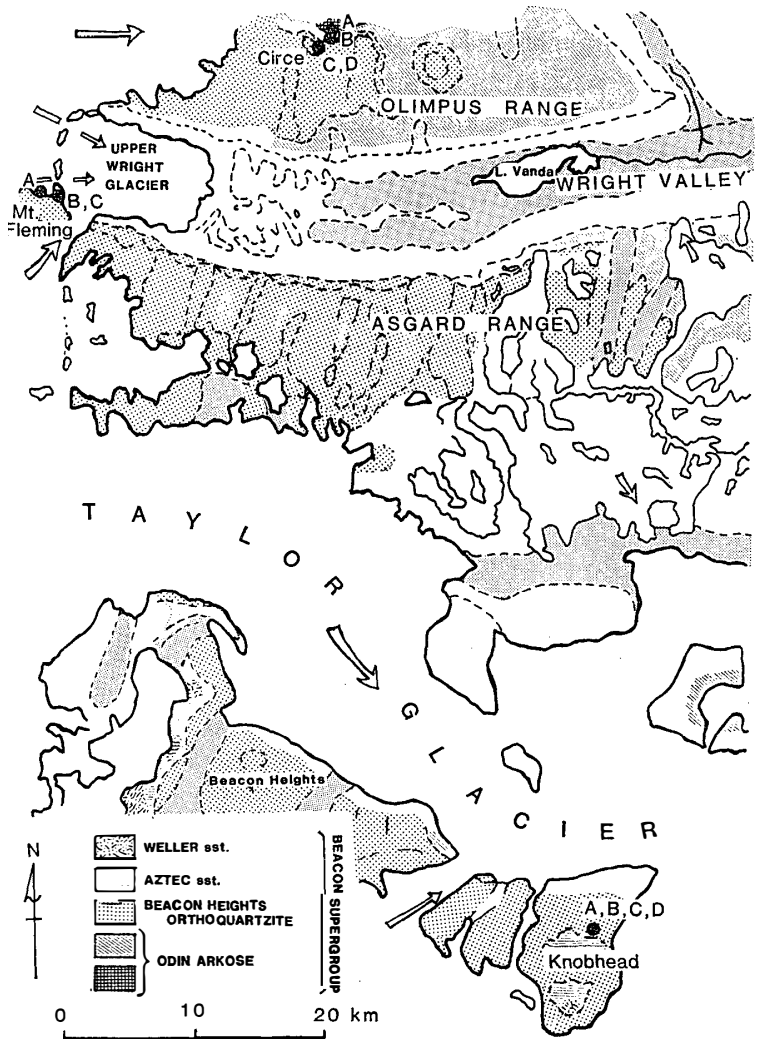

Fig. 5. Geological map and sampling sites of Beacon Supergroup at Dry Valley region.

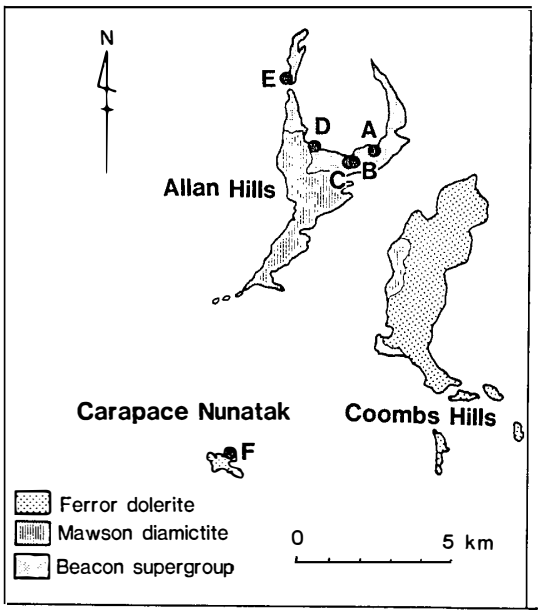

Fig. 6. Geological map of Allan Hills and Carapace Nunatak and sampling sites of Ferrar dolerite (E and F) and Beacon Supergroup (A, B, C and D).

tional Institute of Polar Research, for this study. These sampling sites are identified as the lower boundary of sill "a" as described by McKELVEY and WEBB (1961). In Allan Hills, 19 samples were obtained from 3 different basaltic dykes in the western part of the hills. In Carapace Nunatak, 4 samples were obtained from one site of basaltic body on the north side of the nunatak. On Mt. Fleming, 15 samples were obtained from a dyke on the east ridge.

A total of 216 paleomagnetic samples were collected from the Beacon Supergroup at Mt. Circe, Knobhead, Allan Hills and Mt. Fleming, as shown in Figs. 5 and 6. The sampling sites at Mt. Circe, from lower to higher, are sites A, B, C and D as shown in Fig. 5, and the mutual vertical distances are about 10, 30 and 20 m respectively. Site A is situated 40 m above the upper boundary of a Ferrar dolerite sill of 180 m in thickness, and is located at an altitude of 1500 m. The formation of these sites is identified as Beacon Heights Orthoquartzite (WEBB, 1963). Sampling sites A, B, C and D at Knobhead, with mutual vertical distances of 50, 20 and 20 m respectively from lower to higher, are situated on the north side of that mountain, as shown in Fig. 6. Site A is located at about 2000 m in altitude and probably separated of 140 m above the upper boundary of a dolerite sill. These samples from Knobhead are included in the Aztec siltstone formation (WEBB, 1963). Sampling sites A, B, C and D at Allan Hills, shown in Fig. 6, should be included in the same formation; the altitude is about 2000 m for these sites. Site A is located on the west ridge and sites B and C on the east ridge of the mountain. A dyke of 50–200 cm in thickness, resulting from the Ferrar dolerite sills, invades the Beacon Supergroup at site C, and the samples were collected within 20 m from the dyke. However there is no intrusion of the dyke at sites A and B.

A total of 110 oriented blocks of rocks were collected consisting of Olympus granite, Theseus granodiorite, Vanda lamprophyre, Vanda porphyry and "red dyke" at an altitude of about 200 m above the bottom of Wright Valley, for paleomagnetic investigations. Most of these samples were collected along the north side of the Onyx

River between Vanda Station and the junction of the river and from a valley through Bull Pass. Several samples were obtained from granitic rock of Vida granite 20 m below the lower boundary of sill "a" in Bull Pass. Some of the samples of "red dyke" were collected, 300 m below the lower boundary of sill "a", almost equidistant from the bottom of the valley and the sill boundary. These rocks were collected taking into consideration the distance from the dykes and the sequence of intrusions. These sampling sites are shown in Fig. 4.

4. Equipments and Measurements

A portable engine core drill was designed for paleomagnetic sampling in Antarctic use. It is light in weight, 11 kg; 50% of ethylen-glycole antifreeze liquid is ejected from the installed diamond bit by compressed air to prevent ice formation. The capacity of the engine is 0.8 ps and 7000 rpm; this drill worked at a maximum 1200 rpm below -25°C at 2000 m altitude in Antarctica.

Basic magnetic properties were determined from a magnetic hysteresis loop by means of a vibrating sample magnetometer. At room temperature, saturation magnetization (I_S), saturation remanent magnetization (I_R) and paramagnetic susceptibility (X_p) can be determined from the loop. By use of a special experimental technique to enlarge the abscissa scale for the magnetic field intensity near zero field intensity, the coercive force (H_C) and the remanent coercive force (H_{RC}) were also determined using the same measuring system. The steady applied external magnetic field is from -15 to 15 kOe.

Thermomagnetic (I_S-T) curves were obtained in conditions of atmospheric pressure from 1.1 to 5.3×10^{-2} pa, external magnetic field = 5.0 kOe, and heating and cooling rate = 200°C/h, by use of the vibrating sample magnetometer. The magnetometer can install the cryostat of liquid helium and furnace, and thus I_S-T curves may be obtained from -269 or 30 to 800°C in temperature. The samples for the magnetometer consisted of about 80–100 mg in weight of powder material, and the sensitivity of the magnetic moment was 10^{-4} emu.

The NRM was measured with a spinner magnetometer or a superconducting rock magnetometer. The spinner magnetometer, with two axes of measurement, can detect magnetization from 1×10^{-4} to 5 emu, with measurement error margin of within 1%. The superconducting rock magnetometer consists of three axes of sensor and has 10^{-8} emu sensitivity. As it is difficult to make a nonmagnetic sample holder with less than 10^{-8} emu of remanent magnetization, the moment of magnetization was obtained in the order of more than 1×10^{-7} emu.

The AF demagnetizer consists of a two-axes tumbler and a triple-layers mumetal shield to cancel the effect of the earth's magnetic field. The field intensity in the demagnetizer is less than $100\,\gamma$ at the demagnetizing area. A current of 50 Hz was broadcast by variable transformers for step-by-step AF demagnetization.

The thermal demagnetizer consists of two separate chambers; one furnace for heating the samples and the other for cooling the samples. These chambers are arranged coaxially so that as soon as the samples reach thermal equilibrium in the furnace, the sample carrier can be pushed into the cooling chamber. This demagnetizer has a mumetal shield case to cancel the magnetic field, of three layers for the heating chamber and six layers for the cooling chamber, and the field intensity in the cooling chamber is less than 20 γ.

5. Paleomagnetism of Cenozoic McMurdo Volcanics

5.1. Experimental results

5.1.1. Magnetic hysteresis properties

The magnetic hysteresis properties of typical samples from each site, except (4) Castle Rock, were measured. The values of (I_S), (I_R), (H_C) and (H_{RC}) are summarized in Table 3 together with the intensity of natural remanent magnetization (I_n) and the ratios of I_n/I_S and I_R/I_S.

The ratio of I_n/I_S for all samples ranges from 0.93×10^{-3} to 5.590×10^{-3}, except for (3) Crater Hill, (8) east side of the Gap, (9) Half Moon Crater and (14) Taylor Valley. The ratios for (3) and (9) are as large as 13.113×10^{-3} and 23.798×10^{-3} respectively, whereas those of (8) and (14) are 0.198×10^{-3} and 0.511×10^{-3} respectively. However the ratio of I_R/I_S ranges from 0.088 to 0.332 in all samples. The dispersion of I_R/I_S is much smaller than that of I_n/I_S. Therefore, the intensity of NRM may be classified into three groups, *i.e.* $I_n/I_S>10^{-2}$, $6\times10^{-3}>I_n/I_S>4\times10^{-4}$ and $I_n/I_S<2\times10^{-4}$.

The ranges of H_C and H_{RC} for all samples except (1) Fortress Rocks and (9) are from 95 to 305 Oe and from 123 to 528 Oe respectively. However, H_C values are 30 and 44 Oe and H_{RC} values are 74 and 68 Oe for (1) and (9) respectively. Most pilot samples are likely to have stable remanence, as their ferromagnetic constituents have a single- or pseudosingle-domain structure; but the stability of remanence may be a little worse for (1) and (9), as their ferromagnetic components have a pseudosingle- or multi-domain structure.

5.1.2. Thermomagnetic analysis

The I_S-T curve of pilot samples from each site, except the samples from (4), were measured. Six typical I_S-T curves are shown in Fig. 7. Most of the heating and cooling curves are not exactly identical to each other, which suggests a change in composition during heating. I_S-T curves may be represented by using the sum of ferromagnetic magnetization, antiferromagnetic magnetization and paramagnetic magnetization. All I_S-T curves have a noticeable increase in magnetization below -200°C. The increase in magnetization is due to paramagnetic magnetization of Fe^{2+} in pyroxenes, olivines, ilmenites and other Fe^{2+}-bearing minerals (NAGATA *et al.*, 1972). Experiments have

Table 3. Basic magnetic properties of the Cenozoic volcanics of McMurdo Sound region.

	Sample name	I_n (emu/g)	I_S (emu/g)	I_R (emu/g)	H_C (Oe)	H_{RC} (Oe)	I_n/I_S ($\times 10^{-3}$)	I_R/I_S	Is-T curve		
									Type	Heating (°C)	Cooling (°C)
Hut Point Peninsula	1. Fortress Rock	1.531×10^{-3}	0.79	0.108	30	74	1.938	0.137	1	115	100
	2. Observation Hill	1.340×10^{-3}	1.451	0.26	250	441	0.924	0.179	3	580	555
	3. Crater Hill	5.144×10^{-3}	0.39	0.125	152.5	320	13.113	0.321	4	560, 310	560, 290
	5a. North of Hut Point	6.043×10^{-3}	1.83	0.608	305	487	3.302	0.332	5	570, 40	530, 40
	5b. Near Hut Point	6.988×10^{-3}	1.25	0.285	80.5	270	5.590	0.228	5	540, 120	520, 120
	6. Cape Armitage	2.296×10^{-3}	1.50	0.178	59	243	1.531	0.119	6	475, 130	100
	7. Between Cape Armitage and Scott Base	2.811×10^{-5}	0.017	0.002	78.5	520	1.654	0.106	2	−40, 20	−40, 20
	8. East side of the Gap	1.701×10^{-6}	0.009	0.003	73.5	363	0.189	0.300	2	−25, 100	−25, 100
	9. Half Moon Crater	3.711×10^{-3}	0.156	0.027	44	68	23.789	0.173	4	550, 290	520, 290
	10. Second Crater	3.521×10^{-3}	1.15	0.17	75	152	3.062	0.148	3	510	510
	11. Black Knob	2.121×10^{-3}	0.014	0.004	129	510	1.515	0.286	2	−20, 100	−20, 100
	12. Cape Royds A	1.169×10^{-3}	0.430	0.080	68.5	188	2.719	0.186	5	570, 100	550, 100
	13. Cape Royds B	1.160×10^{-4}	0.295	0.051	66	123	0.393	0.173	5	120, 550	120, 550
	14. Taylor Valley (Normal polarity)	1.581×10^{-3}	2.87	0.49	175	442	0.551	0.171	3	560, 250	540, 130
	Taylor Valley (Reversed polarity)	4.063×10^{-4}	2.12	0.34	128	528	0.192	0.160	5	560, 250	540, 130

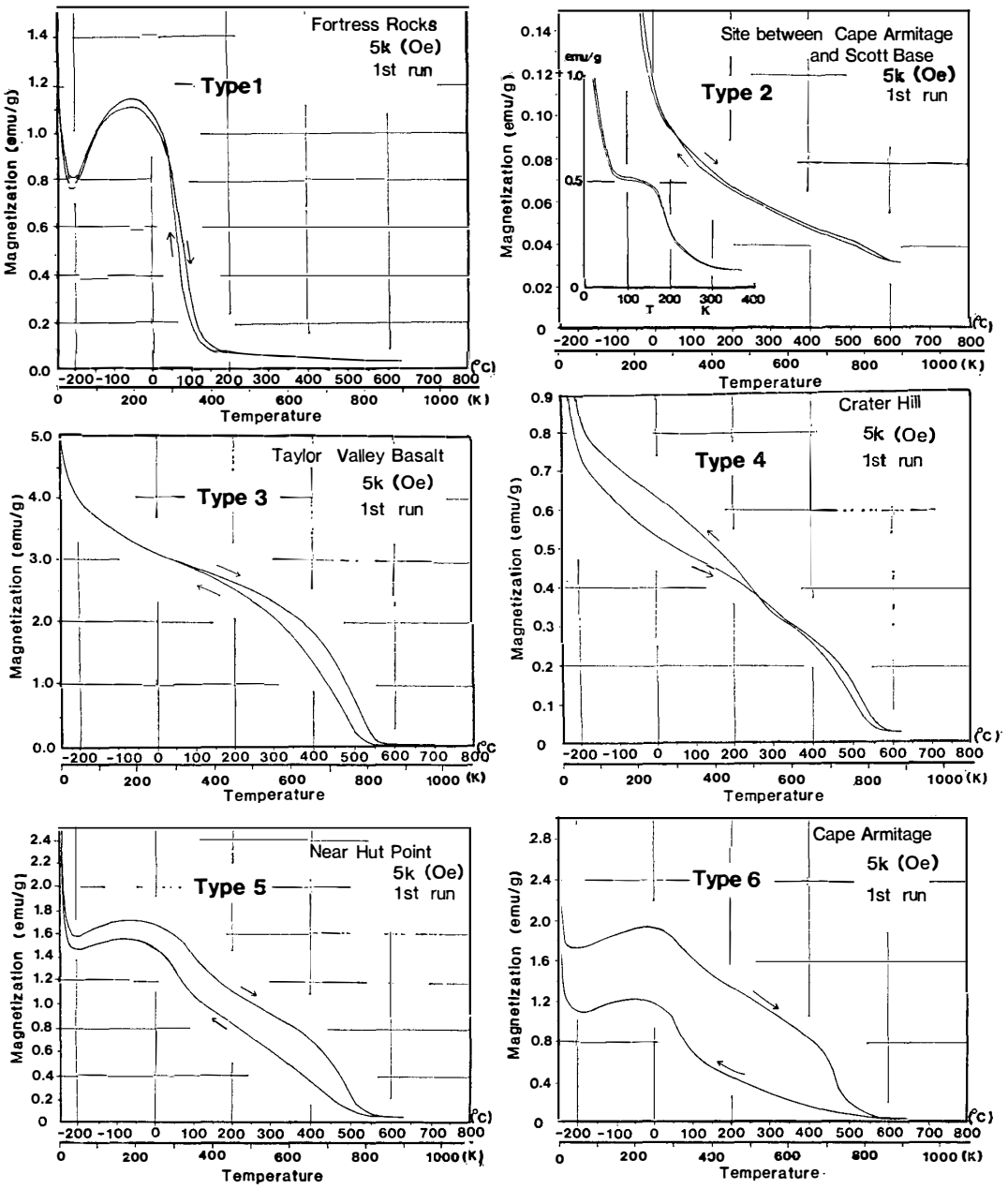

Fig. 7. Typical thermomagnetic curves (I_S-T curves) of six types from the McMurdo volcanics.

been made to try and detect the Néel point of ilmenite ($\theta = 57$ K), if any, but no evidence of the presence of ilmenite has been detected in the I_S-T curves of these samples.

The I_S-T curve can be divided into the following categories based on thermal reversibility: Type 1: Reversible with single Curie point at 115°C. Type 2: Reversible with not well-defined Curie point from 20 to 150°C and one Curie point below 0°C. Type 3: Almost reversible with single Curie point at 570°C. Type 4: Comparatively reversible with two Curie points and increased magnetization after heating. Type 5: Comparatively irreversible with two distinct Curie points and decreased magnetization after heating. Type 6: Irreversible with two distinct Curie points, main Curie point being lowered and magnetization decreasing in cooling curve. The type of I_S-T curve

and Curie points of each pilot sample are listed in Table 3 and typical examples of 6 I_S-T curves are illustrated in Fig. 7. The I_S-T curve from (1) is classified as Type 1. The curve shows a peculiar form, resembling Néel's p-type; magnetization has a peak at about -50°C and decreases from this point. AKIMOTO *et al.* (1957) reported that this remarkable I_S-T curve has a content of $TiFe_2O_4$ of more than 60%. In fact, since the observed Curie point of (1) is at about 115°C, the mol percent of $TiFe_2O_4$ may be estimated at about 70% using the $TiFe_2O_4$-Fe_3O_4 diagram (AKIMOTO *et al.*, 1957). The I_S-T curve of the samples collected from (7) site between Cape Armitage and Scott Base, (8), and (11) Black Knob are classified as Type 2. In this case, no well-defined Curie point is observed in the range from about -40 to 100°C in the heating and cooling curves; titanium-rich titanomagnetites of varying composition are the inferred ferromagnetic minerals. The I_S-T curves of the samples collected from (2) Observation Hill, (10) Second Crater and (14) (normal polarity) are classified as Type 3. The observed distinct Curie point is the only one in the range from 580 to 510°C. The inferred composition of ferromagnetic minerals is almost pure magnetite of constant composition. I_S-T curves of the samples collected from (3) and (9) are classified as Type 4. The I_S-T curve, with an observed Curie point at about 560 and 300°C, is comparatively reversible as a whole. However, it is irreversible under about 300°C, due to magnetization increases in the cooling curve below 300°C. In this case, two kinds of ferromagnetic mineral are inferred, probably almost pure magnetite and titanomagnetite. I_S-T curves of the samples collected from (5a) north of Hut Point, (5b) near Hut Point, (12) Cape Royds A, (13) Cape Royds B and (14) (reversed polarity) are classified as Type 5. The observed Curie point in this type occurs from 570 to 540°C and from 250 to 40°C in the heating curve and from 550 to 530°C and 130 to 40°C in the cooling curve. The main Curie points range from 570–530°C; however, in the case of (13) it occurs at about 120°C with a sub-Curie point at 550°C. The I_S-T curves of samples collected from (5a) and (5b) are very similar to each other. The ferromagnetic minerals in this type may be inferred to be almost pure magnetite and titanomagnetite of constant composition; part of them may change to titanomaghemite or maghemite. The typical irreversible I_S-T curve of a sample collected from (6) Cape Armitage is classified as Type 6. The observed Curie points are from 475 to 570°C in the heating curve and about 100°C in the cooling curve. Since both the Curie point and magnetization decrease clearly in the cooling curve, part of the titanomagnetite may change to titanomaghemite (LARSON *et al.*, 1969).

5.1.3. AF demagnetization of NRM

The pilot samples were demagnetized by step, up to a peak of 500 or 1000 Oe using AF demagnetization. Generally, the AF demagnetization of the intensity of NRM of all pilot samples, except those from (8) and (14), is very stable; usually the decay curve of intensity decreases gradually up to a peak of 500 Oe. Figure 8 shows a representative AF demagnetization curve of stable NRM. The values of the median demagnetization field (MDF) exceed the 200 Oe peak for all pilot samples. These directions of NRM are also very stable showing a peak of at least 500 Oe.

The NRM of matrix samples of palagonitic breccia from (4), originating in depositional remanent magnetization (DRM) or post-depositional remanent magnetization

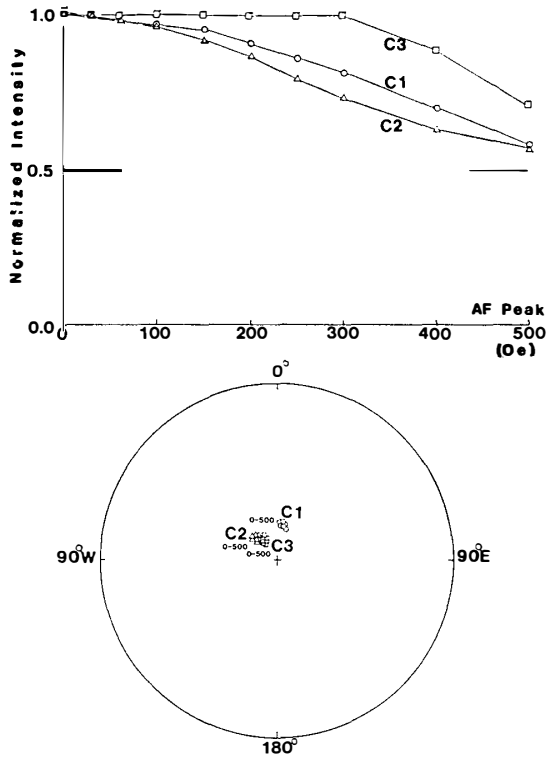

Fig. 8. Representative AF demagnetization curves from Crater Hill.

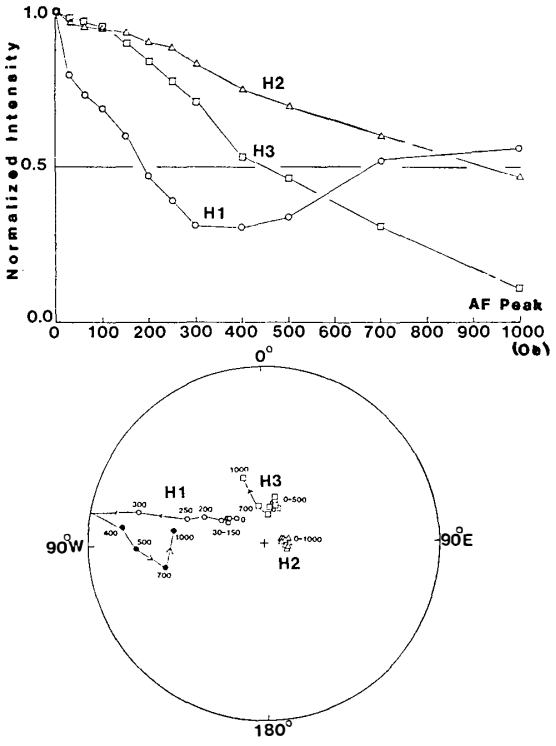

Fig. 9. Representative AF demagnetization curves from east side of the Gap.

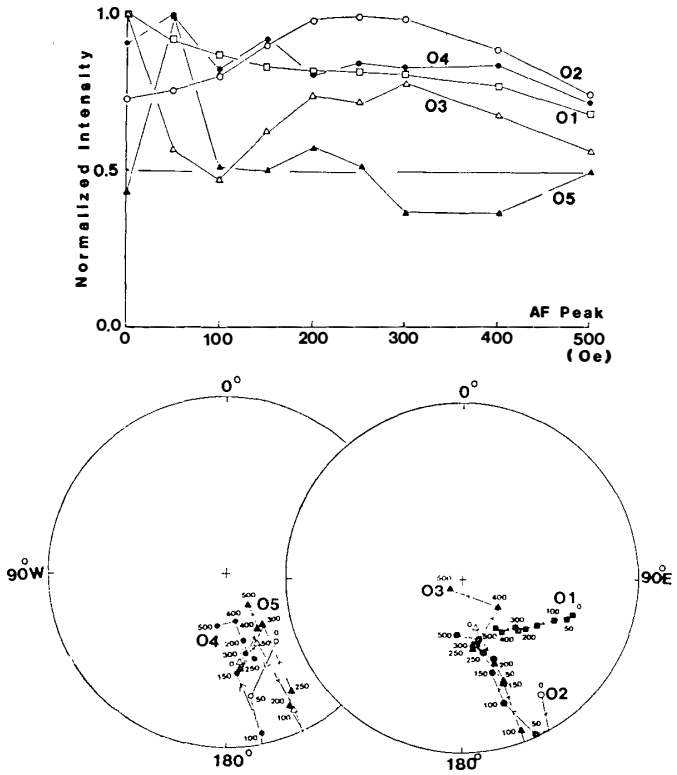

Fig. 10. Representative AF demagnetization curves from Taylor Valley.

(pDRM), is very stable when AF demagnetization of both intensity and direction is applied. On the other hand, one (H1) of the three pilot samples from (8) is unstable against AF demagnetization, as shown in Fig. 9; the intensity decreases gradually up to 350 Oe and then increases up to 1000 Oe. The direction is almost unchanged up to 150 Oe. However, the slope becomes gentle and then positive at 400 Oe. As shown in Fig. 9, the NRM of the other two samples (H2 and H3) are stable up to at least 500 Oe. The AF demagnetization curves of the samples from (14) are shown in Fig. 10. The intensity of the NRM of the reversed magnetized sample (O1) is very stable up to 500 Oe, but the direction of NRM is unstable up to 500 Oe. The NRM of the samples, from magnetized to normal direction, (O2, O3, O4 and O5), appears very unstable both in intensity and direction against AF demagnetization. The direction of NRM shifts from normal to reversed polarity with AF demagnetization. A minimum value is observed in the intensity of the decay curve when the direction is turned towards the horizon by AF demagnetization, and intensity is increased gradually up to 200–300 Oe. It seems that the direction of NRM is clustered into the best grouping when the demagnetizing field is about 350 Oe.

5.1.4. Microscopic observation

All pilot samples were polished for metallic microscopic observation under reflected light. Minerals of ferromagnetic grain and structure are distinguished by color, optical anisotropy and shape of the grains.

The range of diameter of representative magnetic grains in all pilot samples under the microscope is less than 30 μ, and the maximum diameter ranges from 40–300 μ. The main magnetic mineral is identified as hematite for samples from (3) and (9) and as titanomagnetite or magnetite for samples from the other 12 sites excluding (14). In the case of (14), hematite grains and titanomagnetite grains with ilmenite lamellas coexist in reversed samples. However, the main ferromagnetic grains are titanomagnetite in the normal samples. The ilmenite lamellas are shown in Figs. 11 (1) and 11 (2); high temperature oxidation was observed in all titanomagnetite grains in samples from (2) and reversed samples from (14), and in some of the titanomagnetite grains in samples from (5a), (5b) and (10). Titanomaghemite, low temperature oxidation, is observed in some grains in the sample from Cape Armitage, as shown in Fig. 11 (3). In the case of (5a), (5b), (10) and (11) skeletal grains of titanomagnetite of 10–20 μ in length were observed as shown in Fig. 11 (4).

5.1.5. Overall characteristics of magnetic properties

The obtained basic magnetic properties of pilot samples from each site indicate the reliability of NRM. According to the results of AF demagnetization, stable remanence can be removed from NRM by means of an optimum AF demagnetizing field in the case of all samples. Optimum demagnetizing field intensity is estimated at a peak of 350 and 150 Oe for samples of (14) and elsewhere respectively.

Pilot samples of (3) and (9) show a high value of I_n/I_S, I_S-T curve type 2 and mainly hematite magnetic minerals. Saturation magnetization (I_S) of hematite at room temperature is 0.37 emu/g, *i.e.* 1/249, as opposed to that of magnetite. However, the hematite in basaltic samples has a stable and strong NRM. Therefore, the source of

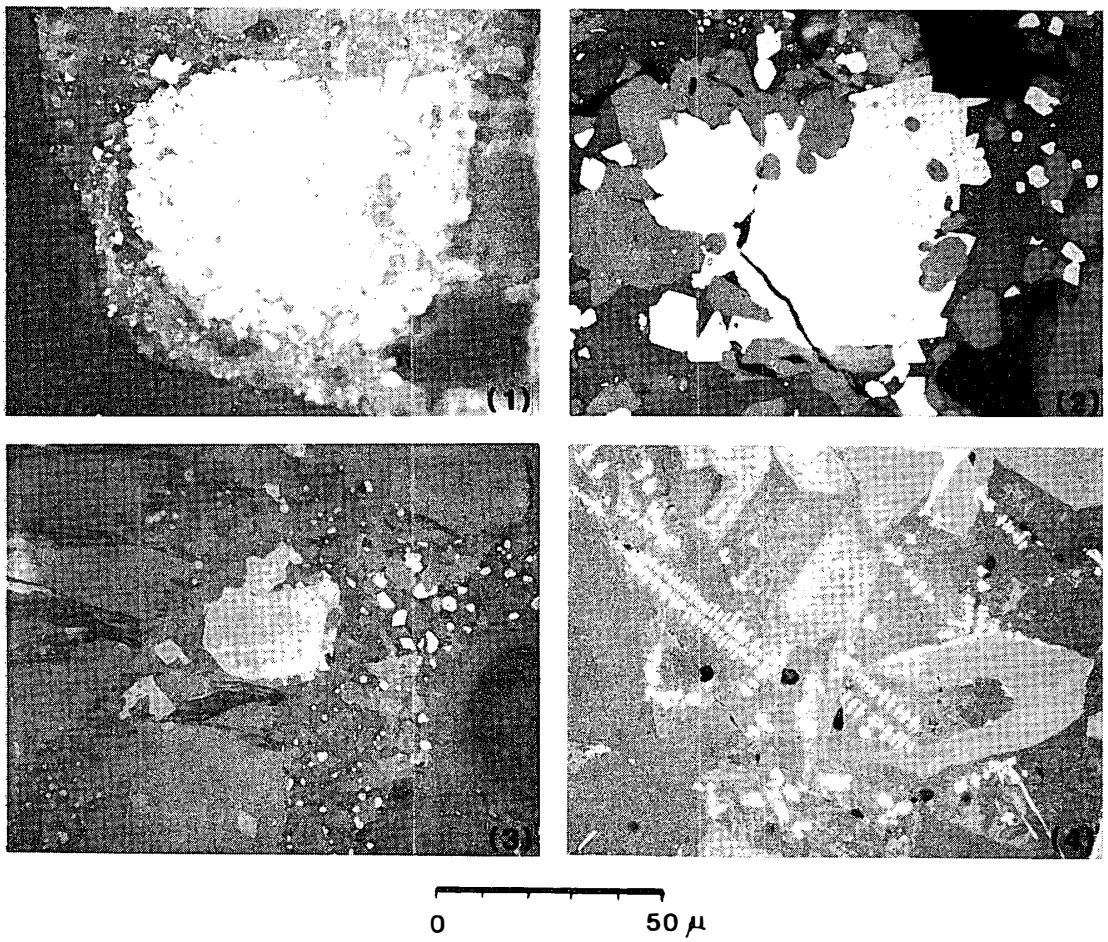

Fig. 11. Photomicrographs of typical magnetic grains in reflected light. (1) Taylor Valley (normal polarity samples), coarse ilmenite lamella. (2) Observation Hill, fine ilmenite lamella. (3) Cape Armitage, titanomaghemite, (4) North of Hut Point, skeletal grain.

NRM with a high I_n/I_S value may be hematite. The existence of hematite in these samples is supported by microscopic observation.

Pilot samples showing type 2 I_S-T curve of (7), (8) and (11) have an NRM intensity of 1.70×10^{-6}–2.81×10^{-5} emu/g. As there is no obvious Curie point above room temperature, these intensities may be weak. As the values of H_C and H_{RC} are 73.5–129 Oe and 363–520 Oe respectively, the NRM of samples of this type is able to have sufficient stability against AF demagnetization.

The existence of titanomaghemite was observed with a microscope in pilot samples of (6). This is consistent with the results of thermomagnetic analysis. In the case of type 5, the deduction of the existence of titanomaghemite from the I_S-T curve is not consistent with the results of microscopical observation. This discrepancy may be due to fine titanomagnetite grains having titanomaghemite, whose structure is difficult to identify with a microscope.

In general, pilot samples with ilmenite lamellas in the major titanomagnetite grains, *i.e.* the samples of (2) and the reversed magnetized sample of (14), have a high value of H_C and H_{RC}, 120–350 Oe and 441–528 Oe respectively. Pilot samples with skeletal

grains, *i.e.* the samples of (5a), (5b), (10) and (11) also have high values of H_C and H_{RC}, namely 75–350 Oe and 152–510 Oe respectively.

Usually skeletal grains are observed in rapidly cooled lava in the sea as pillow basalt. As there is no geological evidence of eruption in the sea at the Hut Point Peninsula, lava with skeletal grains have been formed by rapid cooling by snow or ice.

Since the basic magnetic properties of (5a) and (5b) are very similar and the distance between the two sampling sites is about 200 m in the same volcanic ridge, these lavas may be included in the same lava flow. All pilot samples have a stable component of remanence based on the synthetic basic magnetic properties.

5.2. Paleomagnetic discussion

The NRM of every sample was measured and it was then demagnetized in an optimum AF demagnetization field. As mentioned above, the optimum demagnetizing field intensity was found to be 150 Oe for all samples except those from (14), based on AF demagnetization curves. In the case of samples from (14), a peak of 350 Oe was adopted. Table 4 shows the number of examined specimens (N) collected at the same site, the intensity of NRM (R), the mean inclination (Inc) and declination (Dec) of NRM before AF demagnetization (Demag=0) and after optimum AF demagnetization, for 14 groups. This table shows the estimate of precision (K), the semiangle of the cone of confidence of 95% probability (α_{95}), the paleolatitude (pLat) and the paleolongitude (pLon) of VGP.

In the case of samples from (5a) and (5b), as mentioned above, both lava flows may be the same as the NRM, showing similar magnetic properties and almost the same direction. The sampling site of the lava is referred to as (5), near Scott Hut, in Table 4.

The mean intensity of NRM of these basaltic rocks ranges from 5.21×10^{-4} to 5.93×10^{-3} emu/g for the original NRM and 1.34×10^{-4} to 4.74×10^{-3} emu/g after AF demagnetization with optimum field. In the case of samples from (7), (8) and (11), individual NRM intensity deviated widely from the mean intensity, *i.e.* from 1.87×10^{-2} to 1.70×10^{-6} emu/g despite their coming from the same site. The samples from (2) and (6) were magnetized to the reversed polarity. In the case of samples from (14), the main inclination is normal polarity, although it changes to reversed when AF demagnetization is applied. Samples from the other 11 groups are magnetized to normal polarity.

Obtained Quaternary paleomagnetic data collected from Hut Point Peninsula as summarized in Table 4 will be compared first with the previous data as given in Table 5, where the lava at 250 m north of Scott Base (E) can be considered as practically the same lava as (3), (7) and (8). This paleomagnetic polarity is normal magnetization. The maximum difference in the angle of NRM direction (Θ) between (3), (7) and (8) is $\Theta=10.8°$, and the difference in angle of the NRM direction of (E) from that of (3) is $\Theta=13.0°$. Since these deviation angles are of the same order of magnitude as the α_{95} values of the respective rock specimens, it may be concluded that the mutual agreement of paleomagnetic direction among the four sample groups is reasonably good. The deviation of paleomagnetic direction for Observation Hill is 9.4° between sample (2) in Table 4 and samples from near the Nuclear Power Plant (D) in Table 5. The

Table 4. Paleomagnetic results of McMurdo volcanics.

Sampling site	Demag. (Oe)	N	R (emu/g)	Inc	Dec	K	α_{95}	pLat	pLon
1. Fortress Rock	0	13	3.442×10^{-3}	−84.2°	107.5°	40.3	6.6°		
	150		1.454×10^{-3}	−85.2	118.6	38.8	6.7	71.4°S	139.8°E
2. Observation Hill	0	25	0.969×10^{-4}	84.2	214.1	85.3	3.2		
	150		1.002×10^{-3}	85.0	201.0	106.6	2.8	85.4°S	116.8°E
3. Crater Hill	0	10	2.615×10^{-3}	−77.8	320.9	145.1	4.0		
	150		1.658×10^{-3}	−78.3	322.6	139.2	4.1	75.2°S	79.4°E
4. Castle Rock	0	3	5.210×10^{-4}	−82.3	6.2	362.1	6.6		
(matrix samples)	150		3.530×10^{-4}	−80.3	6.8	925	4.1	83.1°S	5.1°E
5. Near Scott Hut	0	14	5.925×10^{-4}	−72.8	60.6	31.5	7.2		
	150		4.473×10^{-4}	−72.1	58.8	29.8	7.4	61.7°S	64.8°E
6. Cape Armitage	0	1	2.969×10^{-4}	37.3	237.4				
	150		1.516×10^{-4}	76.2	239.6			67.6°S	72.3°E
7. Between Cape Armi-	0	6	4.466×10^{-4}	−77.8	303.1	30.6	12.3		
tage and Scott Base	150		3.736×10^{-4}	−78.2	301.0	34.0	11.7	70.7°S	103.3°W
8. East side of the Gap	0	7	9.428×10^{-4}	−88.0	298.8	25.1	12.3		
	150		2.976×10^{-4}	−88.9	331.7	23.3	12.8	79.8°S	172.7°E
9. Half Moon Crater	0	6	3.534×10^{-3}	−59.5	285.2	131.8	5.9		
	150		1.967×10^{-3}	−60.8	284.5	130.7	5.9	43.7°S	100.0°W
10. Second Crater	0	4	1.906×10^{-3}	−76.8	44.4	228.4	6.1		
	150		6.979×10^{-3}	−77.1	44.9	197.7	6.6	72.0°S	58.4°E
11. Black Knob	0	6	5.253×10^{-4}	−73.4	290.5	49.6	9.6		
	150		1.306×10^{-4}	−73.5	284.1	48.8	9.7	60.1°S	110.3°W
12. Cape Royds A	0	28	1.247×10^{-3}	−85.8	225.0	76.9	3.1		
	150		0.844×10^{-3}	−85.6	234.4	67.9	3.3	71.2°S	171.5°W
13. Cape Royds B	0	48	1.106×10^{-3}	−83.4	84.5	137.7	1.8		
	150		0.549×10^{-3}	−82.8	82.8	160.7	1.6	72.4°S	112.4°E
14. Taylor Valley	0	41	9.594×10^{-4}	−47.9	163.7	2.0	22.7		
	350		8.398×10^{-4}	59.1	158.7	75.8	2.6	51.5°S	43.3°W

Table 5. Previous Cenozoic VGP for Antarctica.

	Sampling site	N	R (emu/cc)	Inc	Dec	K	α_{95}	pLat	pLon	Ref.
A.	North side, Twin Crater	6	6.5	−23°	322°	870	2.3°	21.4°S	53.6°W	1
B.	South end, Second Crater	8	4.0	−80	208	537	2.4	59.3°S	175.5°W	1
C.	South end, Half Moon Crater	1	10.2	−78	61			70.7°S	78.1°E	1
D.	Observation Hill near Nuclear Power Plant	9	2.7	84	319	89	5.5	67.5°S	146.1°E	1
E.	Flows, 250m north of Scott Base	9	5.7	−88	196	1836	1.2	74.0°S	170.7°E	1
F.	Cenozoic volcanics of Cape Hallett (72°S, 171°E)	23		80	208	48	4.2	81°S	94°E	3
G.	Tertiary dykes Marie Byrd Land							62°E	64°E	2
H.	Pleistocene volcanics Marie Byrd Land							78°S	128°W	2
I.	Upper Miocene from Hallett group			83.4	206		11.8	80.5°S	138.9°E	4

References: 1. KYLE and TREVES (1974), 2. SCHARON *et al.* (1969), 3. TURNBULL (1959), 4. DELISLE (1983).

main inclination of the samples from Observation Hill (Inc = −84.2°) is almost the same as the mean value of subsurface samples from the Observation Hill Sequence obtained by DVDP 2 (MCMAHON and SPALL, 1974a, b). The deviation value is Θ=38.7° for (9) and (C) from Half Moon Crater as compared with Tables 4 and 5. Taking into account the α_{95} values, the two paleomagnetic directions of Observation Hill are in reasonably good agreement with each other, but the Θ value of the Half Moon Crater basalt considerably exceeds their α_{95} values in the two tables. Since sample number N=1 for (C) in Table 5, the statistical reliance of the paleomagnetic direction may be considered poor in this case. The lavas from (5a) and (5b), listed together with (5) near Scott Hut in Table 4, have a similar NRM direction with only 7.3° for the Θ value and normal polarity. Their lavas may be considered the same lava group; from the viewpoint of field observation it can be considered the same lava unit. Since the deviation angle Θ between Fortress Rocks (1) and Cape Royds (13) is 11.3°, as the direction deviation angle is not of the same magnitude as the α_{95} values of the respective sampling sites, individual paleomagnetic directions are statistically significant. Therefore, it is considered that the eruptive sequence of the two lava flows is not exactly the same.

The positions of the VGP of the 14 groups of sites as plotted in Fig. 12 are confined to the polar cap area within 30° colatitude. Previous data for the Cenozoic VGP of Antarctica are plotted in Fig. 13. In Figs. 12 and 13, individual VGP positions are clustered in a wide area in the southern hemisphere. In Fig. 12, the latitude of VGP for the samples collected from the north side of the Twin Crater (A) in Table 5 is very

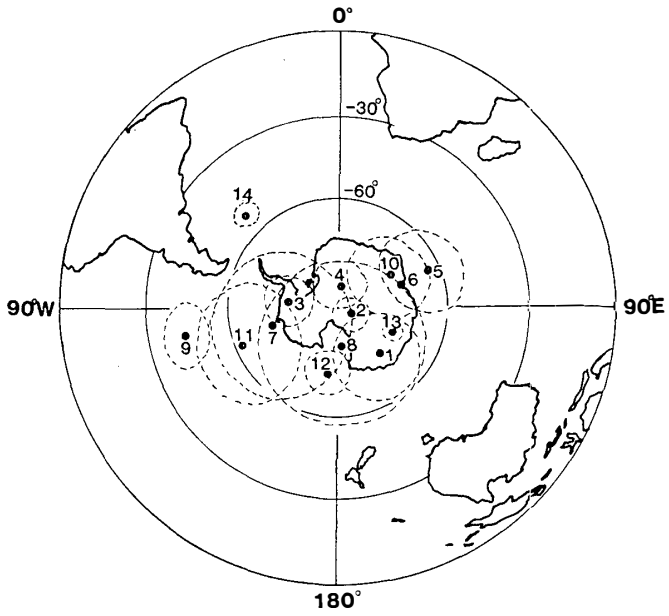

Fig. 12. VGP positions from McMurdo volcanics, equal-area projection. 1. Fortress Rock, 2. Observation Hill, 3. Crater Hill, 4. Castle Rock (matrix), 5. Near Scott Hut, 6. Cape Armitage, 7. Between Cape Armitage and Scott Base, 8. East side of the Gap, 9. Half Moon Crater, 10. Second Crater, 11. Black Knob, 12. Cape Royds A, 13. Cape Royds B, 14. Taylor Valley.

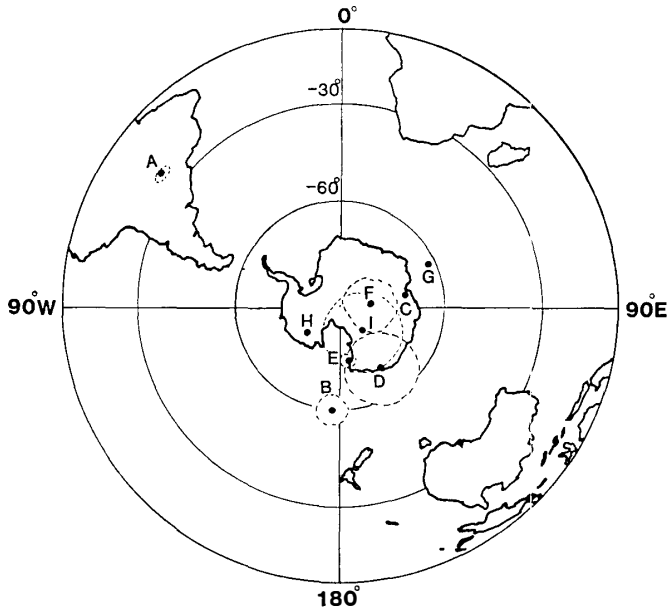

Fig. 13. Previous Cenozoic VGP positions for Antarctica. Equal-area projection. A–E. Hut Point Peninsula (KYLE and TREVES, 1974), A. North side of Twin Crater, B. South end of Second Crater, C. South end of Half Moon Crater, D. Observation Hill, near Nuclear Power Plant, E. Flows of 250 m north from Scott Base, F. Cenozoic volcanics of Cape Hallett (TURNBULL, 1959), G and H. Marie Byrd Land (SCHARON et al., 1969), G. Tertiary, H. Pleistocene volcanics, I. Northern Victoria Land, Hallett group (DELISLE, 1983).

low, $-21.4°$, taking into account of α_{95} value compared with other Cenozoic data for Antarctica. From this viewpoint, the NRM direction is anomalous, and probably represents a certain local geomagnetic anomaly.

McELHINNY and WELLMAN (1969) summarized the polar-wander path in Cenozoic age for the fragments of Gondwanaland and Europe. According to their results, the polar-wander path of between 10 and 15° has occurred since the Eocene period. However the inferred path from the Plio-Pleistocene to the recent age is a few degrees nearby the geographical South Pole. Consequently the influence of the polar-wander path can be neglected for the VGP distributions in the Quaternary age.

VGPs from the Plio-Pleistocene to the Quaternary age in the northern hemisphere are clustered quite clearly around the geographic pole rather than the geomagnetic pole, and the mean of the sixty-seven lies at 88.8°N, 131.9°W with α_{95} of 1.9, which is not significantly different from the geographic pole as defined by MCELHINNY (1973). Almost the same results were obtained for Cenozoic volcanics in New Zealand (GRINDLEY *et al.*, 1977) and Réunion Island (CHAMALAUN, 1968) in the southern hemisphere. From the viewpoint of sea-floor spread, the Australian continent used to be adjacent to the Australian-Antarctic ridge; during the past 43 m.y. the two continents drifted apart to their present positions (LE PICHON and HEIRTZLER, 1968). The distance between the Australian-Antarctic ridge and Antarctica is estimated to be about 2000 km. As mentioned above, the oldest samples in this study may be estimated to be 2.9 m.y. old. If the speed of spread of the Antarctic plate is assumed to be 5 cm/year, the normal speed of sea-floor spread, Antarctica was almost exactly in the present position 2.9 m.y. ago. Therefore, the Quaternary VGP of Antarctica are clustered into the narrow area around the geographical South Pole. The discrepancy between this estimation and the obtained result may be due to the high latitude location of the sampling sites, which gives the result that VGP displacement angles δ_i, showing the angular distance between VGP and the present geomagnetic field, are systematically greater in the southern hemisphere than in the northern one, and in both hemispheres the standard deviation of δ_i averaged over circles of latitude decreases toward the equator (COX and DOELL, 1964). Based on these viewpoints, the distributions of VGP, as shown in Fig. 12 and Fig. 13, do not show exactly the mean VGP positions. However, observed Cenozoic VGP of Antarctica may suggest that the rift area of the geomagnetic field by nondipole field is confined to the polar cap area within a radius of about 30° and the center of the cluster is quite close to the geographical pole.

The historical sequence of lava flow ejections in this area and geomagnetic pole movement will be clarified to a certain extent by synthetically referring to the field evidence of geological and geochronological data of lava and the present paleomagnetic results. The Black Knob lava, which is 0.43 m.y. in K-Ar age and normal in magnetic polarization is probably the youngest volcanic rock in Hut Point Peninsula (WELLMAN, 1964). Lavas from Black Knob, southwest of Black Knob, Fortress Rock, Scott Hut and Second Crater belong to the Twin Crater Sequence, and all these lavas are normally magnetized. The K-Ar age of the lava from the southwest of Black Knob has been determined as 0.57 ± 0.03 m.y. (ARMSTRONG, 1978). The lava of near Scott Hut is under lava of southwest of Black Knob, so that the age of these lavas must be older than 0.57 m.y. The lavas of Fortress Rocks and of Second Crater are older than the Black

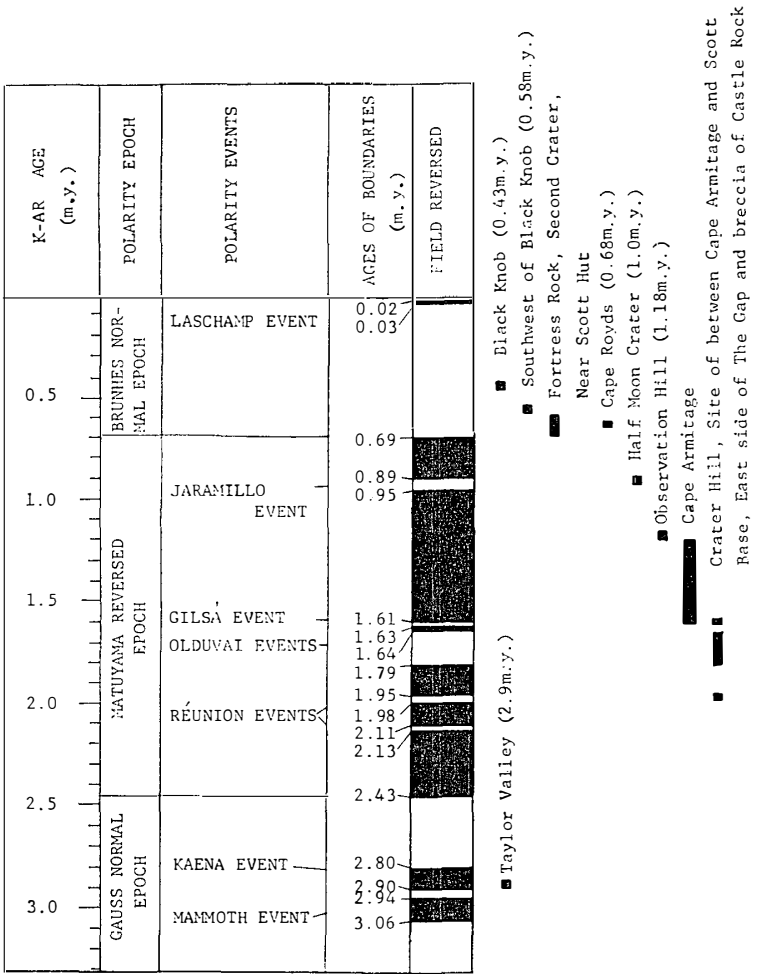

Fig. 14. Eruptive sequence of McMurdo volcanics and world standard paleomagnetic stratigraphy (Cox, 1969).

Knob lavas and are normally magnetized, whence these two lavas are presumed to have flowed out during a period from 0.69 to 0.43 m.y. ago (see Fig. 14). Since the Half Moon Crater lava is 1.0 ± 0.15 m.y. (ARMSTRONG, 1978) in K-Ar age and normally magnetized, it is most likely that the Half Moon Crater volcanic activity took place during the Jaramillo Event, *i.e.* 0.89 to 0.95 m.y. in age (Cox, 1969), as illustrated in Fig. 14. Both the Observation Hill lava and the Cape Armitage lava gave reverse magnetic polarity. As the K-Ar age of the Observation Hill lava is 1.18 ± 0.03 m.y. (FORBES *et al.*, 1974), its magnetic polarity is in accordance with the world standard paleomagnetic data (Cox, 1969) (Fig. 14). Since the trachyte of the Observation Hill intrudes into Cape Armitage lava at a locality between Observation Hill and the Cape Armitage (KYLE and TREVES, 1974), the Cape Armitage lava should be older than Observation Hill lava. The Castle Rock palagonitic breccia consists of numerous fragments of large grain size (5 to 20 cm diameter) and the palagonitic matrix; mainly tuff including small fragments of basalt less than 5 mm in diameter. The matrix of the Castle Rock breccia is systematically magnetized into the normal direction (Table 4), but the direction of NRM of the large basaltic conglomerates is widely dispersed.

The Castle Rock breccia is considered as a subglacial or submarine deposit (KYLE and TREVES, 1974). Thus, the most plausible interpretation of the paleomagnetic result of Castle Rock is that this breccia is a product of the deposition of tuff and basaltic materials during a geomagnetic normal polarity epoch 1.1 m.y. ago, resulting thus in an acquisition of DRM or pDRM in the matrix and random orientation of large size conglomerates which were unable to follow the geomagnetic force. It is most likely, from this viewpoint, that the formation of the Castle Rock breccia took place before the Gilsa Event (1.61 to 1.63 m.y. in age) during normal polarity. The Crater Hill lavas are normally magnetized at the top of the Crater Hill and between Cape Armitage and Scott Base. Since these lavas are overlain by the Observation Hill trachyte (KYLE and TREVES, 1974), they must be older than 1.18 m.y. in age. Thus, the age of formation of the Crater Hill lavas is presumed to be older than the Gilsa Event for the same reason as applied to the Castle Rock breccia. In general, as the construction of the Hut Point Peninsula seems to be earlier than Pliocene, the lower boundary of the Crater Hill Sequence and the Castle Rock Sequence may be 200 m.y.

Since both kenyte lava flows from Cape Royds are magnetized to normal polarity and the estimated age is 0.68 ± 0.14 m.y. (TREVES, 1967), the inferred eruptive sequence is the early Matuyama reversed epoch.

The sampling site of basalt at the Taylor Valley in this study corresponds to the site for age determination by ARMSTRONG (1978). The obtained ages range from 2.87 ± 0.15 to 2.93 ± 0.10 m.y. using the K-Ar method. As the NRM direction after AF demagnetization up to 350 Oe shows reversed polarity, the eruptive sequence of basalt from the Taylor Valley can be assigned to the Kaena Event in the Gauss normal epoch as shown in Fig. 14.

5.3. Concluding remarks

From the synthetic experimental evidence of basic magnetic properties, it is deduced that all samples from the Hut Point Peninsula, Cape Royds and Taylor Valley have a stable component of natural remanent magnetization. The results of paleomagnetic studies of 13 basaltic lavas and one pyroclastic breccia in the McMurdo volcanics since the late Pliocene period are summarized in the VGP distribution chart in Fig. 12 and in the geological history diagram with a geomagnetic polarity scale in Fig. 14. The ellipse confidence for VGP in Fig. 12 suggests that the positions of VGP are confined to the polar cap area within 46° colatitude, and those of 12 groups (excluding the basaltic samples from the Half Moon Crater and the Taylor Valley) are distributed within a polar cap area of 30° in colatitude. The center of distribution of VGP is in almost the same position on the geographical South Pole. It seems, therefore, that Antarctica existed in almost exactly the same position as the present at least by the late Pliocene time. The reason for this distribution of VGP is not continental drift, but is due to the nondipole geomagnetic field. An overall summary of paleomagnetic, geological and geochronological data gives the following time sequence of geologic history in Hut Point Peninsula, Cape Royds and Taylor Valley, from the latest to the earliest; Twin Crater and Cape Royds (Brunhes Epoch), Half Moon Crater (Jaramillo Event), Observation Hill and Cape Armitage (Matuyama Epoch), Crater Hill and Castle Rock (Olduvai or Reunion Events) and Taylor Valley (Kaena Event).

6. Paleomagnetism of Ferrar Dolerite

6.1. Magnetic hysteresis properties

The basic magnetic properties (I_S), (I_R), (H_C) and (H_{RC}) of pilot samples were determined from the hysteresis curve, as shown in Table 6. The intensity of NRM, (I_n) and the ratios (I_n/I_S) and (I_R/I_S) are also listed in the table. For hysteresis analyses, 4 samples were selected from the Wright Valley; A from the south slope of the Olympus Range behind Vanda Station; B, C and D from the Bull Pass; 2 from the Allan Hills and one each from the Carapace Nunatak and Mt. Fleming, based on differences of color and grain size in the rock.

Table 6. Basic magnetic properties of Ferrar dolerite from the McMurdo Sound region.

Sample name	I_S ($\times 10^{-3}$ emu/g)	I_R ($\times 10^{-3}$ emu/g)	H_C (Oe)	H_{RC} (Oe)	I_n (emu/g)	I_n/I_S ($\times 10^{-3}$)	I_R/I_S
Wright Valley A	10	2.0	101	556	6.206×10^{-5}	6.206	0.200
B	41	4.1	72.5	273	2.160×10^{-5}	0.527	0.100
C	7	2.0	63	417	2.162×10^{-5}	3.089	0.286
D	6	1.4	58	326	1.510×10^{-5}	2.517	0.233
Allan Hills A	502	201.0	205	767	5.636×10^{-4}	1.123	0.400
B	1.6	0.26	18.5	526	2.346×10^{-7}	0.147	0.163
Carapace Nunatak	253	11.0	16	102	3.812×10^{-4}	1.507	0.044
Mt. Fleming	15	1.7	313	1273	1.497×10^{-5}	0.998	0.113

In the case of the 3 pilot samples from the Wright Valley, the ratio I_R/I_S was of a similar magnitude, but I_n/I_S showed considerable variation. The values of H_C and H_{RC} suggest that the main magnetic grains in these samples have a single- or pseudosingle-domain structure. In general, fine-grained samples have large H_C and H_{RC} values in comparison with coarse-grained. It may be concluded that the dolerite sill in the Wright Valley is capable of having a stable NRM.

The two pilot samples from the Allan Hills are different from each other in grain size and color. Sample A is fine-grained and dark in color in comparison with sample B. The values of H_C and H_{RC} suggest that the magnetic grains may have a single-domain structure in sample A and a single- or pseudosingle-domain structure in sample B.

The pilot sample from the Carapace Nunatak is the most coarse-grained of all

the pilot samples. The values of H_C and H_{RC} suggest that the magnetic grains have an almost pseudosingle- or multi-domain structure.

The pilot sample from Mt. Fleming shows the finest grain among the pilot samples. As the sample has high values of H_C and H_{RC}, the magnetic grains in this sample probably consist of a single-domain structure and the NRM may be the most stable in this study.

6.2. AF demagnetization

The pilot samples were demagnetized at 50 or 100 Oe steps up to 800 Oe. The number of chosen pilot samples was; one from the Carapace Nunatak, 3 from the Wright Valley and Mt. Fleming and 5 from the Allan Hills. The AF demagnetization curves obtained are shown in Fig. 15. The intensity of NRM of the samples from the Wright Valley was 6.26×10^{-5} to 1.16×10^{-5} emu/g. The intensity of remanence in two of the samples decreased smoothly up to 800 Oe. The median demagnetization field (MDF) of these exceeded 800 Oe. In the case of the remaining sample, the intensity decayed gradually up to 300 Oe, after which there was almost no change up to 800 Oe. The value of MDF was about 250 Oe. The direction of NRM changed within only 3° up to 200 Oe, but showed a large scatter for higher demagnetization steps.

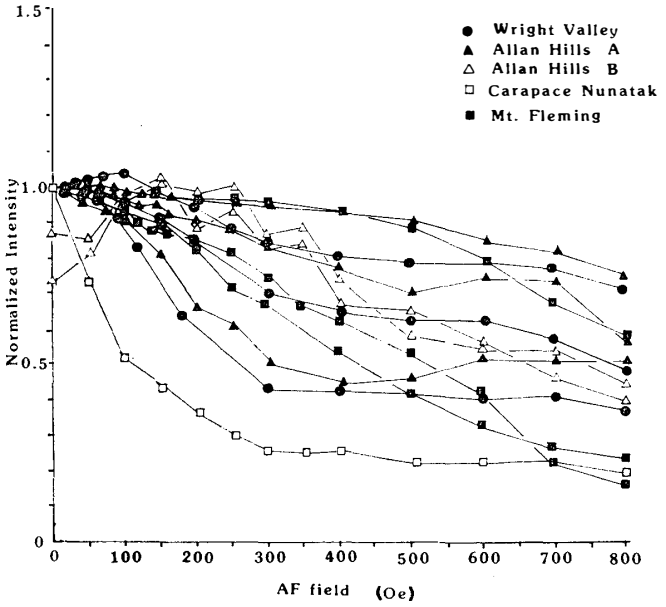

Fig. 15. AF demagnetization curves of NRM for Ferrar dolerite, McMurdo Sound region.

The AF demagnetization curves obtained were 3 and 2, for the samples of Allan Hills A and B respectively. The intensity of NRM before AF demagnetization for sample A was 2.62×10^{-4} to 6.61×10^{-4} emu/g. In general, the NRM of Allan Hills A was demagnetized smoothly up to at least 500 Oe, with MDF values exceeding 300 Oe. The direction of the NRM changed less than 12° in AF demagnetization up to 800 Oe. In the case of Allan Hills B, the intensity of the two pilot samples increased up to 200 Oe and then decreased gradually up to 800 Oe. The direction of NRM for

these samples changed within 6° up to 800 Oe. Their basic intensity was very weak (2.35×10^{-7} and 2.04×10^{-7} emu/g), but the NRM was generally stable against AF demagnetization.

AF demagnetization showed that the sample from the Carapace Nunatak is not as stable as the samples from the Wright Valley and the Allan Hills. The intensity of NRM for these samples was 3.50×10^{-4} emu/g. The intensity decreased rapidly up to 300 Oe with MDF of about 100 Oe, and then gradually decreased up to 800 Oe. The direction of NRM changed by about only 6° in the range from 50 to 500 Oe, but it scattered widely at higher fields.

The intensity of NRM for the 3 samples from Mt. Fleming was 4.74×10^{-6} to 1.21×10^{-5} emu/g. The intensity of NRM decreased smoothly up to 800 Oe and the MDF exceeded 400 Oe. As the directional change was within 5° up to 800 Oe, the NRM was very stable against AF demagnetization.

6.3. Thermal demagnetization

Pilot samples from the Wright Valley, Allan Hills A and Mt. Fleming were thermal demagnetized in steps up to 600°C. The representative thermal demagnetization curves obtained are shown in Fig. 16.

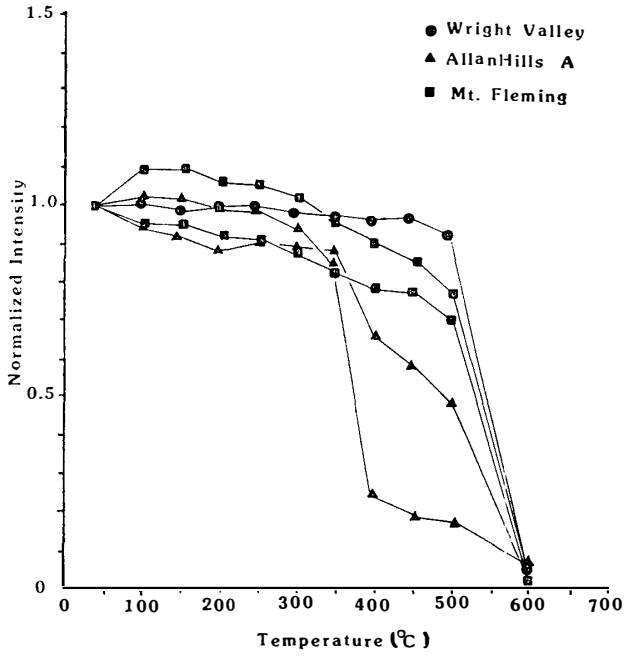

Fig. 16. Thermal demagnetization curves of NRM for Ferrar dolerite from McMurdo Sound region.

The intensity of remanence of the 3 samples from the Wright Valley was different to a factor of two, although the normalized decay curves were very similar to each other; no decrease of intensity up to 500°C, and a steep decrease in the range 500–600°C. The directional remanence was very stable against thermal demagnetization; directional changes were less than 10° up to 500°C, but at 600°C the directions were random and there was no recognizable trace of fossil remanence.

The thermal demagnetization curves of the 3 samples from Allan Hills A showed a large change of intensity up to 400°C. The intensity in one sample decreased steeply between 350 and 400°C and thereafter the decrease became more gradual. In the other two, the intensity decreased gradually between 350 and 600°C; a small blocking component was found between 350 and 400°C. The direction change in the 3 samples was limited to a few degrees within the range 30–500°C.

The NRM of the 3 samples from Mt. Fleming decayed smoothly up to 500°C, although a slight initial increase was observed in one sample between room temperature and 100°C; the intensity decreased steeply in the range 500–600°C. The direction of NRM clustered within 6° against thermal demagnetization up to 500°C. Residual remanences at 600°C were almost zero and the directions scattered widely from the cluster.

Thermal decay curves from these 3 sites (Wright Valley, Allan Hills and Mt. Fleming) clearly show well-defined blocking temperatures. The blocking temperature of the Wright Valley and Mt. Fleming samples exceeds 500°C and there is no recognizable trace of fossil remanence at 600°C. Therefore, it seems that the main magnetic minerals are almost pure magnetite. Since the decay curves of the samples from the Allan Hills show two temperatures, 350–400°C and 500–600°C, the coexistence of titanomagnetite and almost pure magnetite may be inferred in these samples.

6.4. Thermomagnetic curves and microscopic analyses

A typical first run I_S-T curve for the Wright Valley is illustrated in Fig. 17a. The I_S-T curves of the 4 pilot samples are essentially the same; the Curie points are 330 and 543°C in the heating curve and 540°C in the cooling curve. The Curie point at 330°C in the heating curve disappears in the cooling curve, although the I_S-T curve is otherwise reversible. The second run I_S-T curve of this sample is exactly the same as the first run cooling curve. Microscopic observations suggest that the main magnetic minerals are magnetite of 20–100 μ in diameter and sulfide 10–40 μ in diameter. A minor quantity of hematite grains were also observed around small holes and cracks. As the thermal demagnetization of NRM of the samples from the Wright Valley shows a single blocking temperature higher than 500°C (Fig. 16), the carrier of the NRM can be identified as magnetite with a Curie point at 543°C.

The I_S-T curves of Allan Hills A are shown in Fig. 17b. The 1st run (temperature up to 600°C) was reversible, while the 2nd run (to 750°C) was irreversible. A single Curie point at 565°C was observed in both heating and cooling of the 1st and 2nd runs. Since the intensity decreases by about 13% after heating while the Curie point remains unchanged, part of the magnetite grains may have been oxidized to hematite. Consequently, the I_S-T curve becomes irreversible when the sample is heated up to 750°C. The magnetic grains in this pilot sample are titanomagnetite, 40–150 μ in diameter. Almost all of these grains are cut by ilmenite lamellas, indicating that they were oxidized at high temperature. Therefore, the sample has a high coercive force of $H_C =$ 250 Oe in spite of the large grain size and a high Curie point of 565°C. The I_S-T curves for Allan Hills B could not be obtained because of the weak saturation moment of $I_S = 1.6 \times 10^{-3}$ emu/g; there were almost no opaque minerals in this sample when examined under a microscope.

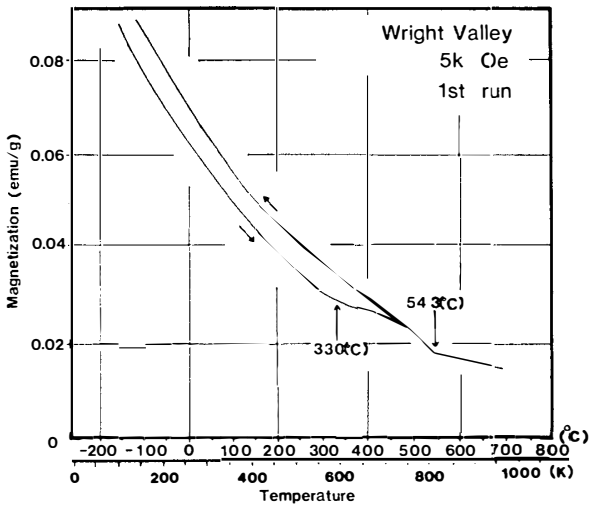

Fig. 17a. A thermomagnetic curve of Ferrar dolerite from Wright Valley.

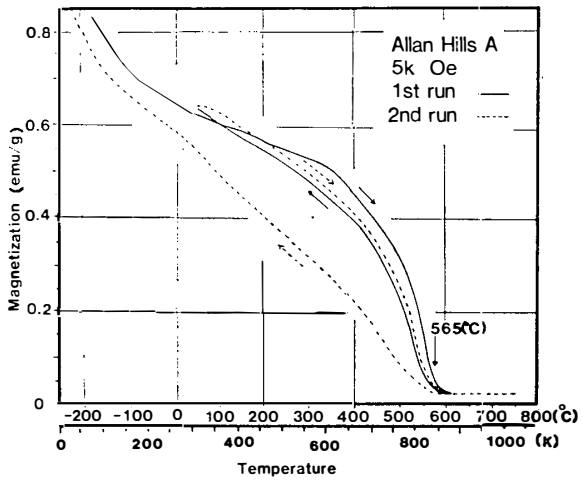

Fig. 17b. Thermomagnetic curves of Ferrar dolerite (dyke, Allan Hills A) from Allan Hills.

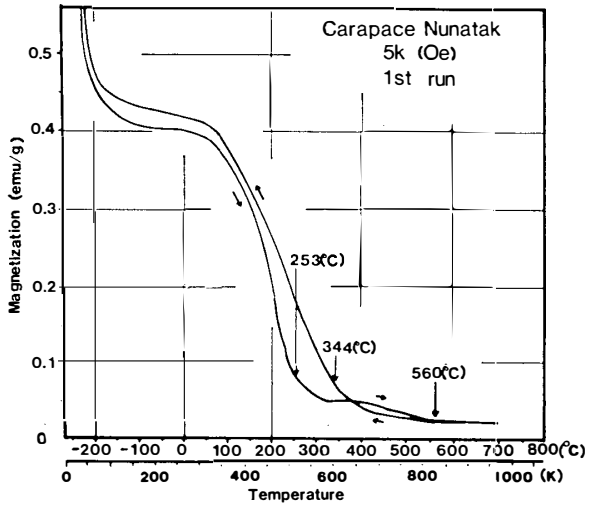

Fig. 17c. A thermomagnetic curve for Ferrar dolerite (basaltic rock) from Carapace Nunatak.

The I_S-T curve of the Carapace Nunatak, illustrated in Fig. 17c, is irreversible. Curie points were observed at 253 and 560°C in the heating curve, and 560 and 344°C in the cooling curve. In the I_S-T curve, a noticeable increase of magnetization may be observed at temperatures below −200°C. This may be due to the paramagnetic component (NAGATA *et al.*, 1972). The main Curie point at 253°C moved to 344°C, and the intensity increased by about 8% compared with the initial value on heating. It is possible that the titanomagnetite grains underwent low temperature oxidation (titanomaghemite). If this is the case, the Curie points of 250, 344 and 560°C may be identified as those of titanomaghemite, titanomagnetite and magnetite respectively. However, titanomaghemites were not observed under the microscope. The diameter of the titanomagnetite grains ranged between 80 and 250 μ.

The I_S-T curve of Mt. Fleming is essentially the same as that of the Wright Valley. Curie points were observed at 364 and 570°C in the heating curve and 570°C in the cooling curve. The intensity increased by about 26% after heating, as compared with the initial value. The result of thermal demagnetization showed that about 80% of the NRM still remained at 500°C and then decreased steeply. Therefore, the carrier of the NRM must be mainly magnetite with a Curie point of 575°C. Actually a small amount of magnetite, at most 8 μ in diameter, was observed under the microscope. The transition point at 364°C may indicate the beginning of the dissolution of pyrrhotite; fine-grained pyrrhotite was observed under the microscope.

6.5. Paleomagnetic discussion

The NRM of 64 samples was measured, and these samples were then demagnetized up to 150 Oe to detect stable remanence. The average NRM data from each site together with previous data are listed in Table 7 with calculated VGP position. Table 7 shows the mean intensity of the NRM (In), and the mean inclination (Inc) and declination (Dec) of the NRM before (Demag=0) and after optimum AF demagnetization (Demag=150) for the 4 groups.

Deviation of individual intensity was within 15% of the mean value at each site in the Wright Valley, the Carapace Nunatak and Mt. Fleming. However, it was about 250% for the samples from the Allan Hills; intensities for sites A and B were 43.37×10^{-5} and 0.17×10^{-5} emu/g respectively. The rate of NRM decay by AF demagnetization up to 150 Oe was less than 12% for the samples from the Wright Valley, the Allan Hills and Mt. Fleming, but it was 72% for samples from the Carapace Nunatak. Every sample was magnetized in the normal direction (upward). After AF demagnetization up to 150 Oe, the K value and the α_{95} gave reasonably good values for the Wright Valley (K=136, $\alpha_{95}=2.4°$), the Allan Hills (K=44.0, $\alpha_{95}=5.1°$), the Carapace Nunatak (K=74.1, $\alpha_{95}=10.5°$) and Mt. Fleming (K=1466, $\alpha_{95}=1.0°$).

Since the samples from the Carapace Nunatak have low coercive force as $H_C=16$ Oe, unstable NRM against AF demagnetization and a low main Curie point, it seems that they are unable to have stable NRM; magnetic grains in these samples are of a pseudosingle- or multi-domain structure. Consequently, the α_{95} value would be larger than others. On the other hand, the samples from the Wright Valley, the Allan Hills and Mt. Fleming have high H_C values, NRM blocking temperature and Curie points. Therefore, their NRM are fairly stable and the carrier of NRMs would be of a single-

Table 7. Paleomagnetic results of Ferrar dolerite in Antarctica.

Sampling site	N	Demag. (Oe)	$R \times 10^{-5}$ (emu/g)	Inc	Dec	K	α_{95}	pLat (°S)	pLon (°W)
1. Wright Valley	26	0	4.04	−69.0°	237.4°	19.5	6.5°		
		150	3.72	−69.4	237.6	136	2.4	45.3	152.0
2. Allan Hills A	14	0	43.37	−66.6	263.9	40.6	6.3		
		150	38.38	−64.2	259.7	42.9	6.1	42.2	133.8
Allan Hills B	5	0	0.17	−73.2	272.5	73.7	9.0		
		150	0.14	−76.2	277.5	463	3.6	62.5	130.1
Total	19	0	32.0	−68.4	265.7	44.7	5.1		
		150	28.31	−67.6	262.6	44.0	5.1	47.0	133.2
3. Carapace Nunatak	4	0	26.38	−76.2	207.0	56.8	12.3		
		150	7.48	−67.7	226.7	74.1	10.7	40.9	163.4
4. Mt. Fleming	15	0	1.30	−81.0	275.1	1100	1.2		
		150	1.43	−80.5	274.4	1466	1.0	68.6	139.5
5. Theron Mountains	8			−68	64		12	54	136
6. Ferrar Glacier	57			−76	255	52	2.7	58	142
7. Wright and Victoria Valleys	92			−68	250	1877	3	45	140
8. Beardmor Glacier	13			−75	244	18	11	59	139
9a. Dufek Intrusion								60	137
9b. Dufek Intrusion	91			−69	53	12.4	4.5	56.5	168.0
10. Queen Maud Land	32			−52.0	50.9	46.6	3.8	41.8	133.5
11. Southern Victoria Land								54.9	138.0

1–4. This study, 5. BLUNDELL and STEPHENSON (1959), 6. TURNBULL (1959), 7. BULL *et al.* (1962), 8. BRIDEN and OLIVER (1963), 9a. BURMESTER and SHERIFF (1980), 9b. BECK (1972), 10. LØVLIE (1979), 11. KYLE *et al.* (1983).

or pseudosingle-domain structure. From these viewpoints, the VGP data of the Carapace Nunatak can be discarded for this paleomagnetic discussion, and the data of others show significant pole positions of Jurassic time.

The maximum difference in the angles of the mean NRM directions among those 3 sampling sites was 14.1° (between Mt. Fleming and Wright Valley). Even if the previous data are included, the maximum deviation of NRM directions remains the same. In the case of the Wright Valley, the same sampling site was also used in a study by BULL *et al.* (1962). The difference in the angle of mean NRMs is only 4.7° between their value (Inc = −68°, Dec = 250° and α_{95} = 3°) and our value (Inc = −69.4°, Dec = 237.6° and α_{95} = 2.4°). Since this deviation angle is of the same order of magnitude as the α_{95} value of the respective samples, it may be concluded that the mutual agreement of paleomagnetic direction between the two studies is satisfactory.

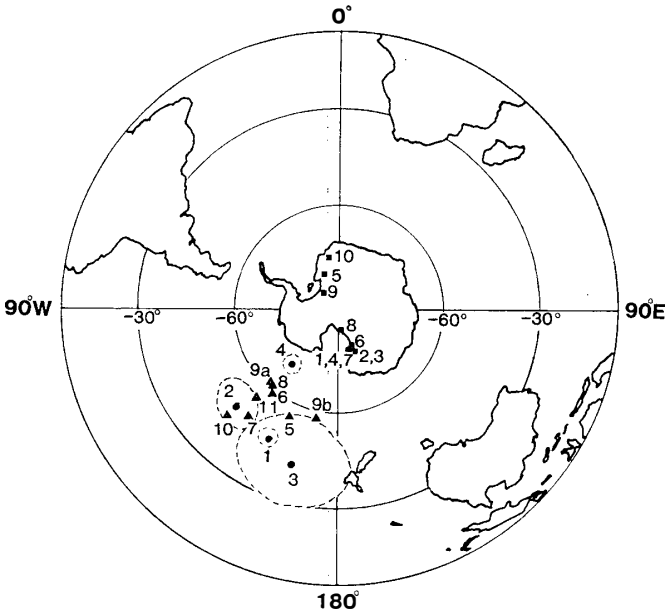

Fig. 18. VGP positions of Jurassic rocks (Ferrar dolerite) for Antarctica (Circle: This study, Triangle: Previous studies) and the corresponding sampling localities along the Transantarctic Mountains (squares). 1. Wright Valley, 2. Allan Hills, 3. Carapace Nunatak, 4. Mt. Fleming, 5. Theron Mountains (BLUNDELL and STEPHENSON, 1959), 6. Ferrar Glacier (TURNBULL, 1959), 7. Wright and Victoria Valleys (BULL and IRVING, 1960), 8. Beardmore Glacier (BRIDEN and OLIVER, 1963), 9a. Dufek Intrusion (BECK, 1972), 9b. (BURMESTER and SHERIFF, 1980), 10. Queen Maud Land (LØVLIE, 1979), 11. Victoria Land (KYLE et al., 1983).

The VGP positions obtained and the circle of 95% confidence from the 4 sites are illustrated in Fig. 18 in addition to the previous Jurassic paleomagnetic poles for East Antarctica. The center of these 10 VGPs, excluding that of the Carapace Nunatak, is located at 53.9°S and 141.8°W and the confidence of radius of 95% circle is 6.3°.

6.6. Concluding remarks

The conclusions to be drawn from the present analysis may be summarized as follows: The samples from the Wright Valley, the Allan Hills and the Mt. Fleming

have a stable NRM representing the magnetic field at the time of the intrusion of Ferrar dolerite. The stability of the NRM was inferred from the results of hysteresis analyses, AF demagnetization and thermal demagnetization. On the other hand, the samples from the Carapace Nunatak may have both a hard and a soft component of NRM. The main magnetic minerals consist of almost pure magnetite in samples from the Wright Valley, the Allan Hills A and the Mt. Fleming, and titanomagnetite in samples from the Carapace Nunatak.

The obtained virtual geomagnetic pole positions in the Jurassic age are 45.3°S, 152.0°W, 47.0°S, 133.2°W and 68.6°S, 139.5°W for the Wright Valley, the Allan Hills and Mt. Fleming respectively. The center of these VGP positions, including the previous Jurassic data in Antarctica, is located on the South Pacific Ocean at 53.9°S, 141.8°W at present.

7. Paleomagnetism of Beacon Supergroup

7.1. Experimental technique

The NRM of rock specimens may be divided into several kinds of magnetization, such as thermal remanent magnetization (TRM), depositional remanent magnetization (DRM), isothermal remanent magnetization (IRM) and viscous remanent magnetization (VRM). These magnetizations are different not only in the mechanism of acquisition but also in their stability against demagnetization. In general, TRM and DRM are very stable (hard) as compared to IRM and VRM (soft). It is possible that the Beacon Supergroup in McMurdo Sound has TRM and the magnetic soft component, besides DRM. We have therefore defined these magnetizations as follows: The soft component is removed from the samples by AF demagnetization in a relatively weak alternating field. The NRM intensity of sediment is considerably weaker as compared to that of igneous rock, ranging from 10^{-7} to 10^{-4} emu/g (*i.e.* NAGATA, 1961). Consequent comparison of the intensities of the stable component of NRM and acquired TRM in the laboratory would suggest the NRM magnetization method. However, this method may result in chemical alteration during heating. Therefore anhysteresis remanent magnetization (ARM) was adopted as a substitute for TRM in this study. ARM has characteristics quite similar to those of TRM, including proportionality with a weak steady magnetic field and magnitude of partial ARM (PATTON and FITCH, 1962), however the low field susceptibility of ARM has a magnetic grain size dependence as suggested by LEVI and MERRILL (1976). Thus, it may be possible to determine the origin of NRM by means of synthesized results from ARM acquisition, AF demagnetization of NRM and ARM, thermal demagnetization of NRM and TRM acquisition properties.

A total of 6 typical samples were selected from each sampling site to examine their NRM characteristics; 3 samples to test AF demagnetization of NRM and another 3 to test thermal demagnetization of NRM. The samples which were used to test AF demagnetization of NRM were examined for ARM acquisition and the effects of AF demagnetization of ARM, and the samples which were used to test thermal demagnetization of NRM were examined for TRM acquisition.

As NRMs of samples of the Beacon Supergroup are fairly weak, a superconducting rock magnetometer was used. In the case of the thermal demagnetizer, the magne-

tic field intensity is less than 20 γ. The applied alternating field ($\tilde{H}$) for AF demagnetization and ARM acquisition is up to 1000 Oe, and the maximum temperature is 600°C for thermal demagnetization and TRM acquisition. The steady magnetic field ($\bar{h}$) is 0.42 Oe for ARM and TRM acquisition and the direction is parallel to $\tilde{H}$.

7.2. Experimental results

The curves obtained for AF demagnetization of NRM and ARM, and ARM

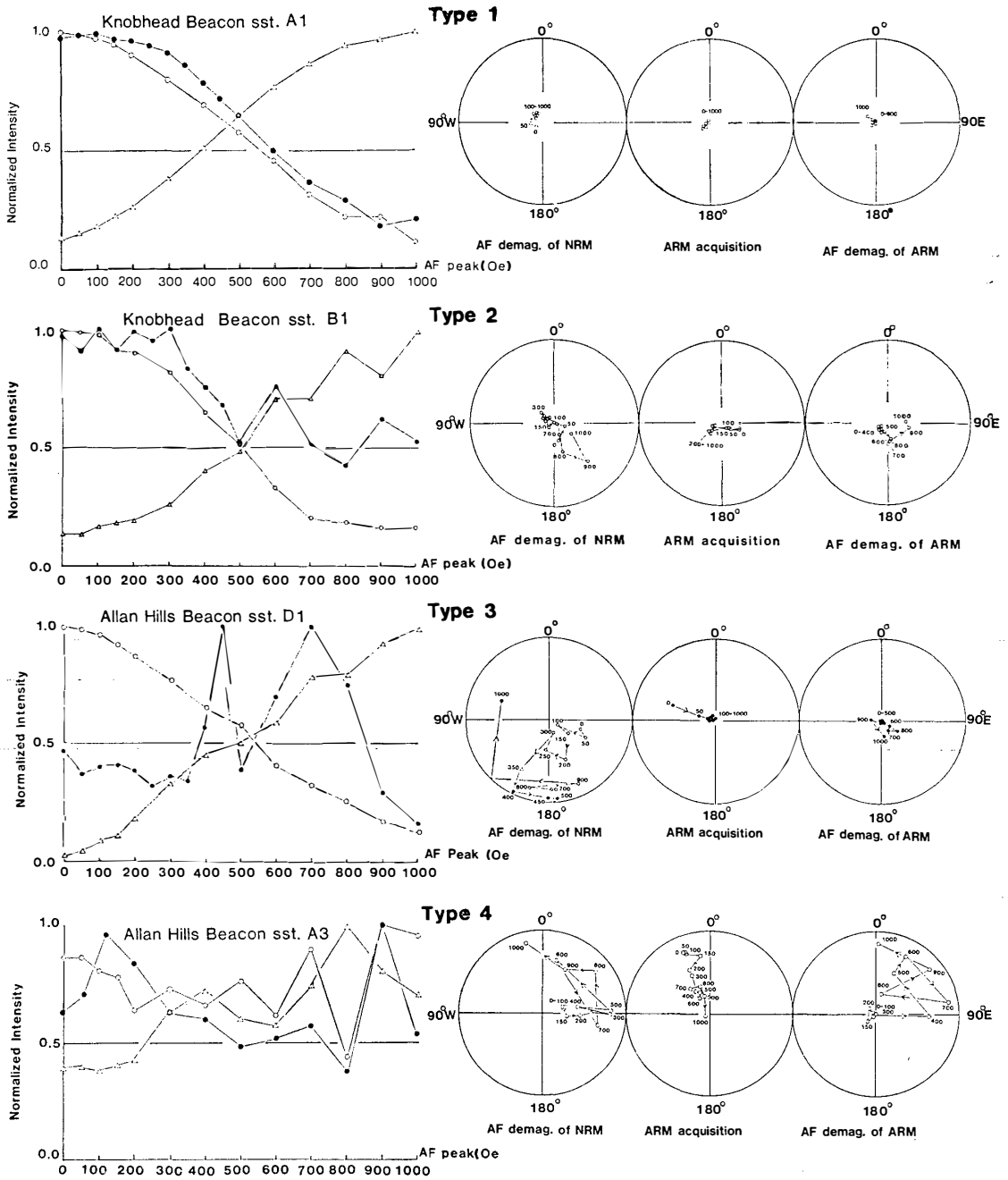

Fig. 19. Typical 4 AF demagnetization groups for Beacon Supergroup (sandstone) in McMurdo Sound region. Solid circles: AF demagnetization curve of NRM. Triangle: ARM acquisition curve. Open circle: AF demagnetization curve of ARM.

acquisition for the 3 representative samples from each respective site were divided into the following categories, as shown in Fig. 19. Type 1: NRM intensity and direction is fairly stable against AF demagnetization up to 1000 Oe. The ARM acquisition curve shows a smooth increase and no saturation up to the maximum field. AF demagnetization of ARM is fairly similar to that of NRM. Thus, the inferred magnetic grains probably have a single domain structure. Type 2: Stable NRM is observed up to approximately 500 Oe but is destroyed in higher fields, ARM acquisition is smooth up to approximately 500 Oe but increases in a zigzag above that field. The AF demagnetization curves of ARM are essentially the same as that of NRM. Type 3: The direction and inclination of NRM are quite unstable against AF demagnetization. However ARM acquisition and AF demagnetization of ARM are fairly stable up to at least 500 Oe. That is, samples of this type are able to have a stable ARM, but the NRM is unstable. Type 4: Both NRM and ARM are fairly unstable up to 1000 Oe against AF demagnetization except when in a weak field. The ARM acquisition curve is also a zigzag on the whole. That is, stable remanent magnetization is impossible. A multi-domain structure for the magnetic grains is inferred. Three representative samples collected from the same site were classified as essentially of the same type, although some may be included in the neighboring type. The types for each site are listed in Table 8 together with the mean NRM and ARM intensities and the NRM/ARM ratios.

Three samples were also selected from each site for step-by-step thermal demagnetization and TRM acquisition. The results of these experiments are classified into

Table 8. Mean intensities of NRM and ARM ($\tilde{H}$=1000 Oe, $\bar{h}$=0.42 Oe, $\bar{h}//\tilde{H}$), and classified types at room temperature of Beacon Supergroup in McMurdo Sound.

Sampling site		NRM (emu/g)	ARM $\bar{h}//\tilde{H}$ (emu/g)	ARM/NRM	Type	
					AF demag. group	Thermal demag. group
Mt. Circe	A	3.28×10^{-6}	9.50×10^{-6}	2.89	1	1
	B	9.03×10^{-7}	1.37×10^{-6}	1.52	1	1
	C	9.41×10^{-6}	9.12×10^{-6}	0.97	1	1
	D	1.42×10^{-6}	3.29×10^{-6}	2.31	1	1
Knobhead	A	1.05×10^{-6}	1.57×10^{-6}	1.50	1	1
	B	3.568×10^{-7}	1.25×10^{-6}	3.51	2	2
	C	7.07×10^{-8}	3.51×10^{-7}	4.96	3, 4	3
	D	1.63×10^{-7}	4.54×10^{-7}	2.78	2, 3	2, 3
Allan Hills	A	6.71×10^{-8}	1.26×10^{-7}	1.88	3	3
	B	9.84×10^{-8}	1.64×10^{-7}	1.67	3, 4	3
	C	3.48×10^{-7}	2.82×10^{-6}	8.11	1, 2	2
	D	3.66×10^{-8}	4.10×10^{-7}	10.97	3	3
Mt. Fleming	A	1.64×10^{-7}	2.75×10^{-7}	1.67	3, 4	3
	B	3.56×10^{-8}	1.85×10^{-7}	5.21	3	3
	C	1.071×10^{-7}	1.49×10^{-7}	1.40	2	2, 3

AF demag. group: AF demagnetization of NRM and ARM, and ARM acquisition.
Thermal demag. group: Thermal demagnetization of NRM and TRM acquisition.

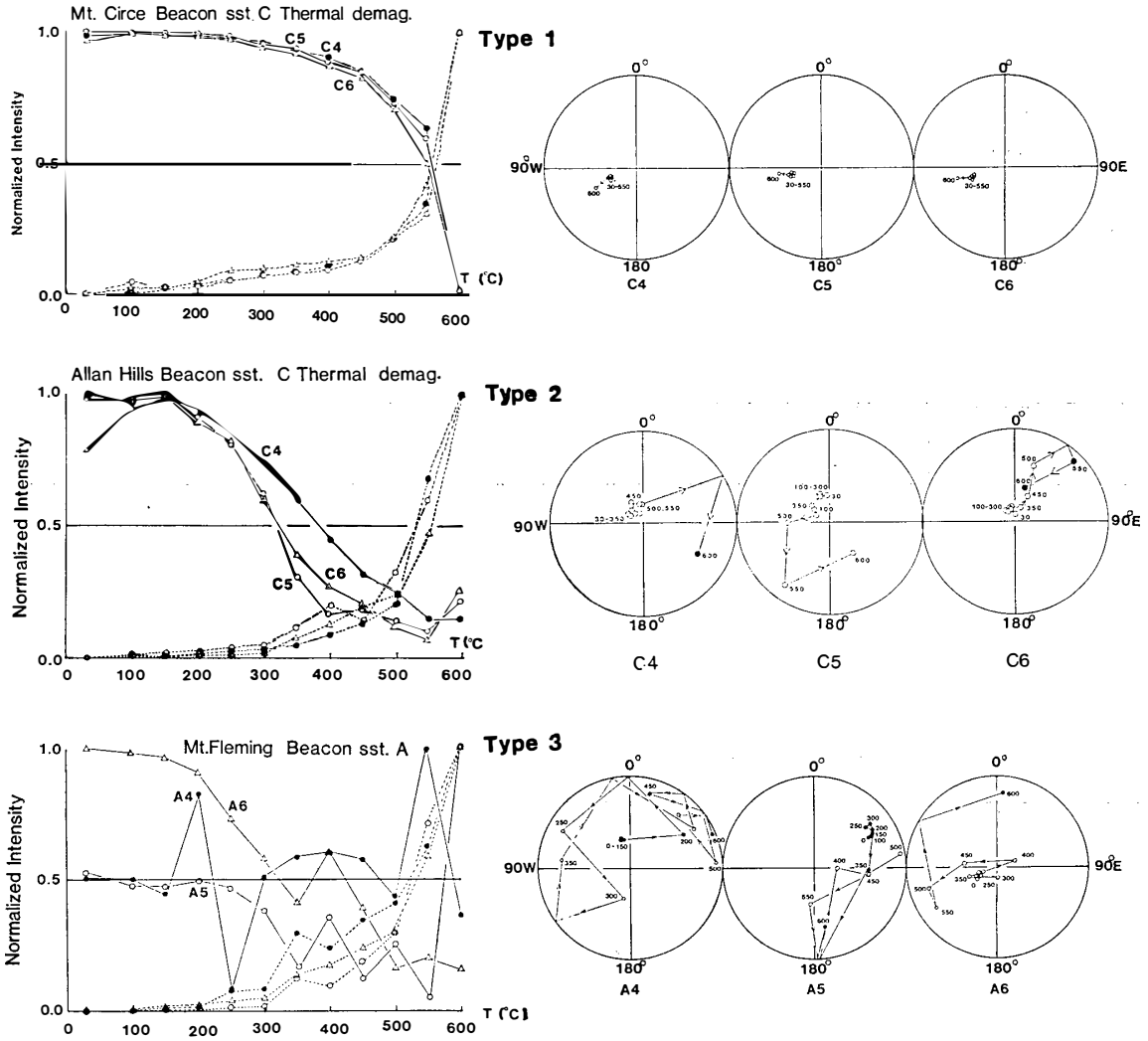

Fig. 20. Typical 3 thermal demagnetization groups for Beacon Supergroup (sandstone) in McMurdo Sound region. Solid line: Thermal demagnetization curve of NRM. Dotted line: TRM acquisition curve ($\bar{h}$=0.42 Oe). The properties of 3 representative samples are shown in each type.

the following categories, as shown in Fig. 20. Type 1: The decay curves of NRM against thermal demagnetization have smooth and clear blocking temperatures of NRM between 550 and 600°C. The directions are fairly stable up to 550°C and disperse at 600°C. Type 2: The intensities decay gradually from approximately 200 to 450°C and the directions are stable up to at least 400–500°C against thermal demagnetization. But both intensity and direction are unstable from 450–500°C to 600°C. That is, various kinds of blocking temperature may be observed from 200 to about 450°C. TRM acquisition increases gradually up to approximately 450°C and then steeply to 600°C. Since no stable NRM were observed at more than 450°C, the increasingly steep magnetization from 450 to 600°C is probably due to chemical alterations of magnetic grains. Type 3: The intensities and directions of NRM are stable to 300°C; this is the most stable type. TRM acquisition increases gradually to 300°C and then zigzag to 600°C; in many cases it is fairly unstable from 200 to 600°C. That is, the inferred

blocking temperature must be very low or undefined. As the results of these thermal examinations are almost identical in samples collected from the same site, the classified types from each site are listed in Table 8.

NRMs of 216 samples collected from 4 formations of the Beacon Supergroup were measured before and after optimum AF demagnetization. Based on the results of AF demagnetization of representative samples, the samples with an optimum 100 or 150 Oe AF demagnetization field were chosen. Obtained results of the mean value are summarized in Table 9. The NRMs of mean intensities of the samples from Mt. Circe are strong, 8.74×10^{-7}–8.82×10^{-6} emu/g, as compared to those from Knobhead,

Table 9. Paleomagnetic results of Beacon Supergroup in McMurdo Sound.

Sampling site		Demag. (Oe)	N	R (emu/g)	Inc	Dec	K	α_{95}	pLat	pLon
Mt. Circe	A	0	6	3.55×10^{-6}	−78.2°	267.7°	1040	2.1°		
		150		3.30×10^{-6}	−77.1	266.9	1258	1.9	61.9°S	223.1°W
	B	0	16	8.74×10^{-7}	−75.4	261.0	123.2	3.3		
		150		8.31×10^{-7}	−72.6	257.0	460.1	1.7	53.5°S	139.4°W
	C	0	17	8.82×10^{-6}	−63.5	254.7	151.2	2.9		
		150		8.51×10^{-6}	−62.3	255.6	169.8	2.7	39.4°S	134.0°W
	D	0	8	1.36×10^{-6}	−75.9	251.7	526.5	2.4		
		150		1.29×10^{-6}	−73.9	247.5	1342	1.5	53.5°S	148.2°W
	Total	150	47	4.00×10^{-6}	−69.9	255.9	118.9	1.9	49.1°S	138.0°W
Knobhead	A	0	37	9.78×10^{-7}	−81.8	277.0	132.4	2.1		
		150		9.79×10^{-7}	−81.7	280.7	354.4	1.3	76.6°S	136.9°W
	B	0	10	3.47×10^{-7}	−75.6	231.3	14.4	13.1		
		150		3.22×10^{-7}	−84.1	245.3	55.5	6.5	69.9°S	165.8°W
	C	0	17	1.51×10^{-7}	−88.1	234.3	5.7	16.4		
		100		1.42×10^{-7}	−87.0	201.5	4.5	19.0		
	D	0	21	1.30×10^{-7}	−75.9	281.5	6.7	13.3		
		100		4.73×10^{-8}	−68.6	245.1	7.5	12.4		
	A+B	150	47	8.39×10^{-7}	−82.4	275.1	159.6	1.7	71.7°S	143.6°W
Allan Hills	A	0	8	7.07×10^{-8}	−65.2	279.1	2.8	41.3		
		100		1.07×10^{-7}	−71.8	273.8	2.6	43.7		
	B	0	14	6.97×10^{-8}	−62.7	196.9	1.7	46.2		
		100		6.86×10^{-8}	−67.0	206.2	2.1	38.3		
	C	0	12	3.06×10^{-7}	−82.1	319.5	13.5	12.3		
		150		3.62×10^{-7}	−78.8	253.5	97.2	5.3	62.3°S	151.4°W
	D	0	17	5.29×10^{-8}	−27.1	221.7	1.9	36.9		
		100		5.62×10^{-8}	−53.3	313.8	2.8	32.0		
Mt. Fleming	A	0	8	1.79×10^{-7}	−67.3	193.5	1.8	34.1		
		100		1.57×10^{-7}	−66.1	206.4	1.7	35.9		
	B	0	15	4.72×10^{-8}	−42.5	190.0	1.2	76.4		
		150		4.12×10^{-8}	3.7	214.1	1.4	59.3		
	C	0	10	1.79×10^{-7}	−77.2	243.8	29.3	9.1		
		150		1.57×10^{-7}	−77.1	244.5	24.5	9.9	58.2°S	154.5°W

Demag.: Optimum AF demagnetization field, N: Sample number, R: Mean intensity of NRM, Inc and Dec: Mean inclination and declination of NRM, K: Precision parameter, α_{95}: Radius of 95% confidence circle about mean direction.

Allan Hills and Mt. Fleming. The samples from Allan Hills and Mt. Fleming are weak, with a magnitude of 10^{-8}–10^{-7} emu/g. Most of the samples are magnetized to the normal polarity but some samples from Allan Hills D and Mt. Fleming B are magnetized to reverse polarity. Individual NRM directions for all samples from one site formed a cluster in the case of the samples from all sites of Mt. Circe, A and B sites of Knobhead and site C of Allan Hills and Mt. Fleming, but were scattered for the others. The mean intensities of clustered samples from each site are generally larger than those of scattered ones; and the mean directions are limited from -62.3 to $-82.3°$ inclination and 230.9 to 280.7° declination.

7.3. Paleomagnetic discussion

TURNBULL (1959) and BULL *et al.* (1962) pointed out that the directional NRMs of the Beacon Supergroup from Ferrar Glacier and the Wright and Victoria Valleys regions were parallel to that of Ferrar dolerite. Obtained results in this study support not only their results but also expand it to include the region from Knobhead to Allan Hills. This uniformity of direction for the Beacon Supergroup and Ferrar dolerite may be caused by the geomagnetic field in this region being constant in direction from the Devonian to the Jurassic period, or by the reheating of the Beacon Supergroup during the intrusion of Ferrar dolerite in the Jurassic period. The following analysis is carried out in order to find a solution to this problem by applying the different types of AF and thermal demagnetization groups and the mean directions of NRM for each site. The significance of each type of AF demagnetization group may be estimated as follows: Types 1 and 2: As the AF demagnetization curves of NRM and ARM are similar, the inferred origin of NRM may be DRM when both intensities differ greatly. Type 3: Although NRM is unstable, it has stable ARM. DRM and TRM cannot be acquired, and the ratio ARM/NRM is large. Type 4: As there is no possibility of stable remanence, it cannot be judged whether the samples were heated or not.

The representative samples from Mt. Circe A, B, C and D, are similar not only in the ratio ARM/NRM but also in their classified type for the AF and thermal demagnetization groups as shown in Table 8; the ratios range from 0.97 to 2.89 and the samples all belong to one type. The sequence of the Beacon Supergroup at Mt. Circe is estimated to be of Devonian time. According to the standard polar-wander path of Gondwanaland (MCELHINNY, 1973), the expected VGP position of Devonian time for Antarctica is situated at the outer boundary of the present-day Weddell Sea. However, the obtained VGP position for whole samples from Mt. Circe yields 49.1°S latitude and 138.0°W longitude with $\alpha_{95}=1.9°$ as shown in Table 9. This discrepancy is probably due to remagnetization by intrusion of Ferrar dolerite in the Jurassic age. A dolerite sill 180 m thick intruded into the boundary between the basement complex and the Beacon Supergroup (MCKELVEY and WEBB, 1961), and the sampling site at Mt. Circe is within a vertical distance of 50 m from the upper boundary of that sill. Taking into account the calculation of temperature in the neighborhood of the intrusive sheet (JAEGER, 1957, 1959), it is possible that the temperature at the sampling site rises to over 570°C; a Curie point at 570°C is estimated for Type 1 of the thermal demagnetization group. The NRM direction for Ferrar dolerite collected from the Olympus Range is $-69.4°$ inclination and 237.6° declination with $\alpha_{95}=2.4°$, magnetized to the

normal polarity (see Chapter 6), while that for Beacon Supergroup for whole samples from Mt. Circe is -69.9, 255.9 and 1.9° respectively, magnetized to the same direction. Since the mutual angular deviation (Θ) of NRM direction between these formations is 6.4°, their NRM directions should correspond to each other, taking into account the α_{95} values. This suggests that the Beacon Supergroup around the sampling sites at Mt. Circe was heated to over 570°C and remagnetized during cooling down through that temperature during the Jurassic age.

The representative samples from Knobhead are of different kinds of type of AF demagnetization group for each site. The samples from sites 1 and 2 are Types 1 and 2 respectively for both the AF and thermal demagnetization groups, and have small ARM/NRM ratios of 1.50 and 3.15. That is, the inferred origin of NRM at these sites is probably TRM for the same reasons as given for the samples from Mt. Circe. The samples from site C are classified as Types 3 or 4 for the AF and thermal demagnetization groups; NRM is generally unstable, but some are capable of stable remanence. Therefore it may be assumed that the samples at site C were not placed under conditions of DRM acquisition, and were not then heated up to Curie temperature. The samples from site D are classified as Types 2 and 3 for both AF and thermal demagnetization groups, having a small ARM/NRM ratio of 2.78; all samples are capable of stable remanent magnetization, and some of them actually show stable NRM. Therefore the formation at this site was probably heated up to the same temperature, limited from 200 to 450°C. Consequently the samples which have a blocking temperature than below temperature would acquire TRM. Dolerite sills intrude into Knobhead at the top (2400 m) and about 540 m below the top (WEBB, 1963). The vertical distance of sampling site A from the lower sill is estimated as about 140 m above. The mean NRM direction for whole samples from sites A and B shows an inclination of -82.4° and a declination of 275.1° with a α_{95} value of 1.7°. TURNBULL (1959) obtained the NRM directions for Ferrar dolerite sills from the upper Ferrar Glacier region. As Knobhead is also situated in the same region, the representative NRM direction for Ferrar dolerite from the upper Ferrar Glacier region, referring to his data, should show an inclination of -76° and a declination of 255° with a α_{95} value of 2.7°. Therefore, since the angular deviation is $\Theta=7.3$°, the directions of both formations are parallel, taking into account the α_{95} values. Therefore these sampling sites may have been heated by a dolerite sill to more than 570°C for site A and less than that temperature for the other sites. Later many samples were remagnetized completely or partially to the geomagnetic field direction during the Jurassic age.

In the case of Allan Hills, the representative samples from site C have stable NRM; they are classified as Types 1 or 2 for the AF and thermal demagnetization groups. As the ARM/NRM ratio is large, 8.11, it may be estimated that the formation was magnetized by DRM rather than by TRM. The samples from sites A, B and D are of Types 3 or 4 AF demagnetization group.

The results of chemical analysis of coal from near site C in Allan Hills are shown in Table 10 together with other coal data from the hills (GUNN and WARREN, 1962). The values of volatile matter, fixed carbon and calorific value suggest that samples (1) and (2) are anthracite but sample (3) is low grade coal. The value of the fuel ratios (volatile matter/fixed carbon), ranging from 16.9 to 20.4, shows that this coal includes

Table 10. Chemical analyses of coals from Allan Hills.

Samples		(1)	(2)	(3)
Moisture	(wt%)	4.80	1.91	2.67
Ash	(wt%)	11.4	12.92	43.4
Volatile matter	(wt%)	12.8	12.32	9.76
Fixed carbon	(wt%)	71.0	72.85	44.17
Sulfur	(wt%)	0.72	4.77	3.02
Calorific value	(cal/g)	6520	6445	3833
Fuel ratio		18.0	16.9	20.4

(1) This study; analyzed by the Coal Mining Research Centre, Japan.
(2) and (3) GUNN and WARREN (1962).

a relatively large quantity of volatile matter in the case of anthracite. That is, it may be concluded that these samples were not heated between the Permian age and the present. Thus, the surface of Allan Hills was probably not heated, and the DRM of the samples from site C survived.

The earth's geomagnetic field from the late Permian to the middle Triassic period showed alternate changes of normal and reversed polarity, but prior to the Permian age showed only reversed polarity (Kiaman interval) (MCELHINNY and BUREK, 1971). Therefore the magnetization polarity of Allan Hills would suggest the age confirmed by fossil evidence, namely from the late Permian to the early Triassic period.

The NRM direction of Ferrar dolerite in this area has an inclination of $-67.6°$ and a declination of 262.6° and a α_{95} value of 5.1°. An angular deviation between the Beacon formation at site C and Ferrar dolerite is $\Theta=11.5°$. That is, both directions are in mutual agreement taking into account these α_{95} values. Since the inferred age of the Beacon Supergroup at Allan Hills form Permian to Triassic (TOWNROW, 1966; BALLANCE and WATTERS, 1971), it may be concluded that the shift of Antarctica against VGP was small from the Permo-Triassic to the Jurassic age. This conclusion is consistent with the results of analysis of Mesozoic rocks from Australia (IRVING, 1963; IRVING *et al.*, 1963); directional magnetizations from lower Triassic to lower Cretaceous are approximately uniform for eastern Australia including Tasmania Island. Hence it seems that Australia separated off from East Antarctica in early Tertiary time.

The representative samples collected from site C at Mt. Fleming are classified as Types 2 or 3 for AF and thermal demagnetization groups, and the ARM/NRM ratio is small, 1.40. The NRM direction of the dyke from which Ferrar dolerite originates, showing an inclination of $-81°$ and a declination of 274° with α_{95} of 1.0°, was obtained at a site separated by 30 m from site C. The angular deviation Θ between the mean NRM direction of the Beacon Supergroup at site C, as shown in Table 9, and that of the dykes is 6.6°; they are mutually parallel taking into account the α_{95} values. A total of 10 samples from site C were collected from the area between a dyke 50 to 100 cm in thickness and 20 m away from the dyke. It is impossible to determine from the NRM direction whether the formation at site C was heated by the dyke or not, because the inferred ages of the Beacon Supergroup and Ferrar dolerite are Triassic and Jurassic respectively and, as mentioned above, the NRM directional change during Misozoic time was small. From the ARM/NRM ratio, however the formation must

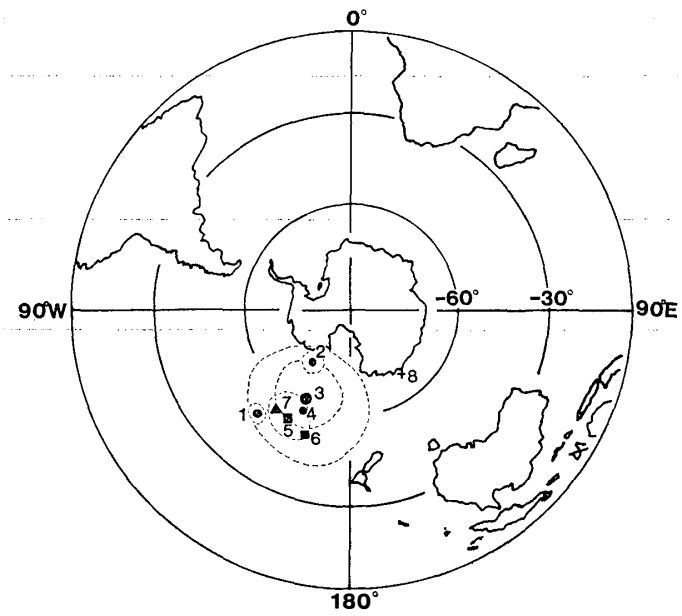

Fig. 21. Obtained VGP positions from Beacon Supergroup in McMurdo Sound. 1. Mt. Circe, 2. Knobhead, 3. Allan Hills, 4. Mt. Fleming, 5. Ferrar Glacier (TURNBULL, 1959), 6. Wright and Victoria Valleys (BULL et al., 1962), 7. Mean VGP position of Ferrar dolerite, 8. Present geomagnetic field direction. 1–4 and 7. This study.

have been heated to above the Curie point. The samples at sites A and B, including the same formations as site C, are of Types 3 or 4 of the AF and thermal demagnetization groups; they were not heated up to the Curie point. From this it may be concluded that the samples which were heated by dykes (site C) have a stable NRM, but samples which were not heated (sites A and B) do not have a stable NRM.

The four obtained VGP positions of the Beacon Supergroup, for (1) Mt. Circe, (2) Knobhead, (3) Allan Hills and (4) Mt. Fleming, are illustrated in Fig. 21 together with those of previous data about the Beacon Supergroup ((5) TURNBULL, 1959; (6) BULL *et al.*, 1962), (7) Ferrar dolerite and (8) the present geomagnetic pole. The VGP of Ferrar dolerite is estimated as the average position of 10 independent data from the whole Transantarctic Mountains. The VGPs of the Beacon Supergroup from the Wright and Victoria Valleys regions (1) and (6) are distributed on the low latitude side. This is consistent with the results of analysis of Ferrar dolerite from the Wright and Victoria Valleys regions; the latitude of VGP is the lowest for these 10 data. In general, VGP distribution in Fig. 21 resembles that of Ferrar dolerite in the Jurassic age fairly closely. VGP (3) shows the location of the geomagnetic pole position for Allan Hills during the Permo-Triassic period. However it is included in the cluster of VGPs from the Beacon Supergroup which were heated by Ferrar dolerite as shown in the figure. Therefore, as mentioned above, Antarctica probably did not shift during the late Permian to Jurassic periods.

7.4. Concluding remarks

The formation of the Beacon Supergroup in Mt. Circe was remagnetized completely by a Ferrar dolerite sill in the Jurassic period; the temperature of the formation in-

creased to more than 570°C. Consequently it acquired a fairly stable TRM and the directional NRM was aligned to that of the sill at Wright Valley. The samples from Knobhead were probably heated to at least the Curie point and remagnetized to the field direction of the Jurassic dyke. However, the increased temperature is probably high, more than 570°C for site A and less than 570°C for sites B, C and D. The samples from sites A, B and D from Allan Hills do not have DRM, although almost samples are able to have stable remanent magnetization. However the sample from site C probably has stable DRM. The direction of NRM is almost parallel to the Jurassic dyke at Allan Hills; East Antarctica probably had almost no shift of VGP from the Permo-Triassic to the Jurassic period. The samples from sites A and B at Mt. Fleming do not have a stable NRM like that of Allan Hills. The samples from site C may have been heated by dykes of Ferrar dolerite and remagnetized to the Jurassic geomagnetic field.

The intensity of the Beacon Supergroup in McMurdo Sound is fairly weak, 9×10^{-6} to 4×10^{-8} emu/g. In general, samples with a stable NRM have a stronger intensity than those with unstable NRM.

8. Paleomagnetism of Basement Complex in Wright Valley

8.1. Basic magnetic properties

8.1.1. Magnetic hysteresis properties

Magnetic hysteresis properties (I_S), (I_R), (H_C) and (H_{RC}) are summarized in Table 11 together with the NRM intensity (I_n) and the ratio of I_n/I_S and I_R/I_S. The value of H_{RC} for granitic rock, Theseus granodiorite and some samples of Vanda porphyry could not be obtained, due to the noise of the instrument.

The I_S value of granitic rock and Theseus granodiorite is generally low, namely 8 to 0.2×10^{-3} emu/g, compared with those for Vanda porphyry and "red dyke" samples which have a range from 105 to 3.5×10^{-3} emu/g. In the case of Vanda lamprophyre, samples C2 to C8 have a small I_S value from 10 to 1×10^{-3} emu/g, but sample C1 has an extremely large 790×10^{-3} emu/g. The I_n/I_S ratios of all samples range from 2.604 to 0.192×10^{-3}, except for Vanda "red dyke", which has low value of 0.122 to 0.016×10^{-3}; however the I_R/I_S ratio does not differ so greatly from the others. The H_C values of granitic rocks range from 11.5 to 56 Oe. The values of Vanda lamprophyre vary from 472 to 9 Oe, and those of Theseus granodiorite, Vanda porphyry and "red dyke" are relatively large, 35 to 99 Oe. These H_C values suggest that the magnetic grains in many samples are single- or pseudosingle-domain structures, but those in granitic rock, collected from the bottom of the valley, and a some samples of the Vanda lamprophyre, probably have a pseudosingle- or multi-domain structure. The H_{RC} values for the Vanda lamprophyre and "red dyke" support the results obtained from the H_C values.

8.1.2. AF demagnetization

Several typical samples from each formation were demagnetized in alternating fields, increased in steps up to a peak of 880 Oe. The results of AF demagnetization of NRM suggests that all the samples except those from Theseus granodiorite and Vanda "red dyke" have stable NRM; the magnitude of the soft magnetic component, *i.e.* isothermal remanent magnetization (IRM) and viscous remanent magnetization (VRM), is not particularly great, as compared to the hard component. The median demagnetization field (MDF) of these samples exceeds 500 Oe and their NRM directions change within 12° during AF demagnetization up to a peak of 600 Oe. Figure 22a shows

Table 11. Basic magnetic properties of basement complex in Wright Valley.

Sample name		Inc	I_n ($\times 10^{-6}$ emu/g)	I_S ($\times 10^{-3}$ emu/g)	I_R ($\times 10^{-4}$ emu/g)	H_C (Oe)	H_{RC} (Oe)	I_n/I_S ($\times 10^{-3}$)	I_R/I_S ($\times 10^{-1}$)	I_S-T curve Type	I_S-T curve Curie point (°C)
Granitic rock	A1	−21.8°	1.687	4.0	1.5	14	—	0.422	0.375		
	A2	−12.2	2.604	1.0	1.0	11.5	—	2.604	1.0		
	A3	−17.2	3.636	8.0	8.0	15.8	—	0.455	1.0		
	A4	−15.5	1.032	0.4	0.4	11.5	—	2.580	1.0		
	A5	−42.0	0.894	1.5	1.5	25	—	0.596	1.0		
	A6	−70.6	0.277	0.2	1.3	56	—	1.385	6.5		
	A7	−75.4	0.144	0.75	1.7	54	—	0.192	2.267		
Theseus	B1	−67	1.649	1.0	0.3	61	—	1.649	0.3		
granodiorite	B2	−76	0.365	0.8	0.18	75	—	0.456	0.225		
Vanda	C1	−17.6	336.7	790	3630	472	688	0.426	4.595	1	570
lamprophyre	C2	−19.2	3.212	2	3.5	23	306	1.606	1.750	3	30–400, 570
	C3	−50.7	6.907	3	7.0	53	711	2.302	2.333	4	30–570
	C4	−41.8	2.793	2	1.3	9	146	1.397	0.650	4	30–570
	C5	−62.1	1.720	2	1.4	11	216	0.860	0.7	4	30–570
	C6	−58.5	8.393	10	40	172	1384	0.839	4.0	4	30–570
	C7	−79.1	2.123	3	4.3	28	308	0.708	1.430	5	30–400
	C8	−71.9	1.533	1	1.0	13	111	1.533	1.0	6	220, 330
Vanda	D1	−38.1	3.800	11	9.0	50	497	0.346	0.818		
porphyry	D2	−24.8	3.473	7.5	8.0	84	—	0.463	1.067		
	D3	−22.5	2.500	3.5	2.5	35	—	0.833	0.833		
"Red dyke"	E1	−31.8	1.663	54	34	79	471	0.0301	0.630	2	350, 560
	E2	−67.6	2.677	22	20	99	514	0.122	0.909	1	570
	E3	−60.3	1.647	105	43	51	352	0.016	0.410	1	570

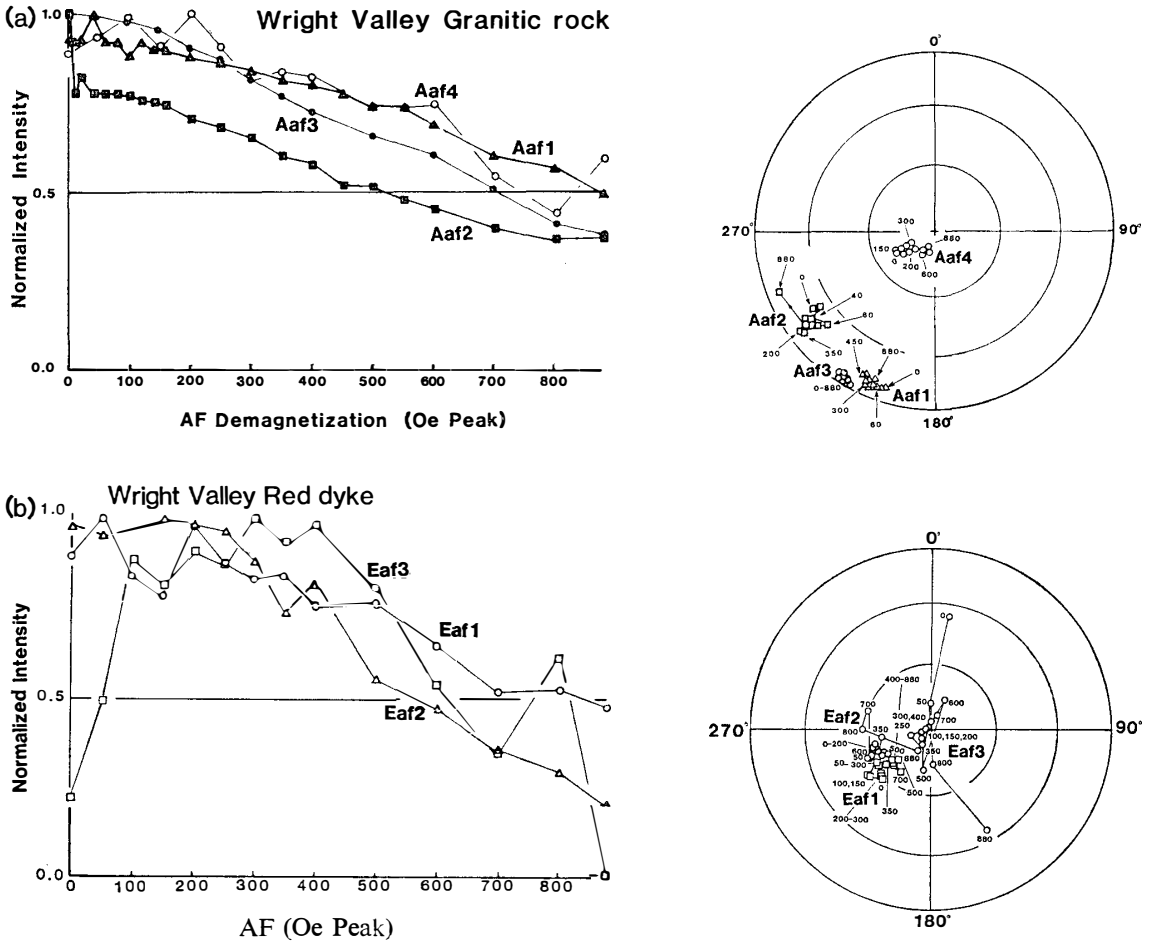

Fig. 22. AF demagnetization curves of NRM for 7 representative samples. (a) Stable NRM, (b) Unstable NRM.

the AF demagnetization curve of 4 samples of granitic rock, as examples of stable NRM. These representative samples were selected from the bottom of Wright Valley (Aaf 1, Aaf 2 and Aaf 3), and from 300 m above the bottom of the valley (Aaf 4). Their NRM intensities range from 2.275×10^{-7} to 2.433×10^{-6} emu/g. The AF demagnetization curves of intensity, with an MDF exceeding 500 Oe, are fairly stable and their NRM directions are also stable up to at least 800 Oe as shown in Fig. 22a. However the samples of Theseus granodiorite and "red dyke" do not have such a stable NRM against AF demagnetization. Figure 22b shows the AF demagnetization curves of Vanda "red dyke" as an example of unstable NRM. The intensities of samples Eaf 1, Eaf 2 and Eaf 3 range from 4.833×10^{-7} to 2.677×10^{-6} emu/g. These AF demagnetization curves suggest that an alternating field around peak of 150 Oe peak removes the unstable component from NRM; every sample is stable against AF demagnetization, at least to 400 Oe.

8.1.3. Thermal demagnetization

Typical samples, selected according to the NRM inclination of each formation, were thermal demagnetized in air in steps of 50 or 100°C, up to 600°C. The field intensity in the thermal demagnetizer is less than 20 γ.

Since the NRM of all samples of granitic rock from the bottom of Wright Valley is distributed along a meridian from middle to low latitude in the southern hemisphere, as described later, each of the three samples was selected from the middle and those from the low latitude groups. The inclination of these samples ranges from -8.5 to $-21.9°$ for Ath 1, Ath 2 and Ath 3 of the low latitude group, and from -46.7 to $-69.0°$ for Ath 4, Ath 5 and Ath 6 of the middle latitude group. The intensities of the low latitude group (1.566–4.140×10^{-6} emu/g) decay steeply between 500 and 600°C; only one clear blocking temperature is observed between 500 and 600°C, as shown in Fig. 23a. The directions of this group show almost no change up to 500°C and then scatter from the cluster at 600°C. For the middle latitude group, the NRM changes gradually, not only in intensity (1.034–5.797×10^{-6} emu/g) but also in its direction, with thermal demagnetization up to 500°C; the NRM direction of in the middle latitude systematically shifts to low latitude, simultaneously with the decay of intensity up to 500°C, but scatters widely at 600°C. Although residual remanent magnetizations of random direction were observed at 600°C, this is probably merely the noise of the thermal demagnetizer. Thermal demagnetization curves of granitic rocks collected from 20 m below the lower boundary of sill "a" shown in Fig. 23a. Both the intensity and direction of NRM are stable up to 400°C, but intensities decay and directions scatter at above that temperature.

The result of thermal demagnetization of samples of Bth 1 and Bth 2 of Theseus granodiorite were thermal demagnetized as shown in Fig. 23b. The initial intensities of Bth 1 and Bth 2 are 2.796×10^{-7} and 3.467×10^{-7} emu/g, respectively; both samples then demagnetize steeply between 300 and 400°C. The corresponding directions, originally with high inclination of -79.5 and $-77.0°$ respectively, show almost no change up to 300 or 400°C; they then shift systematically to low latitude at 500°C. Residual remanent magnetization after heating to 600°C is probably due to the noise of the thermal demagnetizer.

Since the NRM directions of all samples of the Vanda lamprophyre are distributed along a meridian from 0 to 90° in latitude in the southern hemisphere, two or three samples were selected from each of the high, middle and low latitude groups for thermal demagnetization. Their I_S-T curves are illustrated in Figs. 23c and 23d. Before demagnetization the intensities of Cth 1 and Cth 2 of the low latitude group ranged between 3.431×10^{-4} and 3.933×10^{-7} emu/g respectively. They gradually thermally demagnetize up to 300°C, and decay steeply between 500 and 600°, as shown in Fig. 23c. Their NRM directions show no large changes up to 600°C, but do shift a little towards lower latitudes with the increasing demagnetizing temperature. The thermal demagnetization curves of the high latitude group, Cth 6, Cth 7 and Cth 8, as shown in Fig. 23c, are very similar to those of the Theseus granodiorite. The intensities, ranging from 6.201×10^{-7} to 2.057×10^{-6} emu/g show almost no change up to 300°C and then demagnetize steeply from 300 to 400°C. Their NRM inclinations, distributed from -68.0 to $-84.6°$ in inclination, show almost no change up to 300°C, although they shift broadly from 400 to 600°C. Consequently it seems that the observed residual remanence at more than 400°C may be merely the noise of the thermal demagnetizer. The I_S-T curves of the middle latitude group (Cth 3, Cth 4 and Cth 5), as shown in Fig. 23d, show intensities ranging from 1.1×10^{-6} to 7.7×10^{-6} emu/g, which decay

gradually between 300 and 600°C, although there is almost no change up to 300°C. The directions of the three samples show a tendency to shift towards low latitude, synchronizing with the decay of intensity by thermal demagnetization up to 500°C. Since the directions of the three samples are random at 600°C, the residual remanences are probably the noise of the demagnetizer. These I_S-T curves are therefore fairly

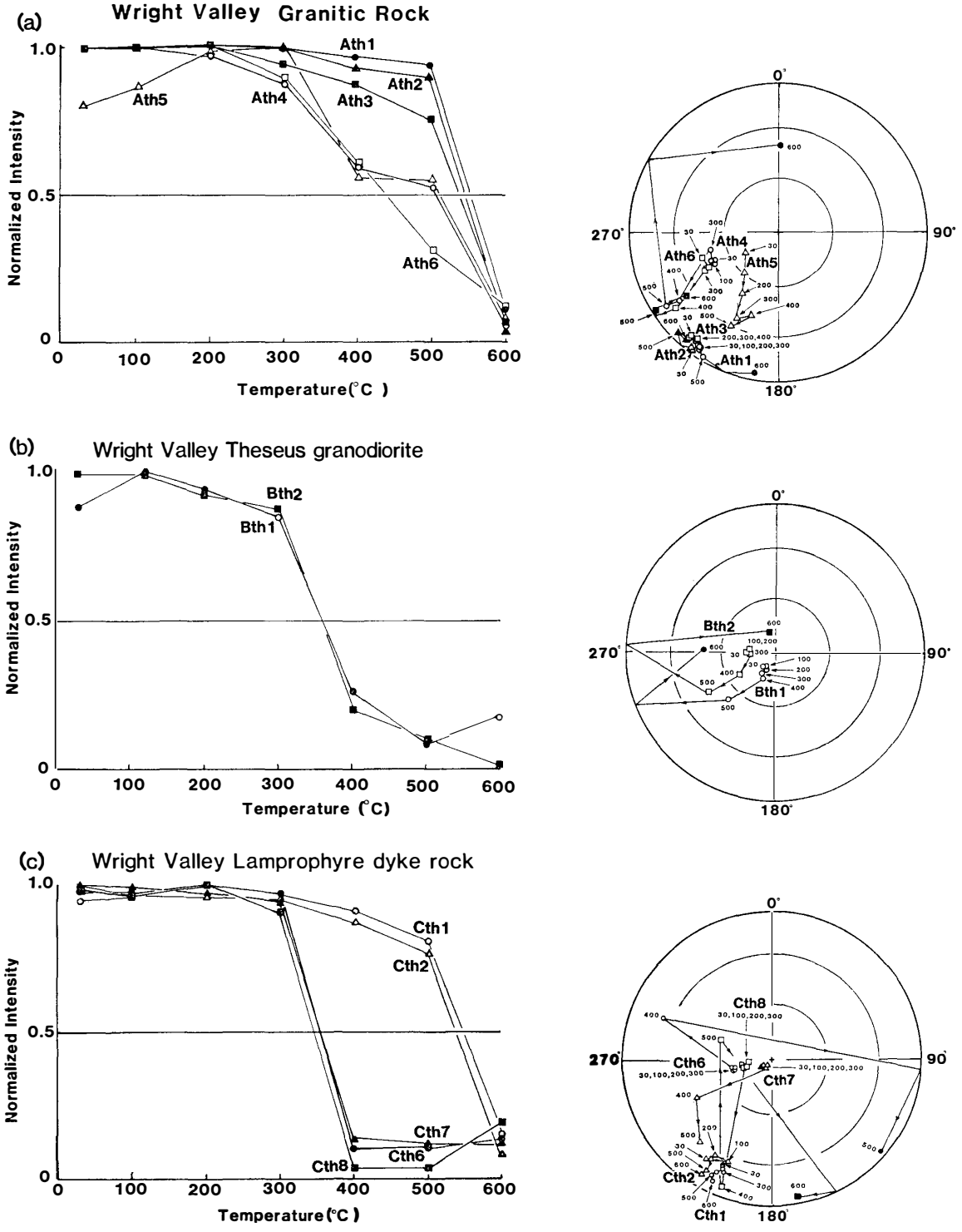

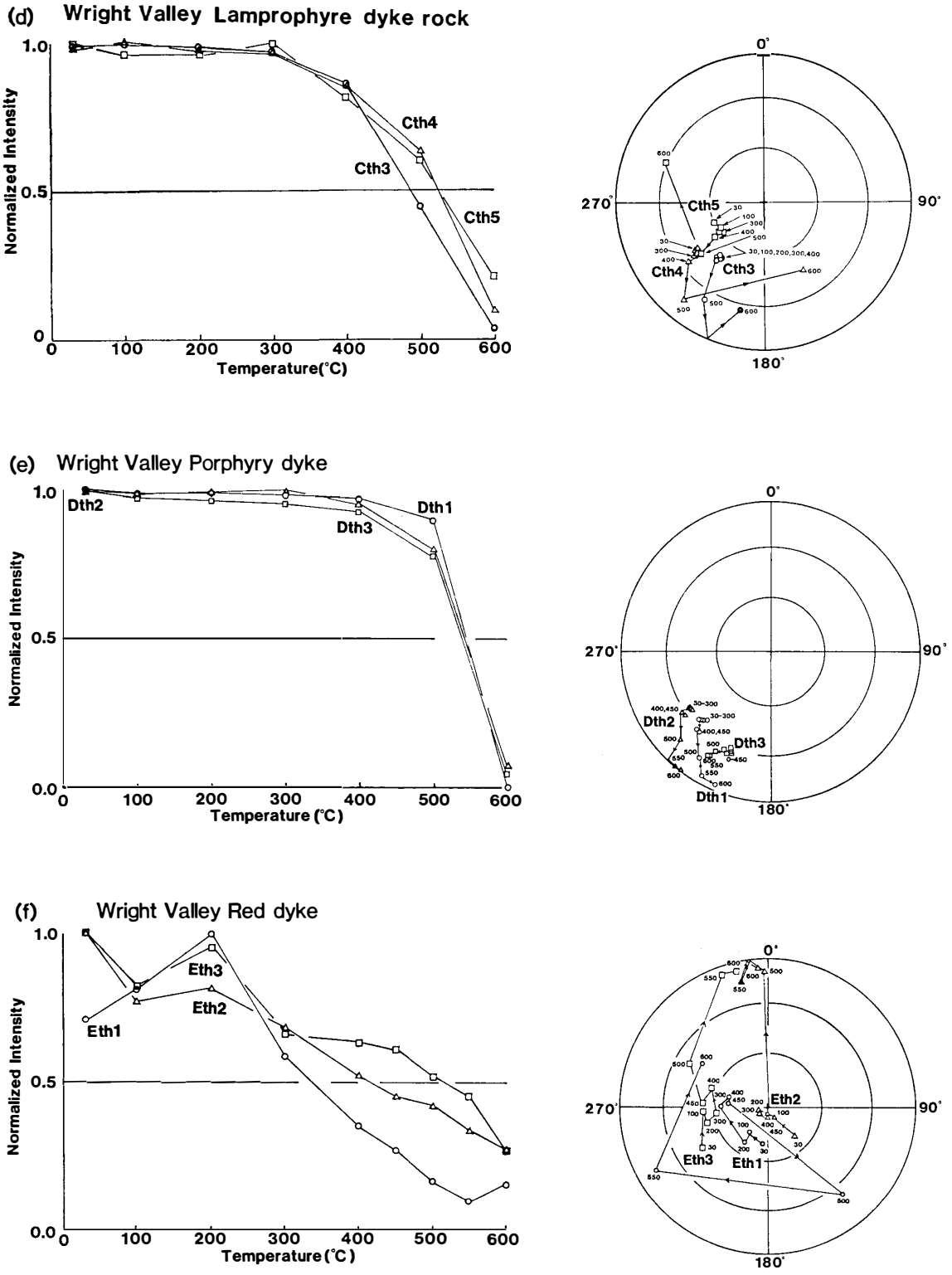

Fig. 23. Thermal demagnetization curves of representative samples of basement complex. (a) Granitic rocks, (b) Theseus granodiorite, (c) and (d) Vanda lamprophyre, (e) Vanda porphyry, (f) "Red dyke".

similar to those of the middle latitude group of granitic rocks collected from the bottom of Wright Valley.

The thermomagnetic curves of Vanda porphyry Dth 1, Dth 2 and Dth 3, shown in Fig. 23e, are fairly similar to those of the low latitude group of granitic rock collected from the bottom of Wright Valley, and of Vanda lampropyre. That is, their original NRM intensity, ranging from 3.473 to 3.723×10^{-6} emu/g, does not show much decay up to 500°C and then decays steeply from 500 to 600°C. Their NRM directions, remain at low inclination, with almost no change, up to 400°C then shifts back towards low latitude and scatters at 600°C.

The NRMs of samples Eth 1, Eth 2 and Eth 3 of the Vanda "red dyke" are unstable against thermal demagnetization, compared with those of other formations, as shown in Fig. 23f. The samples of Eth1 and Eth 3 were collected from the bottom of Wright Valley; the samples of Eth 2 were collected from 300 m above the bottom of the valley. Their NRM intensities, which intensity ranging from 4.833×10^{-7} to 2.677×10^{-6} emu/g, decay smoothly from 200 to 600°C. The NRM directions are relatively stable from 300 to 450°C in the case of Eth 1, and from 100 to 450°C in the case of Eth 2 and Eth 3.

8.1.4. Thermomagnetic curves

The I_S-T curves for granitic rock, Theseus granodiorite and Vanda porphyry could not be obtained because of instrumental noise. The obtained I_S-T curves of typical samples of Vanda lamprophyre and "red dyke" are classified into six types, as shown in Fig. 24. Type 1: Irreversible, with a single Curie point at 570°C; the ferromagnetic minerals are probably magnetite of constant composition, but may show low temperature oxidation (titanomaghemite) due to increasing magnetization during heating. Type 2: Irreversible, with two distinct Curie points at 350 and 570°C in the heating curve and one at 570°C in the cooling curve. Since the Curie point at 350°C is not present in the cooling curve and intensities of this type increase to double magnitude after heating, some of the magnetic grains probably change to titanomaghemite. Type 3: Reversible with an area of undefined Curie points and distinct Curie point at 570°C. Titanomagnetite grains of various composition and magnetite are inferred. Type 4: Reversible, with an area of undefined Curie points, and a minor one at 570°C. Titanomagnetite grains of varying composition and a small quantity of magnetite are inferred. Type 5: Reversible, with no well-defined Curie point. Titanomagnetite of varying composition is inferred. Type 6: Irreversible, with two Curie points at 220 and 330°C in the heating curve, and no well-defined Curie points in the cooling curve. Titanomagnetite may show chemical alteration during heating. These classified types for each sample are shown in Table 11. A relationship between the NRM inclination and the Curie point of these representative samples can be identified in the case of the samples of Vanda lamprophyre. That is, the samples of Types 1 and 3 have clearly distinct Curie points for magnetite, and have a low inclination of about $-20°$; those of Types 5 and 6 have a lower Curie point at more than 500°C and have high inclinations of 70–80°; that of Type 4 is midway between these two cases. However there is no correlation between the Curie points and the inclinations in the case of the "red dyke". Pilot samples from "red dyke", with all samples showing a Type 2 I_S-T curve, magnetized at an inclination of about -32–$-65°$.

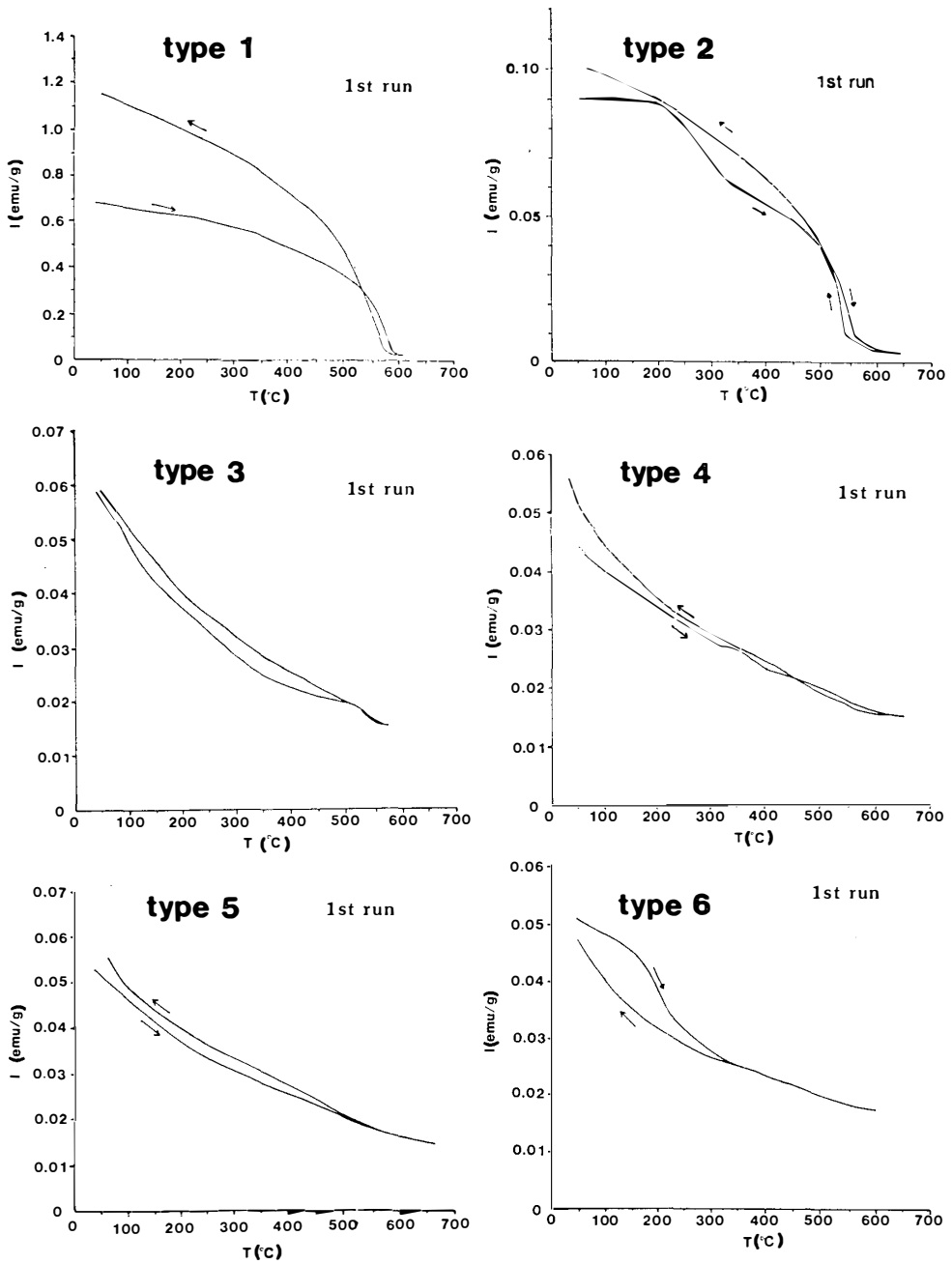

Fig. 24. Classified 6 types of thermomagnetic curves for Vanda lamprophyre and "red dyke".

8.2. Directional NRM against demagnetization

The NRM of every sample before and after AF demagnetization in fields of up to 140 Oe were measured, and the samples were then thermal demagnetized at 300, 400, 500 and 550°C in air, based on the results of thermal demagnetization of representative samples. The results obtained from demagnetizations are summarized in Table 12 and plotted in Figs. 25a to 25d. Table 12 shows the number of examined specimens (N) collected from the same formation, the mean intensity of NRM (R), the mean inclination (Inc) and declination (Dec) of NRM, the estimate of precision (K), the semiangle

of the cone of confidence of 95% probability (α_{95}), and the paleolatitude (pLat) and paleolongitude (pLon) of the virtual geomagnetic pole (VGP).

The individual NRM directions of granitic rock from the bottom of Wright Valley, plotted after demagnetization step, are shown in Fig. 25a, using the symbol of a circle, together with the direction of the present earth's geomagnetic field. These specimens have magnetization directions significantly different from the earth's field in McMurdo Sound area. The NRM directions for a major part of the specimens are found in low to middle latitudes in the southern hemisphere, although one is located at high latitude. This distribution pattern is not changed by AF demagnetization up to 140 Oe. However the NRM directions distributed from middle to high latitudes tend to shift towards low latitudes through thermal demagnetization, as shown in Fig. 25a. The individual directions after thermal demagnetization at 500°C lie along a great circle of low inclinations. The directions of 9 specimens at 550°C have a cluster at the same position as that of 500°C, but the others scatter from the cluster. A remarkable feature of the mean NRM direction as indicated by thermal demagnetization shows that inclination decrease is observed up to 550°C between -26.5 and $-2.7°$, but declination does not show much change from 220.5 to 216.7°, as shown in Table 12. Using the mean value at 550°C gives only 9 clustered specimens for statistical calculation. The value of confidence of α_{95} has minimum value at 500°C, namely 8.1°. Although the precision is calculated taking into consideration the reliable directions, the most significant cluster is produced by thermal demagnetization at 500°C for granitic rock from the bottom of Wright Valley. The mean differential magnetization between the original NRM and the NRM after thermal demagnetization to 500°C is calculated as Inc $=-66.6°$ and Dec $=274.7°$, although the value of confidence is large, namely $\alpha_{95}=24.5°$. This NRM direction shows a similar to that of Ferrar dolerite in Wright Valley, namely Inc $=-69.4°$, Dec $=237.6°$ and $\alpha_{95}=2.4°$.

The directions of the original NRM of granitic rock, symbolized by a square, collected 20 m below the lower boundary of dolerite sill "a", has a cluster with confidence of $\alpha_{95}=4.7°$; but these are scattered by thermal demagnetization, as shown in Fig. 25a. The clearest precision and confidence are observed at the original NRM. The inclina-

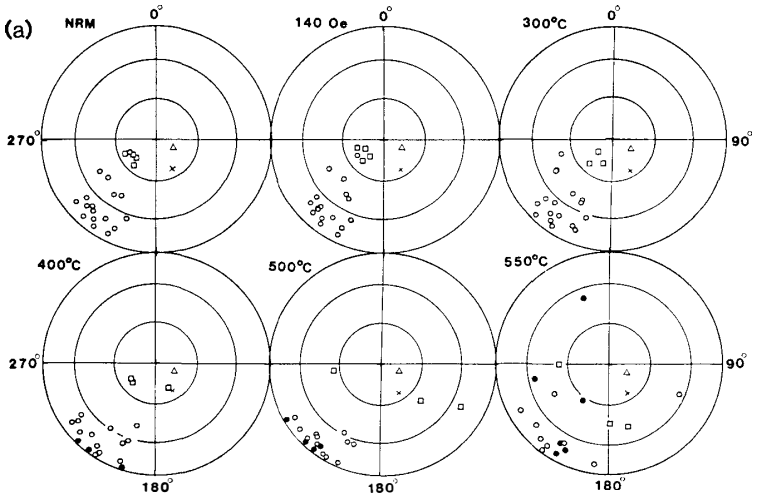

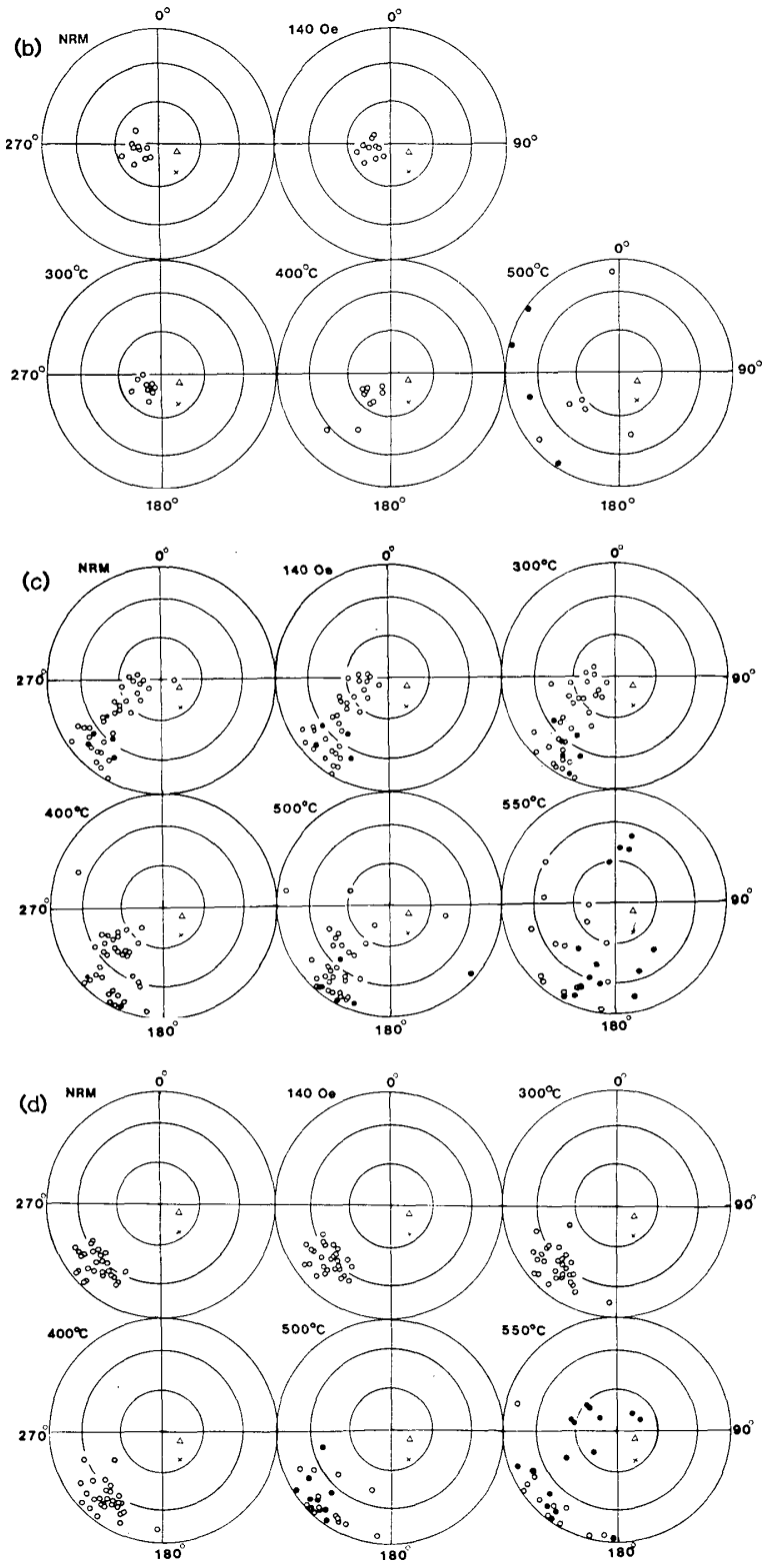

Fig. 25. Change of the directional NRM against AF demagnetization at 300, 400 and 550°C. Triangle: Direction of geomagnetic dipole in present, Cross: Geomagnetic field direction at Wright Valley, Open circle and square: Normal polarity, Solid circle: Reversed polarity. Equal-area projection. (a): Granitic rock, (b): Theseus granodiorite, (c): Vanda lamprophyre, (d): Vanda porphyry.

Table 12. Change of the directions of NRM by AF and thermal demagnetizations.

Sample name		NRM	140°Oe	300°C	400°C	500°C	550°C
A. Wright Valley granitic rocks Bottom of valley	N	16	16	16	16	16	9
	R (emu/g)	2.09×10^{-6}	2.02×10^{-6}	1.89×10^{-6}	1.77×10^{-6}	1.67×10^{-6}	1.40×10^{-6}
	Inc	−26.5°	−26.9	−24.3	−13.5	−9.0	−2.7
	Dec	220.5°	219.8	218.7	215.9	216.7	217.4
	K	17.8	17.3	17.7	20.6	21.5	24.9
	α_{95}	8.7°	8.8	9.0	8.3	8.1	10.5
	pLat	4.4°N	4.6°N	3.0°N	3.3°N	5.4°N	8.5°N
	pLon	20.9°E	20.2°E	19.4°E	17.4°E	18.5°E	19.6°E
20m below from bottom of sill "a"	N	4	4	3	3	3	
	R (emu/g)	1.40×10^{-7}	1.38×10^{-7}	1.17×10^{-7}	8.78×10^{-7}	1.85×10^{-7}	
	Inc	−69.1°	−73.4	−70.9	−73.2	−9.4	
	Dec	237.7°	237.0	222.7	217.8	152.6	
	K	376.2	247.6	218.7	30.3	2.2	
	α_{95}	4.7°	5.9	8.4	22.8	122.8	
	pLat	44.9°S	51.1°S	45.5°S	48.5°S	6.3°S	
	pLon	151.8°W	155.1°W	164.8°W	169.8°W	134.0°E	
B. Theseus granodiorite	N	10	10	10	10	10	
	R (emu/g)	2.63×10^{-7}	2.43×10^{-7}	2.29×10^{-7}	9.13×10^{-8}	1.11×10^{-7}	
	Inc	−75.5°	−76.8	−75.8	−63.6	−24.3	
	Dec	255.3°	255.3	230.2	221.5	252.4	
	K	84.0	105.8	130.2	22.4	2.4	
	α_{95}	5.3°	4.7	4.3	10.4	41.0	
	pLat	54.4°S	59.5°S	54.0°S	35.5°S	8.7°S	
	pLot	142.7°W	144.4°W	162.0°W	163.3°W	128.1°W	
C. Vanda lamprophyre	N	39	39	38	36	31	29
	R (emu/g)	1.06×10^{-4}	1.05×10^{-4}	9.94×10^{-5}	8.96×10^{-5}	9.29×10^{-5}	4.46×10^{-5}
	Inc	−37.5°	−35.3	−36.8	−30.3	−20.3	17.4
	Dec	228.1°	228.6	224.4	218.3	219.8	210.0
	K	4.3	3.9	5.2	12.3	15.0	1.9

	α_{95}	12.6°	13.5	10.5	7.1	6.9	28.5
	pLat	12.5°N	11.2°N	11.5°N	6.3°N	0.9°N	19.6°N
	pLon	25.7°E	26.5°E	23.7°E	18.6°E	20.8°E	13.4°E
D. Vanda porphyry	N	28	28	27	27	27	25
	R (emu/g)	3.59×10^{-6}	3.57×10^{-6}	2.85×10^{-6}	2.76×10^{-6}	2.39×10^{-6}	1.57×10^{-6}
	Inc	−25.1°	−26.8	−24.3	−21.7	−6.6	24.1
	Dec	227.8°	228.6	224.5	222.4	223.0	236.8
	K	39.1	42.0	38.2	41.9	13.0	3.0
	α_{95}	4.4°	4.3	4.6	4.4	8.0	20.3
	pLat	4.7°N	5.8°N	3.8°N	2.0°N	5.8°N	19.2°N
	pLon	28.1°E	28.8°E	25.0°E	23.2°E	24.9°E	41.5°E
E. Vanda "red dykes"	N	13	13	13	13	13	
	R (emu/g)	2.34×10^{-6}	2.05×10^{-6}	1.93×10^{-6}	1.45×10^{-6}	1.20×10^{-6}	
	Inc	−53.4°	−61.7	−59.7	−66.8	−53.0	
	Dec	238.1°	238.4	260.6	252.6	269.9	
	K	6.9	22.0	26.5	22.5	4.7	
	α_{95}	17.7°	9.0	8.2	8.9	21.6	
	pLat	26.9°S	35.5°S	37.5°S	38.3°S	32.7°S	
	pLon	146.2°W	141.8°W	127.5°W	135.6°W	116.5°W	

tion and declination of the original mean NRM direction are Inc = −69.1° and Dec = 237.7° respectively, with a confidence of α_{95} = 4.7° (see Table 12). This direction is fairly consistent with that of sill "a".

The individual NRM directions of specimens from Theseus granodiorite make a cluster around −75.5° inclination, 255.3° declination, with a confidence of α_{95} = 5.3°, as shown in Fig. 25b and Table 12. These original directions are further clustered by AF demagnetization at 140 Oe and thermal demagnetization at 300°C, but are scattered by thermal demagnetization at 400 and 500°C. The best clustering is observed after thermal demagnetization at 300°C. The inclination and declination of the mean NRM at that temperature are −75.8 and 230.2°, respectively, with a confidence of α_{95} = 4.3°. As the angular deviation between this direction and that of sill "a" is only 6.8°, taking into account the α_{95} values, the two directions are in reasonably good agreement with each other.

The original NRM directions of specimens from the Vanda lamprophyre are distributed around high to low latitude along 228.1° of the meridian shown in Fig. 25c. The patterns of direction changes and intensity variations are quite different from dyke to dyke. In general only small changes are produced by AF demagnetization at 140 Oe and by thermal demagnetization at 300°C; the inclination and declination of the mean NRM as shown in Table 12 do not show a large change, maintaining the same order of confidence, α_{95} ranges from 10.5 to 13.5°. However, these directions are considerably clustered by thermal demagnetization at 400 and 500°C, although a few of them scatter from the cluster. In particular, the inclinations observable at high and middle latitude decrease notably at these temperatures. This characteristic behavior under thermal demagnetization is essentially similar to that of the granitic rock from the bottom of Wright Valley. After thermal demagnetization at 550°C results in no recognizably significant distributions of NRM. For Table 12, data referring to the scattering of Vanda lamprophyre from a cluster by thermal demagnetization at 400 and 500°C, was disregarded for statistical calculation. Since the clearest precision and confidence, K = 15.0 and α_{95} = 6.9°, are obtained by thermal demagnetization at 500°C, the inclination of −20.3° and the declination of 219.8° at that temperature are the most significant paleomagnetic directions for the Vanda lamprophyre.

The distribution of NRM directions from Vanda porphyry samples are shown in Fig. 25d. All specimens have middle to low inclinations for their intial magnetization, with a direction of magnetization significantly different from the earth's geomagnetic field, and they are clustered with a precision of K = 39.1 and a confidence of α_{95} = 4.4°. This distribution characteristic is not changed by AF demagnetization at 140 Oe. However it is changed by thermal demagnetization from 300 to 500°C; the mean direction shifts to low inclination while maintaining a cluster, although a few specimens scatter simultaneously from the cluster. A clear cluster still lies on the equator at 550°C, but many specimens scatter further from the position which existed at 500°C. A total of 9 specimens showing reverse magnetization have inclinations that tend to cluster at high inclinations as shown in Fig. 25d, but the mean direction of these points is consistent with the direction of the magnetic field in the thermal demagnetizer, and these intensities are weak, less than 30% of their original values. It may be, therefore, that the mean direction scattered from the cluster is in fact merely the noise of the mag-

netometer. These samples are disregarded for statistical calculation in Table 12. That is, the original mean NRM direction with an inclination of $-25.1°$ and a direction of 227.8° is settled at -6.6 and 223.0° respectively by thermal demagnetization up to 500°C.

In the case of the "red dyke" rocks, the individual directions of NRM, magnetized at normal polarity, do not make such a clear pattern. However NRMs after AF demagnetization at 140 Oe make a cluster around an inclination of $-61.7°$ and a declination of 238.4°, with α_{95} of 8.1, as shown in Table 12. This tendency of clustering formation is not changed by thermal demagnetization at 300 and 400°C, but these directions are dispersed by thermal demagnetization at more than 500°C.

These results may be summarized as follows: The mean NRM direction of each formation, except for the "red dyke" rocks, is not effectively changed by AF demagnetization at 140 Oe. In the case of the specimens from the "red dyke" rocks, the individual NRM directions are gathered into one direction by AF demagnetization. The mean NRM directions of granitic rocks collected from the bottom of Wright Valley, Vanda lamprophyre and porphyry are shifted gradually to low inclination by thermal demagnetization, and settled along the 210–230° meridian of low latitude at 500–550°C. The differential direction of NRM between the original mean NRM and after thermal demagnetization at 500–550°C is fairly similar to that of Ferrar dolerite for these rocks. The specimens collected from 20 m below the lower boundary of dolerite sill "a", Theseus granodiorite, and the "red dyke" rocks have only a stable NRM direction, similar to that of Ferrar dolerite. That is, they show both or the other one of the NRM direction of Ferrar dolerite in Jurassic age and that of the horizontal component in Cambro-Ordovician age.

From the thermal demagnetizations of all specimens and their basic magnetic properties, the magnetization mechanism for the rock formations of the basement complex in Wright Valley can be explained as follows: The ambient geomagnetic field when the basement complex was formed in 480–500 m.y. (lower Ordovician to early Cambrian) was almost horizontal in McMurdo Sound. This region was then heated up to 500°C by the intrusion of dolerite sills in 160 m.y. (Jurassic age) at the bottom of Wright Valley. Consequently the NRM directions of specimens magnetized in the Cambro-Ordovician age, which have a high blocking temperature of higher than 500°C, have survived (primary magnetization). However, the primary magnetizations of the specimens, which have a blocking temperatures lower than 500°C, have completely disappeared, and the specimens have been remagnetized (secondary magnetization) in the direction of the geomagnetic field when the dolerite sills were intruded into the area during the Jurassic age. On the other hand, before thermal demagnetization those specimens which include in both magnetite and various compositions of titanomagnetite show a superposition of both the primary and secondary magnetization directions at room temperature. The results of basic magnetic analyses suggest that the granitic rocks collected from 20 m under the lower boundary of the dolerite sill, and Theseus granodiorite, have a main NRM blocking temperature of below 400°C and mainly secondary magnetization; granitic rocks collected from the bottom of the valley, and Vanda lamprophyre, have various kinds of blocking temperature, and the NRM directions are distributed between the primary and secondary magnetization directions;

Vanda porphyry has a main blocking temperature of more than 500°C and shows mainly the primary magnetization. With the Vanda "red dyke", the directions of the stable component of magnetization resemble to that of only secondary magnetization NRM direction, although it shows the high magnetite Curie point. The results of thermal demagnetization of the NRM of these samples suggest that the main blocking temperature depends on a 300°C Curie point rather than a 570°C one.

8.3. Paleomagnetic discussion

The VGP positions obtained from the mean NRM direction of each formation and sampling site are shown in Table 13 and illustrated in Fig. 26. Rb-Sr ages are determined as 500 ± 43 m.y. (FAURE and JONES, 1973) for granitic rock and 470 ± 7 and 480 ± 44 (JONES and FAURE, 1967; FAURE and JONES, 1973) for Vanda porphyry. The intrusive sequence of Vanda lamprophyre is younger than granitic rock but older than Vanda porphyry according to field evidence (MCKELVEY and WEBB, 1961). Therefore it is possible that the basement complex of Wright Valley records the secular variation of the geomagnetic field for 20–30 m.y. in the Cambro-Ordovician age. The VGP positions for granitic rock, Vanda lamprophyre and porphyry obtained by thermal demagnetization at 500°C are located near the equator of present-day Africa. However these positions cannot be distinguished clearly from each other within 95% level of confidence (See Table 12). The deviation angles (Θ) between these mean NRM directions are within 8.8° which is of the same order of magnitude as the α_{95} values of the respective rock formations. Since Vanda lamprophyre and porphyry are included in

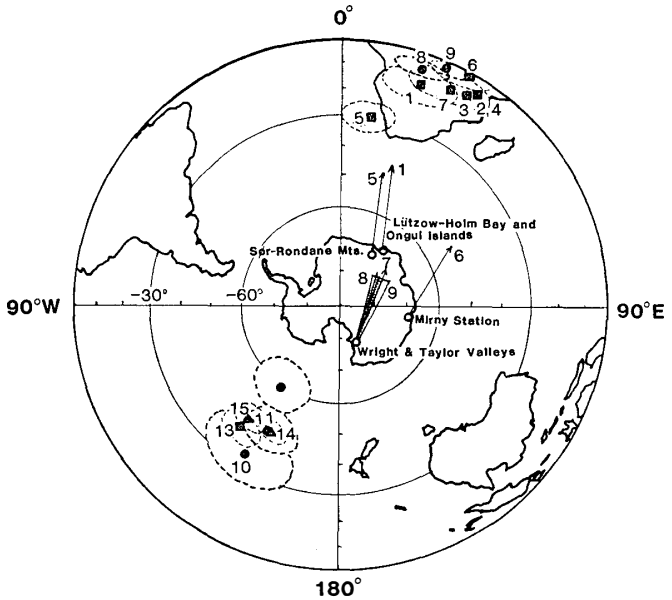

Fig. 26. Positions of VGP in Cambro-Ordovician age for Antarctica and the declinations of NRM. 1. Ongul Islands (NAGATA and SHIMIZU, 1959), 2 and 3. Ongul Islands (NAGATA and YAMA-AI, 1961), 4. Lützow-Holm Bay (KANEOKA et al., 1968), 5. Sør Rondane Mts. (ZIJDERVELD, 1968), 6. Mirny Station (MCQUEEN et al., 1972), 7. Taylor Valley (MANZONI and NANNI, 1977), 8–12. This study, 13. Wright Valley (Ferrar dolerite), 14. This study, 15. Wright and Victorial Valleys (Ferrar dolerite; BULL et al., 1962). Equal-area projection.

Table 13. Paleomagnetic results of the Cambro-Ordovician rocks and Ferrar dolerite for Antarctica.

Sampling site	N	Inc	Dec	α_{95}	pLat	pLon	Remarks
1. Ongul Islands	18	51°	337°	7°	19°S	17°E	NAGATA and SHIMIZU (1959)
2. Ongul Islands	5	49	350	—	9°S	32°E	NAGATA and YAMA-AI (1961)
3. Lützow-Holm Bay	7	60	341	—	21°S	24°E	NAGATA and YAMA-AI (1961)
4. Lützow-Holm Bay	4	46.5	353	—	7°S	33°E	KANEOKA *et al.* (1968)
5. Sør Rondane Mts.	16	64	341.5	4.5	28.5°S	9.5°E	ZIJDERVELD (1968)
6. Mirny Station	37	16.9	294.2	15.6	1.5°S	28.5°E	MCQUEEN *et al.* (1972)
7. Taylor Valley	51	0.6	222.6	10.9	9.3°S	26.7°E	MANZONI and NANNI (1977)
8. Wright Valley	16	−9.0	216.7	8.1	5.4°S	18.5°E	This study. Granitic rocks from bottom of Wright Valley. Thermal demag. at 500°C.
9. Wright Valley	58	−13.2	222.4	5.2	2.5°S	23.8°E	This study. Vanda lamprophyre and porphyry from Wright Valley. Thermal demag. at 500°C.
10. Wright Valley	13	−61.7	238.4	9.0	35.5°S	148.1°W	This study. Vanda "red dyke". AF demag. at 140 Oe.
11. Wright Valley	4	−69.1	237.7	4.7	44.9°S	151.8°W	This study. Granitic rocks from 20m below of lower boundary of Ferrar dolerite.
12. Wright Valley	10	−75.8	230.2	4.3	54.0°S	162.0°W	This study. Theseus granodiorite. Thermal demag. at 300°C.
13. Wright and Victoria Valleys	58	−64	247	4	40°S	140°W	BULL *et al.* (1962)
14. Wright Valley (Ferrar dolerite)	26	−69.4	237.6	2.4	45.3°S	152°W	This study.
15. Wright and Victoria Valleys (Ferrar dolerite)	83	−68	250	3	45°S	140°W	BULL *et al.* (1962)

the same age as Victoria Intrusive (McKELVEY and WEBB, 1961), these two data are combined in Table 13. This experimental result suggests that the geomagnetic field in this region was constant in direction for 20–30 m.y. in the Cambro-Ordovician period (500 m.y. ago), since the reheating of the whole area during the last phase of the Victoria Intrusive in the Ordovician (470–480 m.y. ago).

MANZONI and NANNI (1977) obtained a VGP position of 470 m.y. ago from lamprophyre dykes, maybe the same sequence as the Vanda lamprophyre, in Taylor Valley which is 20 km south of Wright Valley. Their VGP position is located in almost the same area as our VGP positions. The Θ value for VGPs for the lamprophyre dykes in Wright and Taylor Valleys is 11.8°. With the α_{95} value of Taylor Valley lamprophyre ($\alpha_{95}=10.9$), the separate VGP positions are in reasonably good agreement with each other. McQUEEN *et al.* (1972) reported a VGP position of the Cambro-Ordovician age from charnockitic rocks (502 ± 24 m.y. in age) at Mirny Station (66°33′S, 93°01′E). This value, as shown in Table 13, is located in almost the same position as the data from the Wright and Taylor Valleys.

High-grade metamorphic rocks with pegmatite and metabasite dykes are distributed along most parts of the coast line of Lützow-Holm Bay, including Syowa Station (69°01′S, 35°35′E), (*e.g.* TATSUMI and KIKUCHI, 1959). Geochronological investigations by the Pb-U and Rb-Sr radiometric method show that most of the rock formations have a metamorphic age of around 500 m.y. in this region, namely the Cambro-Ordovician age. Paleomagnetic investigations of these formations have been carried out by NAGATA and SHIMIZU (1959, 1960), NAGATA and YAMA-AI (1961) and KANEOKA *et al.* (1968). They reached the general conclusion that the pole-position of the earth's magnetic dipole was situated near the equator in the Cambro-Ordovician age as shown in Table 13 and Fig. 26; VGPs from the Wright and Taylor Valleys, Mirny Station and Lützow-Holm Bay were located around 0.9°N–21°S in the latitude of Africa. The mean VGP position of these 9 data yields 9.5°S latitude and 24.5°E longitude.

However a VGP position of the same age from the Sør Rondane Mountains (72°S, 24°E) was isolated from the other data in East Antarctica as shown in Fig. 26. It can not be concluded that this deviation of the VGP for Sør Rondane Mountains is due to significant geomagnetic secular variation or the influence of a non-dipole components of the geomagnetic pole, taking into account the α_{95} and Θ values; the angular deviation Θ is 11.7° between this location and the closest neighboring data (Ongul Islands (1) in Table 13) and the value of α_{95} for each is 7 and 4.5° respectively.

Taking into account these VGP distributions, paleomagnetic results may be concluded as follows: Antarctica was located in approximately the position of present-day Africa below the equator in the Cambro-Ordovician age; Antractica had few tectonic motions for 20–30 m.y. during that age as compared to the geomagnetic dipole; the Transantarctic Mountains should be included in East Antarctica.

The directions of MRM declination in the Cambro-Ordovician age for the whole of East Antarctica are shown according to the location of respective sampling sites in Fig. 26. A representative declination for Ongul Islands and Lützow-Holm Bay is adopted from the data of NAGATA and SHIMIZU (1959), as the number of examined samples is statistically very small in the case of the others. Ranges of 95% confidence of declination obtained in this study for granitic rock (α_{95} (Dec) = 4.7°) and Vanda lam-

prophyre and porphyry (α_{95} (Dec) $=3.5°$) are also illustrated in Fig. 26. A remarkable characteristic of these directions is that they are approximately parallel in the case of the samples from Ongul Islands and Sør Rondane Mountains, and those from Mirny Station, Taylor Valley and Wright Valley. The angular deviation is 15–20° for these two groups. On the assumption that the structure of the earth's geomagnetic field in the Cambro-Ordovician age was similar to that of the present, the standard precision of the nondipole geomagnetic field at low in latitude in the southern hemisphere is probably 8–10° (Cox, 1962). That is, the angular deviation of declination is twice that of the nondipole precision. If the magnetization age is assumed to be almost the same, a simple interpretation may be proposed as follows: In the Cambro-Ordovician age rock formations were magnetized in the same direction at these locations, and a rift later formed in East Antarctica between Queen Maud Land and Wilkes Land. The most reliable possibility for the location of the boundary of the rifting zone may be along the Amery Ice Shelf to the Lambert Glacier. According to deep seismic soundings and aeromagnetic data by the Soviet Antarctic Expedition in 1973, a crustal feature of the Mac. Robertson–Princess Elizabeth Land through the Lambert Glacier is large-scale normal faulting and the resulting development of a deep graben filled with low-density rocks; the density is 2.3 and the density of country rock is 2.8. Beneath the graben, the crustal thickness is as low as 22–24 km, while on both sides of the graben, the crust is 30–34 km thick (KURININ and GRIKUROV, 1982; FEDOROV *et al.*, 1982). They suggested that the beginning of rifting was in the late Mesozoic period according to geological evidence. The features of topography under the ice sheet in these areas suggest that a large valley extends to the south from the Amery Ice Shelf (*i.e.* BAKAYEV, 1966). The magnetization directions of Cambro-Ordovician rocks in East Antarctica support their results completely and suggest that the rifting angle is about 15–20°.

The VGP position of samples collected from 20 m below the lower boundary of the Ferrar dolerite sill is fairly consistent with that of Ferrar dolerite as obtained by BULL and IRVING (1960) and BULL *et al.* (1962); their ellipses of 95% confidence overlap each other as shown in Fig. 26. It seems therefore that the granitic rocks were heated to above the Curie point by contact with a contacted dolerite sill. The VGP position of Theseus granodiorite collected from the bottom of the valley is near that of Ferrar dolerite, but is not completely consistent, taking into account the α_{95} value. The geological evidence shows that the three dolerite sills which intruded in Wright Valley were not intruded simultaneously; these are referred to as "a" "b" and "c" from lower to higher altitude (MCKELVEY and WEBB, 1961). On the other hand there is a possibility that a hidden sill intruded into the basement complex under the surface of the bottom of Wright Valley. Although no dolerite sills were observed within a 85.7 m core by the Dry Valley Drilling Project (DVDP) No. 4 (CARTWRIGHT *et al.*, 1974) at Lake Vanda in the middle of Wright Valley, a dolerite sill of 39.53 m thickness was observed under 12.6 m of sediment by DVDP 13 core at Don Juan Pond in upper Wright Valley (MUDREY *et al.*, 1975). Therefore it is difficult to determine which sills strongly affected the magnetic properties of the rock formations at the bottom of Wright Valley. Since the thickness of sills "a" "b" and "c" are 250, 180 and 120 m respectively (MCKELVEY and WEBB, 1961) and the vertical distance from the lower

boundary of sill "a" to the bottom of the valley is estimated at about 600 m, thermal influence by sill "a" was probably of the most importance for these formations. A mathematical estimate of the temperature in the neighborhood of a cooling intrusive sheet was given by CARSLAW and JAEGER (1959). The assumptions on which the calculation was based, and the notation used, are as follows: A dolerite sill of thickness $2a$ and temperature V_0, intrudes into the infinite country rock mass of constant temperature V_1. The physical properties of the sill and the country rock are the same, as thermal conductivity K, density ρ, specific heat c and diffusibility κ, where $\kappa = K/c$. The temperature after t time is given by

$$V = \frac{1}{2}(V_1 - V_0)\left\{\operatorname{erf}\frac{a-x}{2\sqrt{\kappa t}} + \operatorname{erf}\frac{a+x}{2\sqrt{\kappa t}}\right\}, \quad \cdots\cdots(1)$$

where x is the distance from the center of the sill, and

$$\operatorname{erf} x = \frac{2}{\sqrt{\pi}}\int_0^x e^{-\xi^2}\, d\xi \quad \cdots\cdots(2)$$

is the tabulated error function. When the values K, ρ and c are supposed as 0.006, 2.6 and 0.25 respectively; $\kappa \simeq 0.01$ in eq. (1). The correlations among x and t are shown in Fig. 27, where $V_0 = 0°C$, $V_1 = 1100°C$ and $a = 120$ m. The maximum temperature attained in granite at a distance of 120 m from the point of contact of a dolerite sheet 240 m thick would be nearly 300°C after 625 year; at a distance of 600 m from the point of contact it would be approximately 100°C after 15000 year. From this viewpoint, it would be impossible to raise the temperature at the bottom of the valley up to 500°C by simple heating of sill "a". The same results were obtained even though the physical properties were different from each other by JAEGER (1957, 1959). Since

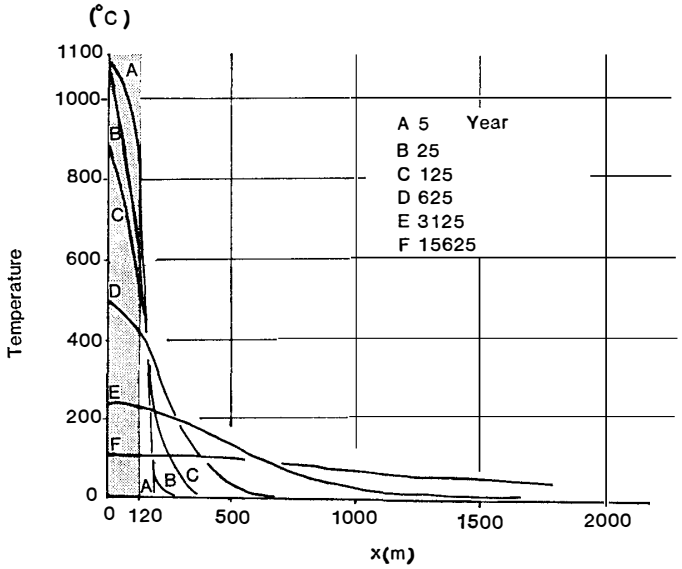

Fig. 27. Temperature in the neighborhood of a Ferrar dolerite sill. Thickness of the sill $2a = 240$ m, temperature of the sill $V_1 = 1100°C$, diffusibility $\kappa = 0.01$, distance x m from the center of the sill.

the vertical distances between the centers of the sills are estimated as 490 m for "a"–"b" and 650 m for "b"–"c", sills "b" and "c" would have almost no thermal effect at the bottom of Wright Valley. Therefore the most prominent thermal source for that location may be a huge hidden dolerite body. According to BULL *et al.* (1962), the directions of magnetization of sills "a", "b" and "c" are consistent with each other to within 95% confidence. Since the ellipse of α_{95} for Theseus granodiorite does not overlap with them, it is possible that the formations at the bottom of Wright Valley could have been heated by hidden sills rather than by sills "a", "b" and "c". The maximum increase in temperature caused by intrusion for granitic rocks 20 m below the lower boundary of sill "a" is estimated at more than 600°C according to Fig. 27. Their Curie points are estimated at 300–400°C by thermal demagnetization; all directions disperse at this temperature (see Fig. 25a). Therefore these granitic samples must have been heated by sill "a" to a temperature above the Curie point and were remagnetized at that time; later the magnetization directions of these samples were probably remagnetized to that of Ferrar dolerite.

8.4. Concluding remarks

The specimens collected from granitic rocks, Theseus granodiorite, Vanda lamprophyre and porphyry in Wright Valley have fairly stable magnetization, and the "red dyke" rocks have a component of stable magnetization against AF demagnetization; magnetic grains in these samples probably have an almost single- or pseudosingle-domain structure. Almost all the specimens are magnetized to the normal polarity and their directions are limited to be the 220–250° meridian.

Formations at the bottom of Wright Valley were heated up to 500°C, probably by the intrusion of a large hidden dolerite body of the Jurassic age. Consequently, the primary magnetizations acquired in the Cambro-Ordovician age survived in the case of the samples which have a higher Curie point than 500°C, but the samples with a lower one were remagnetized to a geomagnetic field direction in the Jurassic age. In the case of granitic rock, Vanda lamprophyre and porphyry, superposition of primary and secondary magnetization is observable at room temperature. These two kinds of magnetization can be separated by thermal demagnetization at 500°C. On the other hand, the samples of Theseus granodiorite and "red dyke" were remagnetized completely and have only the secondary magnetization direction.

Obtained VGP positions of the Cambro-Ordovician age of primary magnetization in Wright Valley are located in present-day Africa below the equator. These positions are consistent with the other 7 previous data for rock of the same age in East Antarctica. The direction of mean declination at each site is approximately parallel for the samples from Ongul Islands and Sør Rondane Mountains, and for those from Mirny Station, Taylor Valley and Wright Valley. The angular deviation between these two groups is 15–20°. The simplest interpretation of this is that East Antarctica rifted along the Amery Ice Shelf to the Lambert Glacier at a relative angle of 15–20°. The limited distribution of these VGPs suggest that Antarctica had very few tectonic motions for 20–30 m.y. during the Cambro-Ordovician age in relation to the geomagnetic dipole field. The Transantarctic Mountains should be considered a part of the East Antarctic plate.

9. Synthesizing Paleomagnetic Discussions and Concluding Remarks

The results of analyses of Cenozoic volcanic rocks, 13 basaltic leva flows and one pyroclastic breccia, in McMurdo Sound, dating from late Tertiary to Quaternary age, show that the distributions of VGP are clustered within a polar cap area of approximately 30° in colatitude. The center is in almost the same position as the geographical South Pole rather than the present geomagnetic dipole. This indicates that Antarctica was situated in almost exactly the same position as at present by at least late Pliocene time. This distribution of VGP is caused by the nondipole geomagnetic field rather than by continental drift.

The eruptive sequence of the McMurdo volcanics in the sampling area from latest to earliest is estimated as follows: Twin Crater and Cape Royds (Brunhes Epoch), Half Moon Crater (Jaramillo Event), Observation Hill and Cape Armitage (Matuyama Epoch), Crater Hill and Castle Rock (Olduvai or Réunion Events) and Taylor Valley (Kaena Event).

The NRMs of Ferrar dolerite collected from the Wright Valley, Allan Hills and Mt. Fleming have a stable TRM for the time of the intrusion of Ferrar dolerite in the Jurassic period. However the samples from Carapace Nunatak are unstable compared with the former. The obtained VGP positions including a previous 7 sites along the Transantarctic Mountains are clustered on a center of 53.9°S, 141.8°W in the present South Pacific Ocean.

The Beacon Supergroup from Mt. Circe, Knobhead and Mt. Fleming have been thermally affected by the intrusion of Ferrar dolerite sills or dykes. Consequently these samples were remagnetized to the Jurassic field direction. Samples from site C in Allan Hills have a stable DRM for the Permo-Triassic period. The NRM direction is almost parallel to that of the Jurassic dyke caused by Ferrar dolerite. This indicates that East Antarctica had no shift against VGP from late Permian to Jurassic time. This estimation is consistent with the results of paleomagnetic analyses of Australia in the Messozoic period.

The formations at the bottom of Wright Valley were heated up to 500°C by the intrusion of a huge hidden Ferrar dolerite body in the Jurassic period. Consequently, the primary magnetization acquired in the Cambro-Ordovician period survived for the

samples which contain magnetite grains and disappeared for the samples which contain titanomagnetite grains. In the case of granitic rock, Vanda lamprophyre and porphyry, a superposition of primary and secondary magnetization caused by Ferrar dolerite is observable at room temperature. On the other hand, the samples of Theseus granodiorite and "red dyke" were completely remagnetized and have mainly secondary magnetization.

The VGPs positions obtained for the Cambro-Ordovician period from primary magnetization at the bottom of Wright Valley are located in present-day Africa below the equator. These positions are consistent with previous data for same period from East Antarctica. This NRM declination suggests that East Antarctica rifted along the Amery Ice Shelf to the Lambert Glacier at a relative angle of 15–20°. These VGP distributions suggest that Antarctica had scarcely any tectonic motions for 20–30 m.y. during the Cambro-Ordovician period, and that the boundary of East and West Antarctica is located in the Ross and Weddell Seas.

Up to now there have been only a limited number of paleomagnetic results for Antarctica, as most of the work has revolved around studies of Ferrar dolerite in the Jurassic age and the basement complex in the Cambro-Ordovician ages. McELHINNY (1973) summarized the previous data and estimated the polar-wander path for East Antarctica, as shown in Fig. 28. The paleomagnetic results obtained in this study not only verify the reliability of previous VGP positions of the Cambro-Ordovician and Jurassic ages, but also determine new VGP positions for the Permo-Triassic and Cenozoic ages.

The apparent polar-wander path for East Antarctica was obtained by McELHINNY (1973) as shown in Fig. 28 using only a limited number of paleomagnetic results; the path is traced using one Cambro-Ordovician positions, one Jurassic and two Cenozoic.

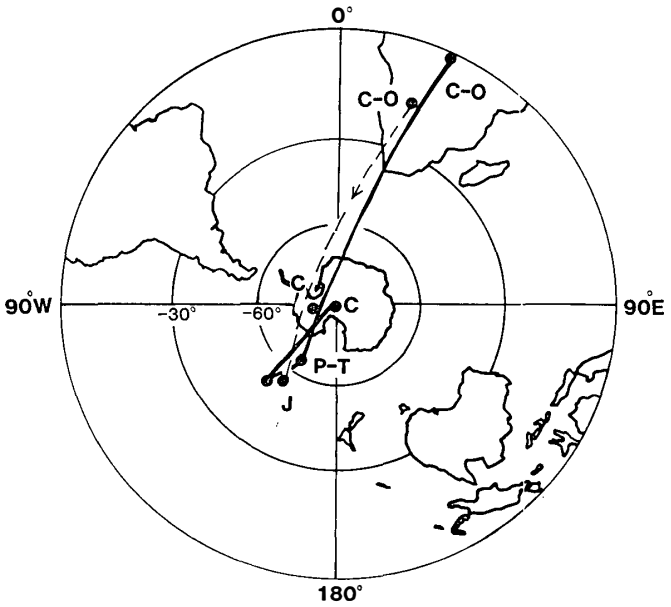

Fig. 28. Apparent polar-wander paths for Antarctica. C-O: Cambro-Ordovician, P-T: Permo-Triassic, J: Jurassic, C: Cenozoic age. Solid line: This study, Dotted line: Previous path (McELHINNY, 1973). Equal-area projection.

Attempts to determine the NRM direction of the Devonian and late Permian Beacon Supergroups (sandstone) proved unsuccessful (TURNBULL, 1959; BULL *et al.*, 1962), both results suggesting that they were remagnetized at the time of the intrusion of Ferrar dolerite. Consequently the apparent polar-wander path, using previous data for East Antarctica from the Cambrian to the Mesozoic age could not be determined in detail as for other fragments of the Gondwana continent. The results of this study support the reliability of the apparent polar-wander path for the Cambro-Ordovician and Jurassic ages; furthermore a new VGP position for the Permo-Triassic age has been determined as shown in Fig. 28. Since the distributions of the Cenozoic VGP position are clustered to within about 30° of colatitude in the polar cap area due to the nondipole component of the geomagnetic field, the apparent polar-wander path in the Cenozoic period cannot be determined in detail paleomagnetically. However it suggests that the VGP at that time was located at the geographical South Pole. Even the improved polar-wander path for East Antarctica in Fig. 28 cannot be compared to that for other fragments of Gondwanaland for the whole age because so few points have been located for the age.

Pole positions of the early Paleozoic and Jurassic ages for East Antarctica are plotted in Fig. 29 together with data for Australia, Africa, South America and India. The VGP positions for Antarctica in this figure are summarized in Figs. 18 and 26. For the data of the southern continents and India, the following studies should be referred to: Australia; J1 IRVING (1963): J2 STOTT (1963): O1 MCELHINNY (1973), Africa; J3

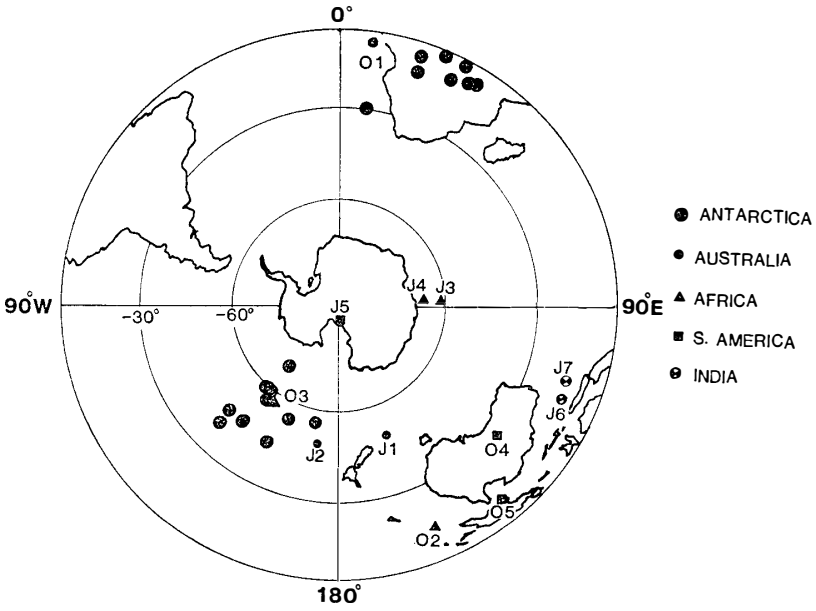

Fig. 29. VGP positions for Jurassic and Ordovician to Cambrian ages relative to the present distribution of Gondwana fragments. Antarctica: Referred in Figs. 18 and 26 (this study). Australia; J1: IRVING (1963), J2: STOTT (1963), O1: MCELHINNY (1973). Africa; J3 and J4: MCELHINNY and JONES (1965), O2: BROCK (1967), O3: HELSLEY (1965). South America; J5 CREER (1962), O4 CREER (1965), O5: CREER (1970). India; J5: RADHAKRISHNAMURTY (1963). J1–J6: Jurassic VGPs, O1–O5: Ordovician or Cambrian VGPs. Equal-area projection.

and J4 McElhinny and Jones (1965): O2 Brock (1967): O3 Helsley (1965), South America; J5 Creer (1970): O4 Creer (1965): O5 Creer (1970), India; J6 Radhakrishnamurty (1963): J7 Clegg (1958). Data obtained from formations similar geologically and geochronologically to Ferrar dolerite is found in J1 and J2 for Tasmania dolerite and J3 and J4 for Karroo dolerite in Africa. The ages of other Jurassic pole positions also correspond to that of Ferrar dolerite. The VGP of Early Paleozoic pole positions are plotted from the Cambrian to the Ordovician age.

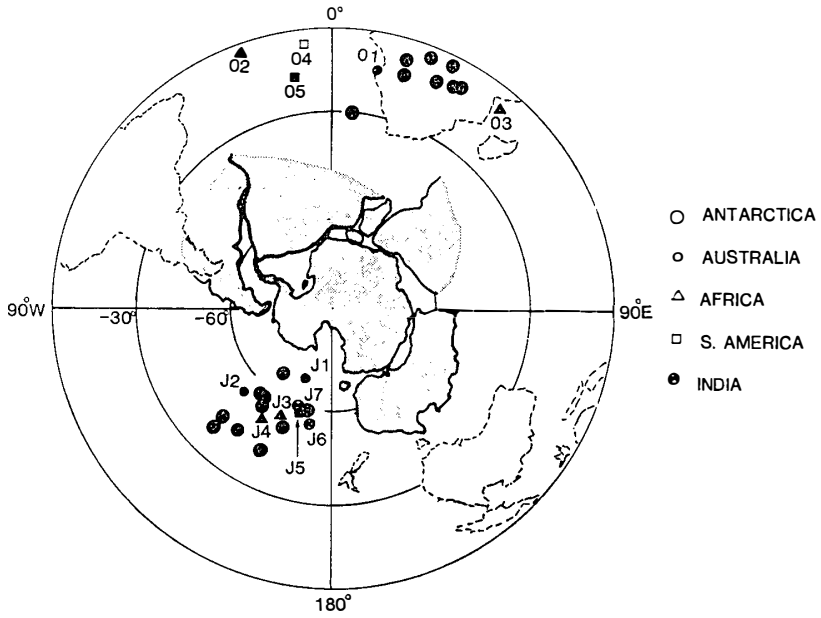

Fig. 30. VGP positions relative to due Smith and Hallam (1970) reconstruction of Gondwanaland. The poles are labelled as in Fig. 29. Equal-area projection.

Many reconstructions of Gondwanaland are available; we have selected the one made by Smith and Hallam (1970), which is geometrically and geologically closest. According to their investigation, the rotation pole positions and the angles between each Gondwana fragment are as follows: South America–Africa 44°N, 30.6°W, 57°; India–Antarctica 1°N, 7.7°W, −88.9°; Antarctica–Africa 1.3°N, 36°W, 58.4°; Australia–Antarctica 3.6°S, 40°E, −31°, for latitude, longitude and angle respectively. In Fig. 29, the VGP positions of different continents are widely scattered. However if these positions are rotated about their respective rotation poles, where Antarctica is fixed, individual VGPs are clustered in two separate areas as shown in Fig. 30. That is, the Jurassic poles for every continent are gathered around the VGP positions of Ferrar dolerite, and clustered around the lower latitude of the Atlantic Ocean and present-day Africa according to early Paleozoic data. It has been commonly accepted for many years that the southern continents including India were once a continuous land mass–Gondwanaland. It began the breakup from Middle Jurassic age at the time of the dolerite intrusion into the continent; the paleomagnetic data strongly support the reconstruction model by Smith and Hallam (1970).

10. Summary

The samples collected from the McMurdo Sound region from the Cambro-Ordovician to the Cenozoic age were examined magnetically for their hysteresis properties, thermomagnetic properties, and stability against AF and thermal demagnetization. Based on the results of these examinations, samples with stable remanent magnetization were subjected to paleomagnetic investigation. The results are as follows:

1. The VGPs from the late Tertiary to the Quaternary period cluster within about 30° in colatitude, and the center is situated on the geographical South Pole rather than the present-day geomagnetic dipole.
2. The position of Antarctica has hardly changed from at least late Tertiary time.
3. The eruptive sequence of the Cenozoic volcanics of Hut Point Peninsula, Cape Royds and Taylor Valley was determined.
4. The mean VGP positions obtained for Ferrar dolerite in the Transantarctic Mountains in the Jurassic age are located in the present-day South Pacific Ocean.
5. Wide areas of the basement complex and the Beacon Supergroup in the McMurdo Sound region were heated and were remagnetized by the Ferrar dolerite intrusion.
6. The NRM direction of the Beacon Supergroup, with a stable NRM, is parallel to that of Ferrar dolerite.
7. The DRM in the Permo-Triassic age was found in the Beacon Supergroup at Allan Hills. The VGP position is almost the same as in the Jurassic age; Antarctica showed almost no shift from the late Permian to the Jurassic period.
8. From the comparison of paleomagnetic data from Mesozoic time for Antarctica and Australia, both continents were part of Gondwanaland up to at least the Jurassic period.
9. The bottom of Wright Valley was heated to 500°C by a large hidden Ferrar dolerite body in the Jurassic age. Consequently, the NRMs of many formations consist of primary and secondary magnetization superposed.
10. The VGP position in the Cambro-Ordovician age for the Wright Valley is in present at Africa below the equator. This location is consistent with that from the whole of East Antarctica at the same period.
11. From the deviation of the declinations of Queen Maud Land and Wilkes

Land in the Cambro-Ordovician age, we deduce that East Antarctica was rifted along the Amery Ice Shelf and the Lambert Glacier at an angle of 15–20°.

12. Paleomagnetically, the McMurdo Sound region is part of East Antarctica, and the boundary of East–West Antarctica is in the Ross–Weddell Sea.

13. Newly apparent polar-wander path from the Cambro-Ordovician to the Jurassic age was determined for Antarctica.

14. The reconstruction model of the Gondwanaland by SMITH and HALLAM (1970) is strongly supported by paleomagnetic data in this study.

15. The southern continent including India are continuous large land mass, Gondwanaland, at least the Jurassic age, and the break up had after begun at the time of the Ferrar dolerite intrusion into the Gondwanaland.

Acknowledgments

The author wishes to thank Prof. T. NAGATA, the director of the National Institute of Polar Research (NIPR), and Prof. A. TAKAGI, Tohoku University, for their paleomagnetic suggestions and encouragements. Thanks are also due to Prof. Y. YOSHIDA, NIPR, for supplying some samples for this investigation and for his geoscientific suggestions, to Dr. K. YANAI, NIPR, for his geological suggestions, to Dr. Y. KONO, Kanazawa University, for geophysical information and to Prof. HOSHIAI, NIPR, for his encouragement. This research was carried out in the 1977–1979 austral summer seasons with the support of the U.S. National Science Foundation.

References

AKIMOTO, S., KATSURA, T. and YOSHIDA, M. (1957): Magnetic properties of $TiFe_2O_4$-Fe_3O_4 system and their change with oxidation. J. Geomag. Geoelectr., **9**, 165–178.

ALLAN, A. D. and GIBSON, G. W. (1961): Geological investigation in southern Victoria Land, Antarctica. Part 6-Outline of the geology of the Victoria Valley region. N. Z. J. Geol. Geophys., **5**, 234–242.

ANGINO, E. E., TURNER, M. D. and ZELLER, E. J. (1962): Reconnaissance geology of lower Taylor Valley, Victoria Land, Antarctica. Geol. Soc. Am. Bull., **73**, 1533–1562.

ARMSTRONG, R. L. (1978): K-Ar dating: Late Cenozoic McMurdo volcanic group and Dry Valley glacial history, Victoria Land, Antarctica. N. Z. J. Geol. Geophys., **21**, 685–698.

BAKAYEV, V. G. ed. (1966): Atlas Antarktiki (Atlas of Antarctica), Tom 1. Moskva, Glavnoe Vpravlenie Geodezii i Kartografii, 255p.

BALLANCE, P. F. and WATTERS, W. A. (1971): The Mawson diamictite and the Carapace sandstone, formations of the Ferrar group at Allan Hills and Carapace Nunatak, Victoria Land, Antarctica. N. Z. J. Geol. Geophys., **14**, 512–527.

BECK, M. E. (1972): Paleomagnetism and magnetic polarity zones in the Jurassic Dufek intrusion, Pensacola Mountains, Antarctica. Geophys. J. R. Astron. Soc., **28**, 49–63.

BLUNDELL, D. J. and STEPHENSON, P. J. (1959): Paleomagnetism of some dolerite intrusions from the Theron Mountains and Whichaway Nunatak, Antarctica. Nature, **184**, 1860.

BRIDEN, J. C. and OLIVER, R. L. (1963): Paleomagnetic results from the Beardmore Glacier region, Antarctica. N. Z. J. Geol. Geophys., **6**, 388–394.

BROCK, A. (1967): Paleomagnetic results from the Hook Intrusives, Zambia. Nature, **216**, 359–360.

BULL, C. and IRVING, E. (1960): The paleomagnetism of some hypabyssal intrusive rocks from South Victoria Land, Antarctica. Geophys. J. R. Astron. Soc., **3**, 211–224.

BULL, C., IRVING, E. and WILLIS, I. (1962): Further paleomagnetic results from South Victoria Land, Antarctica. Geophys. J. R. Astron. Soc., **6**, 320–336.

BURMESTER, R. F. and SHERIFF, S. D. (1980): Paleomagnetism of the Dufek intrusion, Pensacola Mountains, Antarctica. Antarct. J. U.S., **15**(5), 43–45.

CARSLAW, H. S. and JAEGER, J. C. (1959): Conduction of Heat in Solid, 2nd ed. Oxford, Oxford Univ. Press, 54.

CARTWRIGHT, K., TREVES, S. B. and TORII, T. (1974): Geology of DVDP 4, Lake Vanda, Wright Valley, Antarctica. DVDP Bull., **3**, 49–74.

CHAMALAUN, F. H. (1968): Paleomagnetism of Réunion Island and its bearing on secular variation. J. Geophys. Res., **73**, 4647–4659.

CLEGG, J. A. (1958): Remanent magnetism of the Rajmahal Traps of North-Eastern India. Nature, **181**, 830–831.

COLE, J. W., KYLE, P. R. and NEALL, V. E. (1971): Contributions to Quaternary geology of Cape Crozier, White Island and Hut Point Peninsula, McMurdo Sound region, Antarctica. N. Z. J. Geol. Geophys., **14**, 528–546.

COX, A. (1962): Analysis of present geomagnetic field for comparison with paleomagnetic results. J. Geomagn. Geoelectr., **13**, 101–112.

COX, A. (1966): Paleomagnetic research on volcanic rocks of McMurdo Sound. Antarct. J. U.S., **1**(4), 136.

COX, A. (1969): Geomagnetic reversals. Science, **163**, 237–245.

COX, A. and DOELL, R. R. (1964): Long period variations of the geomagnetic field. Bull. Seismol. Soc. Am., **54**, 2243–2270.

CREER, K. M. (1965): Paleomagnetic data from the Gondwanic continents. A symposium on continental drift-III. Phil. Trans. R. Soc. London, **A256**, 569–573.

CREER, K. M. (1970): A paleomagnetic survey of South American rock formations. Philos. Trans. R. Soc. London, **A267**, 457–558.

DELISLE, G. (1983): Results of paleomagnetic investigations in northern Victoria Land. Antarctic

Earth Science, ed. by R. L. OLIVER, P. R. JAMES and J. B. JAGO. Cambridge, Cambridge Univ. Press, 146–149.

DEUTSCH, S. and GRÖGLER, N. (1966): Isotopic age of Olympus granite-gneiss (Victoria Land-Antarctica). Earth Planet. Sci. Lett., **1**, 82–84.

DEUTSCH, S. and WEBB, P. N. (1964): Sr/Rb dating of basement rock from Victoria Land; Evidence for a 1000 million year old event. Antarctic Geology; Proceedings of the first International Symposium on Antarctic Geology, Cape Town, 1963, ed. by R. F. ADIE. Amsterdam, North-Holland, 557–562.

FAURE, C. and JONES, L. M. (1973): Isotopic composition of strontium and geologic history of the basement rocks of Wright Valley, South Victoria Land, Antarctica. N. Z. J. Geol. Geophys., **17**, 611–627.

FEDOROV, L. V., GRIKUROV, G. E., KURININ, R. G. and MASOLOV, V. N. (1982): Crustal structure of the Lambert Glacier area from geophysical data. Antarctic Geoscience, ed. by C. CRADDOCK. Madison, Univ. Wisconsin Press, 931–936.

FORBES, R. B., TUNER, D. L. and CARDEN, J. R. (1974): Age of trachyte from Ross Island, Antarctica. Geology, **2**, 297–298.

FUNAKI, M. (1979): Paleomagnetism of Hut Point Peninsula volcanic sequence. Mem. Natl Inst. Polar Res., Spec. Issue, **14**, 186–193.

FUNAKI, M. (1983a): Paleomagnetic investigation of McMurdo Volcanics, Antarctica. Nankyoku Shiryô (Antarct. Rec.), **77**, 1–19.

FUNAKI, M. (1983b): Paleomagnetic investigation of Ferrar dolerite in the McMurdo Sound region, Antarctica. Nankyoku Shiryô (Antarct. Rec.), **77**, 20–32.

FUNAKI, M. (1983c): Paleomagnetic investigation of the Beacon Group in the McMurdo Sound region, Antarctica. Nankyoku Shiryô (Antarct. Rec.), **78**, 1–14.

GOLDICH, S. S., NIER, A. O. and WASHBURN, A. L. (1958): A^{40}/K^{40} age of gneiss from McMurdo Sound, Antarctica. Trans. Am. Geophys. Union, **39**, 956–958.

GRINDLEY, G. W., ADAMS, C. J. D., LUMB, J. T. and WATTERS, W. A. (1977): Paleomagnetism, K-Ar dating and tectonic interpretation of upper Cretaceous and cenozoic volcanic rocks of the Chatham Islands, New Zealand. N. Z. J. Geol. Geophys., **20**, 425–467.

GUNN, B. M. (1962): Differentiation in Ferrar dolerites, Antarctica. N. Z. J. Geol. Geophys., **5**, 820–863.

GUNN, B. M. and WARREN, G. (1962): Geology of Victoria Land between the Mawson and Mulock Glaciers, Antarctica. N. Z. Geol. Surv. Bull., n.s., **71**, 157p.

HAMILTON, W. (1967): Tectonics of Antarctica. Tectonophysics, **4**, 555–568.

HARRINGTON, H. J. (1958): Nomenclature of rock units in the Ross Sea region, Antarctica. Nature, **182**, 290.

HELSLEY, C. E. (1965): Paleomagnetic results from the middle Cambrian of northwest Africa. Trans. Am. Geophys. Union, **46**, 67.

IRVING, E. (1963): Paleomagnetism of the Narrabeen Chocolate Shales and the Tasmanian dolerite. J. Geophys. Res., **68**, 2283–2287.

IRVING, E., ROBERTSON, W. A. and STOTT, P. M. (1963): The significance of the paleomagnetic results from Mesozoic rocks of Eastern Australia. J. Geophys. Res., **68**, 2313–2317.

JAEGER, J. C. (1957): The temperature in the neighborhood of a cooling intrusive sheet. Am. J. Sci., **225**, 306–318.

JAEGER, J. C. (1959): Temperatures outside a cooling intrusive sheet. Am. J. Sci., **257**, 44–54.

JONES, L. M. and FAURE, G. (1967): Age of the Vanda porphyry dykes in Wrighy Valley, southern Victoria Land, Antarctica. Earth Planet. Sci. Lett., **3**, 321–324.

KANEOKA, I., OZIMA, M., OZIMA, M., AYUKAWA, M. and NAGATA, T. (1968): K-Ar age and paleomagnetic studies on rocks from the east coast of Lützow-Holm Bay, Antarctica. Nankyoku Shiryô (Antarct. Rec.), **31**, 12–20.

KURININ, R. G. and GRIKUROV, G. E. (1982): Crustal structure of part of East Antarctic from geophysical data. Antarctic Geoscience, ed. by C. CRADDOCK. Madison, Univ. Wisconsin Press, 895–901.

KYLE, P. R. and TREVES, S. B. (1973): Review of the geology of Hut Point Peninsula, Ross Island, Antarctica. DVDP Bull., **2**, 1–10.

KYLE, P. R. and TREVES, S. B. (1974): Geology of Hut Point Peninsula, Ross Island. Antarct. J. U.S., **9**(5), 232–234.

KYLE, P. R., SUTTER, J. F., MCINTOSH, W. C., CHERRY, E. and NOLTIMIER, H. (1983): $^{40}Ar/^{39}Ar$ age spectra and paleomagnetic measurements of Ferrar Supergroup samples from the Transantarctic Mountains, Antarctica. Antarctic Earth Sciences, ed. by R. L. OLIVER, P. R. JAMES and J. B. JAGO. Cambridge, Cambridge Univ. Press, 242.

LARSON, E. E., OZIMA, M., OZIMA, M. NAGATA, T. and STRANGWAY, D. W. (1969): Stability of remanent magnetization of igneous rocks. Geophys. J. R. Astron. Soc., **17**, 263.

LE PICHON, X. and HEIRTZLER, J. R. (1968): Magnetic anomaleis in the Indian Ocean and sea-floor spreading. J. Geophys. Res., **73**, 2101–2117.

LEVI, S. and MERRILL, R. T. (1976): A comparison of ARM and TRM in magnetite. Earth Planet. Sci. Lett., **32**, 177–184.

LØVLIE, R. (1979): Mesozoic paleomagnetism in Vestfjella, Dronning Maud Land, East Antarctica. Geophys. J. R. Astron. Soc., **59**, 529–537.

MCDOUGALL, I. (1963): Potassium-Argon measurements on dolerites from Antarctica and South Africa. J. Geophys. Res., **68**, 1535–1545.

MCDOUGALL, I. and GHENT, E. D. (1970): Potassium-Argon dates on minerals from the Mt. Falconer area, Lower Taylor Valley, South Victoria Land, Antarctica. N. Z. J. Geol. Geophys., **13**, 1026–1029.

MCELHINNY, M. W. (1973): Paleomagnetism and Plate Tectonics. Cambridge, Cambridge Univ. Press, 358p.

MCELHINNY, M. W. and BUREK, P. J. (1971): Mesozoic paleomagnetic stratigraphy. Nature, **232**, 98–102.

MCELHINNY, M. W. and JONES, D. L. (1965): Paleomagnetic measurements of some Karroo dolerite from Rhodesia. Nature, **206**, 921–922.

MCELHINNY, M. W. and LUCK, G. R. (1970): Paleomagnetism and Gondwanaland. Science, **168**, 830–832.

MCELHINNY, M. W. and WELLMAN, P. (1969): Polar wandering and sea-floor spreading in the Southern Indian Ocean. Earth Planet. Sci. Lett., **6**, 198–204.

MCKELVEY, B. C. and WEBB, P. N. (1959): Geological investigations in southern Victoria Land, Antarctica. N. Z. J. Geol. Geophys., **2**, 718–728.

MCKELVEY, B. C. and WEBB, P. N. (1961): Geological investigations in southern Victoria Land, Antarctica. Part 3-Geology of Wright Valley. N. Z. J. Geol. Geophys., **5**, 143–162.

MCMAHON, B. and SPALL, H. (1974a): Results of paleomagnetic investigation of selected cores recovered by Dry Valley Drilling Project. DVDP Bull., **4**, 37–38.

MCMAHON, B. E. and SPALL, H. (1974b): Paleomagnetic data from unit 13, DVDP hole 2, Ross Island. Antarct. J. U.S., **9**(5), 229–232.

MCQUEEN, D. M., SCHARNBERGER, C. K., SCHARON, L. and HALPERN, M. (1972): Cambo-Ordovician paleomagnetic pole position and rubidium-strontium total rock isochron for charnockitic rocks from Mirny Station, East Antarctica. Earth Planet. Sci. Lett., **16**, 433–438.

MANZONI, M. and NANNI, T. (1977): Paleomagnetism of Ordovician lamprophyres from Taylor Valley, Victoria Land, Antarctica. Pure Appl. Geophys., **115**, 96–977.

MUDREY, M. G., TORII, T. and HARRIS, H. (1975): Geology of DVDP 13-Don Juan Pond, Wright Valley, Antarctica. DVDP Bull., **5**, 78–99.

NAGATA, T. (1961): Rock Magnetism. Tokyo, Maruzen, 350p.

NAGATA, T. and SHIMIZU, Y. (1959): Natural remanent magnetization of Pre-Camprian gneiss of Ongul Islands in the Antarctica. Nature, **184**, 1472–1473.

NAGATA, T. and SHIMIZU, Y. (1960): Paleomagnetic studies on Pre-Cambrian gneiss of Ongul Island, Antarctica. Nankyoku Shiryô (Antarct. Rec.), **10**, 661–668.

NAGATA, T. and YAMA-AI, M. (1961): Paleomagnetic studies on rocks on the coast of Lützow-Holm Bay. Nankyoku Shiryô (Antarct. Rec.), **11**, 225–227.

NAGATA, T., FISHER, R. M. and SCHWERER, F. C. (1972): Lunar rock magnetism. Moon, **4**, 160–186.
PATTON, B. J. and FITCH, J. L. (1962): Anhysteretic remanent magnetization in small steady fields. J. Geophys. Res., **67**, 307–311.
RADHAKRISHNAMURTY, C. (1963): Remanent magnetism of igneous rocks in the Gondwana formation of India. D. Sc. Thesis, Andra University, India, 230p.
RAVICH, M. G. and FEDOROV, L. V. (1982): Geologic structure of MacRobertson Land and Princess Elizabeth Land, East Antarctica. Antarctic Geoscience, ed. by C. CRADDOCK. Madison, Univ. Wisconsin Press, 499–504.
ROBERTSON, W. A. (1963): The paleomagnetism of some Mesozoic intrusives and tuff from eastern Australia. J. Geophys. Res., **68**, 2299–2312.
SCHARNBERGER, C. and SCHARON, L. (1982): Paleomagnetism of rocks from Graham Land and western Ellsworth Land, Antarctica. Antarctic Geoscience, ed. by C. CRADDOCK. Madison, Univ. Wisconsin Press, 371–375.
SCHARON, L., SHIMOYAMA, A. and SCHARNBERGER, C. (1969): Paleomagnetic investigations in the Ellsworth Land area, Antarctica. Antarct. J. U.S., **4**, 94–95.
SMITH, A. and HALLAM, A. (1970): The fit of the southern continents. Nature, **225**, 139–144.
STOTT, P. M. (1963): The magnetization of Red Hill dike, Tasmania. J. Geophys. Res., **68**, 2289–2297.
STUCKLESS, J. S. (1975): Geochronology of core samples recovered from DVDP 6, Lake Vida, Antarctica. DVDP Bull., **6**, 27.
TATSUMI, T. and KIKUCHI, T. (1959): Nankyoku Syowa Kiti fukin no chigaku-teki kansatsu (sono 2) (Report of geomorphological and geological studies of the wintering term (1957–1958) of the First Japanese Antarctic Research Expedition, Part 2). Nankyoku Shiryô (Antarct. Rec.), **8**, 1–21.
TOWNROW, J. A. (1966): Fossil plants from Allan and Carapace Nunatak, and from the upper Mill and Shackleton Glaciers, Antarctica. N. Z. J. Geol. Geophy., **10**, 456–473.
TREVES, S. B. (1962): The geology of Cape Evans and Cape Royds, Ross Island, Antarctica. Antarctic Research, ed. by H. WEXLER, M. J. RUBIN and J. E. CASKEY. Washington, D.C., Am. Geophys. Union, 40–46 (Geophys. Monogr., **7**).
TREVES, S. B. (1967): Volcanic rocks from the Ross Island, Marguerite Bay and Mt. Weaver areas, Antarctica. JARE Sci. Rep., Spec. Issue, **1**, 136–149.
TREVES, S. B. and KYLE, P. R. (1973): Geology of DVDP 1 and 2, Hut Point Peninsula, Ross Island, Antarctica. DVDP Bull., **2**, 11–82.
TURNBULL, G. (1959): Some paleomagnetic measurements in Antarctica. Arctic, **12**, 151–157.
WEBB, P. N. (1963): Geological investigations in southern Victoria Land, Antarctica. Part 4-Beacon group of the Wright Valley and Taylor Glacier region. N. Z. J. Geol. Geophys., **6**, 361–387.
WEBB, P. N. and MCKELVEY, B. L. (1959): Geological investigation in South Victoria Land, Antarctica. Part 1-Geology of Victoria Valley. N. Z. J. Geol. Geophys., **2**, 120–136.
WELLMAN, G. W. (1964): Later geological history of Hut Point Peninsula, Antarctica. Trans. R. Soc. N. Z., Geol., **2**, 147–154.
ZIJDERVELD, J. D. A. (1968): Natural remanent magnetizations of some intrusive rocks from the Sør Rondane Mauntains, Queen Maud Land, Antarctica. J. Geophys. Res., **73**, 3773–3785.

(Manuscript received November 9, 1983; Revised manuscript received May 10, 1984).